Fall 12-13-2022

# Cascadia Subduction Zone Earthquake Vertical Ground Acceleration Investigation and Potential Impact on Bridges in the Pacific Northwest

Rachel C. Bassil
*Portland State University*

# Cascadia Subduction Zone Earthquake Vertical Ground Acceleration Investigation and Potential Impact on Bridges in the Pacific Northwest

by

Rachel Caroline Bassil

A research project submitted in partial fulfillment of the requirements for the degree of

Master of Science
in
Civil and Environmental Engineering

Project Advisor:
Dr. Peter Dusicka

Portland State University
2022

**Abstract**

The effects of vertical ground accelerations during subduction zone earthquakes currently are not sufficiently understood. There are numerous case studies and evidence that effects of vertical ground accelerations can significantly impact the performance of bridges during a seismic event, but most previous research has been focused on shallow crustal earthquakes. Current bridge design codes provide little guidance for accounting for vertical ground accelerations in seismic design, in part because additional information is needed about the characteristics of vertical ground motions during Cascadia Subduction Zone (CSZ) earthquakes in the Pacific Northwest.

For this study, recorded seismic data from recent subduction zone earthquakes was reviewed and compared to predicted CSZ ground motions. Time history data obtained from subduction zone earthquakes in Japan and Chile was used to compute response spectral accelerations for the three axes of motion. These results were then binned based on peak ground acceleration, short period spectral acceleration and 1.0-second period spectral acceleration, and geometric mean results then compared to the geometric mean of the predicted CSZ response spectra from the M9 CSZ Tool. Stations located within deep sedimentary basins were reviewed and compared separately. This study found that recorded subduction zone vertical accelerations and the predicted CSZ earthquake vertical accelerations could impart significant forces and should likely be considered in design of earthquake resistant bridges.

Differences between recorded subduction zone accelerations and predicted CSZ accelerations included magnitude of vertical acceleration, magnitude of vertical to horizontal acceleration ratio (V/H ratio) and spectral period ranges of maximum V/H ratios and decay.

**Contents**

**List of Tables**

**List of Figures**

## 1 Introduction

This paper aims to investigate subduction zone earthquake vertical ground motions and their potential impact on bridges in the Pacific Northwest. As part of this effort, time history data from recorded subduction zone earthquake events was analyzed and compared to predicted ground motions of the Cascadia Subduction Zone (CSZ) M9 Tool. Subduction zone ground motion records were used from Japan's K-NET and KIK-net Strong Motion Seismograph Networks and Chile's SIBER-Risk Strong Motion Database. Ground motion stations considered were located on soils classified as Site Class B based on $V_{S30}$ shear wave velocity data available. Sites that were located outside of deep sediment basins were investigated and compared separately from sites inside of deep sediment basins in order to compare the effects of deep basin amplification between historical ground motions and predicted ground motions.

## 2 Background

Research dating back to the 1990's has provided evidence that the effects of vertical ground accelerations have been underestimated and, in some cases, under designed by previous and current bridge design codes. Vertical ground motions can significantly affect the performance of bridges by increasing axial demands at columns, and moment demands at the face of the bent cap and in the middle of the span. Numerous investigations have shown that vertical ground acceleration effects have contributed to observed failures in highway bridges.

But the effects of vertical ground accelerations during subduction zone earthquakes currently are not sufficiently understood. While numerous studies investigating the vertical ground motion effects for shallow crustal earthquakes have been completed, the same is not true for vertical ground motion effects of subduction zone events. This is likely due in part to the more frequent occurrence of shallow crustal earthquakes and the spurred research funding from resulting bridge damage. Because subduction zone earthquakes are less frequent, there are fewer resulting ground motion records and less earthquake damage reconnaissance information available. Subduction zone earthquakes have different characteristics than shallow crustal earthquakes including significantly longer duration (more cycles), stronger motion at longer periods, and larger magnitudes. Because of this, it is possible that vertical ground accelerations could impact structures differently during subduction zone seismic events and therefore merits its own investigation.

## 3 Bridge Design Guidance

AASHTO Guide Specifications for LRFD Seismic Bridge Design (AASHTO Seismic Guide Specifications) only provides guidance to account for vertical ground accelerations for long flexible spans, eccentric load paths bridges, and critical and essential bridges within 6 miles (near fault) of an active surface or shallow fault (Section 3.4.3.1, Section 3.4.4, Section 4.2.2, Section 4.7.2, Section C3.4).

Section 4.7.2 of the AASHTO Seismic Guide Specifications state that specific recommendations for assessing vertical acceleration effects are not provided in the

AASHTO Seismic Guide Specifications until more information is known about the characteristics of vertical ground motion in those areas affected by subduction zones in the Pacific. The AASHTO Seismic Guide Specifications advise designers to be aware that vertical acceleration effects may be important and should be assessed for essential and critical bridges. The AASHTO Seismic Guide Specifications direct designers to reference Caltrans Seismic Design Criteria (Caltrans 2006).

The Caltrans Seismic Design Criteria guides designers to account for the effects of vertical ground accelerations by applying an equivalent static vertical load to the superstructure. Multi-span girder bridges located at sites with peak horizontal ground accelerations equal to or greater than 0.6g are required to be designed so that moment demands induced by a uniformly applied vertical force equal to 25% of the dead load applied upward and downward do not exceed the nominal flexural capacity of the superstructure (Sections 3.2.1.4 & 7.2.2).

In 2008, a Caltrans study found that only considering vertical accelerations for sites with a PGA of 0.6g and greater is not an adequate basis to determine the significance of vertical effects. The study also found that the application of 25% static dead load in the upward and downward directions to account for vertical acceleration effects resulted in inadequate reinforcement for a significant number of bridges examined.

The Oregon Department of Transportation Bridge Design Manual and the Washington Department of Transportation Bridge Design Manual do not provide specific guidance on consideration of vertical ground accelerations.

Overall, the bridge design guidance consideration of vertical ground accelerations provided by AASHTO, Caltrans, WSDOT and ODOT only contain guidance for bridges located near shallow crustal faults and not subduction zones. Within this limited guidance, even the shallow crustal fault guidelines for near fault effects have been found to be deficient.

## 4 Recorded Seismic Data Overview

Recorded seismic data from recent subduction zone earthquakes was reviewed and compared to predicted CSZ ground motions. Time history data obtained from Japanese and Chilean events for various stations was converted into response spectral accelerations for the three axes of motion. Vertical to horizontal ratios were compared and binned based on peak ground acceleration (PGA), short period spectral acceleration ($S_s$) and 1.0-second period spectral acceleration ($S_1$). Results were then compared to predicted CSZ response spectra from the M9 CSZ Tool.

The intent of this investigation is to review real earthquake records and the CSZ M9 forecasted ground motions to determine if vertical accelerations during a $M_w$ 9.0 CSZ earthquake will be an important component of earthquake accelerations that effect structures.

## 5 Events

Ground motion data was reviewed for five earthquake events. All events were interplate subduction zone earthquakes with magnitudes greater than 7.0 Mw and with recorded peak accelerations greater than 0.1g. Events were chosen that were sufficiently instrumented with ground motion station recordings located on Site Class B soils; the intent of this was to limit the impacts of acceleration amplification and de-amplification due to site soils. The 8.8 $M_w$ Maule earthquake in Chile (2010) was not included in the reviewed events because data at Site Class B soil stations was not available. See Table 1 for list of reviewed subduction zone earthquake events.

| Event Location | (Mw) | Date |
|---|---|---|
| Illapel, Chile | 8.4 | 9/16/2015 |
| Iquique, Chile | 7.6 | 3/4/2014 |
| Iquique, Chile | 8.2 | 1/4/2014 |
| Miyagi, Japan | 7.1 | 4/7/2011 |
| Tohoku, Japan | 9.0 | 3/11/2011 |

**Table 1: Subduction Zone Earthquakes Reviewed**

## 6 Stations

Ground motion records from Japan's K-NET and KIK-net Strong Motion Seismograph Networks and Chile's SIBER-Risk Strong Motion Database were obtained for the five earthquake events shown in Table 1. Ground motion stations were selected for use that were located within 300km of the event epicenter with recorded peak accelerations greater than 0.1g. To avoid acceleration amplification due to soft soils, stations were selected for review that were located on Site Class B soils with shear wave velocity data indicating 1500m/s $\leq V_{S30} \leq$ 760m/s. Some

K-NET stations did not have $V_{S30}$ data extending the full 30m depth. At these select stations, it was assumed that the deepest $V_{S30}$ value available extended to a 30m depth (i.e., if the deepest $V_{S30}$ data point available was at 20m depth, it was assumed the same value extended from 20m to 30m depth). See Table 2 for stations reviewed.

| Event | Magnitude (Mw) | Station | Max UD (g) | Max V/H (g/g) |
|---|---|---|---|---|
| Illapel | 8.4 | VA03 | 0.14 | 1.81 |
| Illapel | 8.4 | C10O | 0.54 | 0.85 |
| Illapel | 8.4 | CO06 | 0.59 | 0.57 |
| Iquique | 7.6 | TA01 | 0.21 | 1.36 |
| Iquique | 7.6 | T05A | 0.41 | 1.00 |
| Iquique | 7.6 | T06A | 0.28 | 1.18 |
| Iquique | 7.6 | PB11 | 0.33 | 0.93 |
| Iquique | 7.6 | GO01 | 0.48 | 1.53 |
| Iquique | 7.6 | T08A | 0.54 | 1.25 |
| Iquique | 8.2 | TA01 | 0.25 | 1.67 |
| Iquique | 8.2 | T06A | 0.42 | 1.54 |
| Iquique | 8.2 | T05A | 0.68 | 1.41 |
| Iquique | 8.2 | GO01 | 0.37 | 1.20 |
| Iquique | 8.2 | T08A | 0.88 | 1.30 |
| Iquique | 8.2 | PB11 | 1.06 | 1.26 |
| Miyagi | 7.1 | IWTH21 | 0.91 | 1.51 |
| Miyagi | 7.1 | IWTH28 | 0.71 | 1.33 |
| Miyagi | 7.1 | IWTH23 | 2.04 | 2.12 |
| Miyagi | 7.1 | MYGH04 | 1.84 | 2.05 |
| Miyagi | 7.1 | IWTH02 | 2.35 | 2.59 |
| Miyagi | 7.1 | IWT009 | 1.96 | 1.35 |
| Miyagi | 7.1 | MYGH03 | 1.62 | 1.02 |
| Miyagi | 7.1 | MYG012 | 0.91 | 1.00 |
| Tohoku | 9.0 | FKS014 | 0.66 | 2.77 |
| Tohoku | 9.0 | IWTH22 | 0.55 | 1.17 |
| Tohoku | 9.0 | IWT008 | 0.42 | 0.98 |
| Tohoku | 9.0 | IWTH18 | 0.51 | 1.33 |
| Tohoku | 9.0 | IBRH14 | 2.11 | 4.08 |
| Tohoku | 9.0 | IWTH21 | 1.31 | 2.36 |
| Tohoku | 9.0 | FKSH09 | 0.81 | 1.63 |
| Tohoku | 9.0 | MYGH03 | 0.98 | 0.93 |
| Tohoku | 9.0 | IWTH23 | 1.15 | 1.60 |
| Tohoku | 9.0 | MYGH12 | 1.26 | 1.16 |
| Tohoku | 9.0 | MYGH04 | 1.44 | 2.07 |
| Tohoku | 9.0 | IWT009 | 0.92 | 1.34 |
| Tohoku | 9.0 | IBRH16 | 1.71 | 1.94 |
| Tohoku | 9.0 | IWTH02 | 1.86 | 2.28 |
| Tohoku | 9.0 | MYG002 | 1.43 | 1.43 |
| Tohoku | 9.0 | IWTH27 | 1.08 | 1.06 |
| Tohoku | 9.0 | IBRH15 | 2.32 | 1.94 |
| Tohoku | 9.0 | TCGH13 | 1.00 | 0.83 |
| Tohoku | 9.0 | MYG012 | 1.25 | 1.07 |

**Table 2: Ground Motion Stations Reviewed. Maximum Vertical Spectral Acceleration and Maximum Vertical to Horizontal RSA Ratio per Station**

## 7 Data Analysis: Recorded Events, Non-Basin Sites

Recorded subduction zone event time history data was converted into response spectra acceleration (RSA) curves using the software SeismoSignal. Both horizontal directions (East/West and North/South) and vertical (Up/Down) data was developed into RSA curves. Vertical to horizontal (V/H) ratio curves were then developed. To avoid skewing the curves at longer period ranges where the accelerations are low, but V/H ratios can be very large, V/H ratio curves are only shown for accelerations that are equal or greater than 0.5*PGA. This cut off point was selected to capture the portion of the response spectra that would significantly impact structure response. See Figure 1 for examples of developed RSA curves for non-basin stations. See Appendix A for all stations.

The maximum recorded vertical spectral acceleration at the reviewed non-basin stations ranged from 0.14g to 2.3g. The maximum V/H spectral acceleration ratios at the reviewed stations ranged from 0.6 to 4.1. See Table 2.

Figure 2, Figure 3 and Figure 4 (left) show the PGA, $S_s$, and $S_1$ respectively for each site investigated versus the maximum spectral V/H ratio at that site. These figures indicate that most investigated sites had max V/H ratios between 1.0-2.0. It also shows that there is not a strong correlation between increasing or decreasing V/H ratios and PGA, Ss or S1 magnitude.

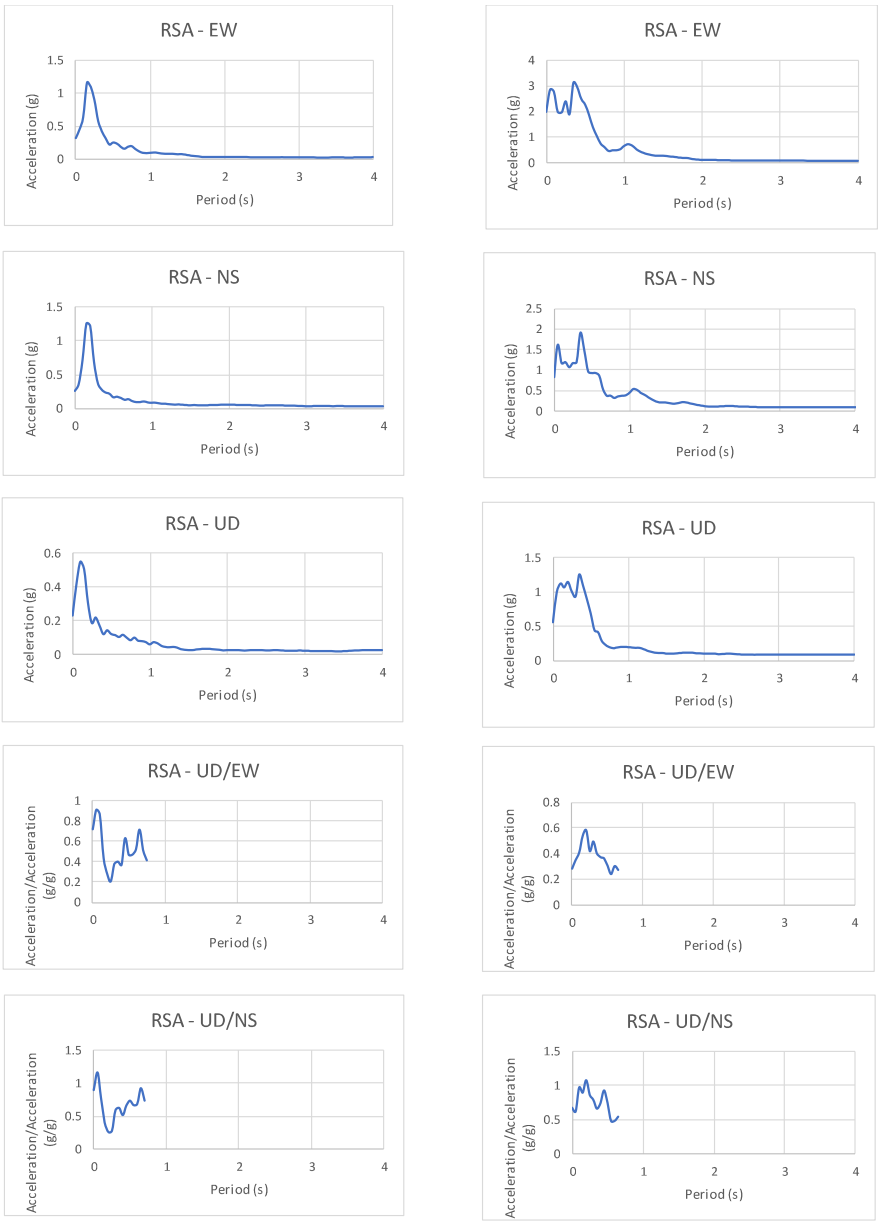


**Figure 1: Examples of RSA and V/H Ratio Curves Developed. Great Tohoku Earthquake Mw 9.0.**

**Stations IWTH22 (left) MYG012 (right). In order from top to bottom: X-direction RSA, Y-direction RSA, Z-direction RSA, X/Z RSA ratio, Y/Z RSA ratio. See Appendix A for RSA curves for all reviewed sites.**

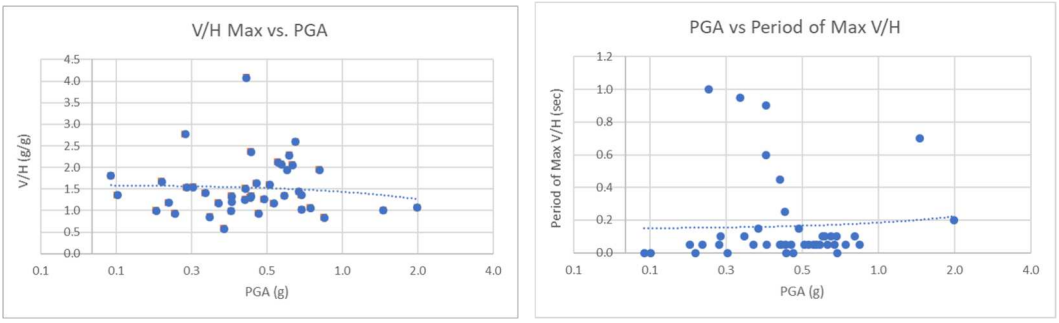


**Figure 2: Japan and Chile Non-basin Sites, V/H Max vs SS (left), SS vs Period of Max V/H (right)**

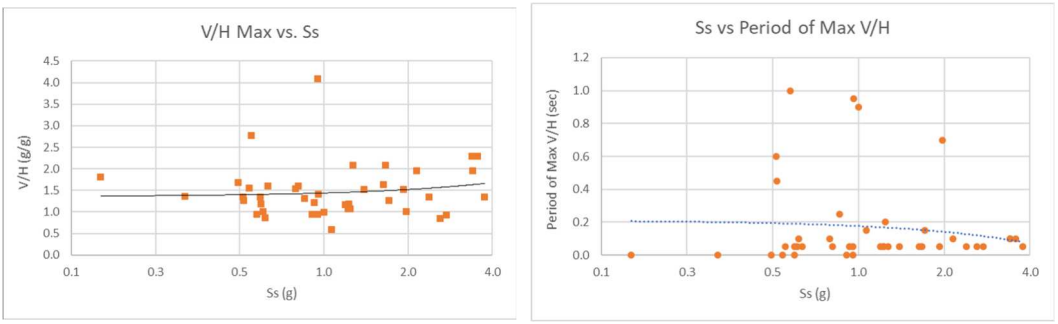


**Figure 3: Japan and Chile Non-basin Sites, V/H Max vs SS (left), SS vs Period of Max V/H (right)**

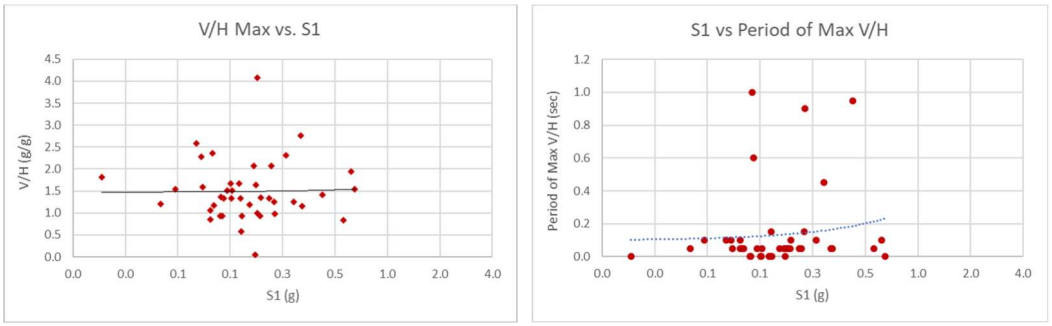


**Figure 4: Japan and Chile Non-basin Sites, V/H Max vs S1 (left), S1 vs Period of Max V/H (right)**

Figure 2, Figure 3 and Figure 4 (right) show the PGA, $S_s$, and $S_1$ respectively for each site investigated versus the spectral period that the maximum spectral V/H ratio occurred. These figures indicate that most sites' max V/H ratio occurred at

periods below 0.2 seconds. It also indicated that there is not a strong correlation between the magnitude of PGA, $S_S$ or $S_1$ and the period where the max V/H ratio occurs.

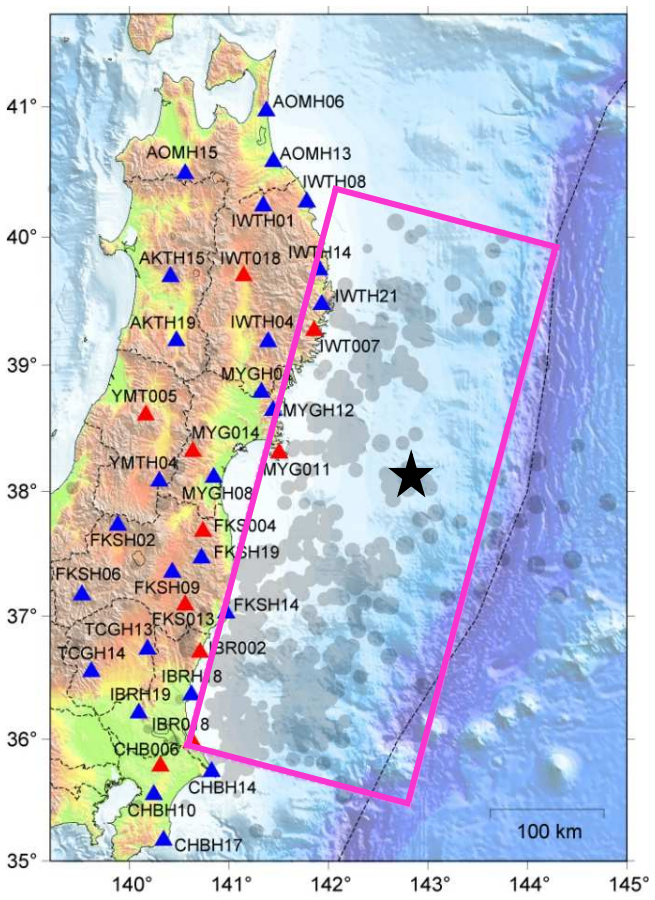


**Figure 5: Tohoku Earthquake Rupture Area**

Station sites were initially binned based on epicentral distance, but early analysis of the Tohoku data indicated that epicentral distance was not a relevant binning parameter. This is likely due to the earthquake's large rupture area, shown in Figure 5, approximately 200km wide by 500km long. Megathrust earthquakes occur due to slip across large areas of subducting plates. A site could be located 200km away

north or south from the epicenter of the Tohoku earthquake and still be located within the rupture area, but if a site was located 200km away east or west of the epicenter it would be well outside of the rupture area. Rupture process information was not readily available for all of the other earthquake events investigated, so for consistency, rupture distance was abandoned as a binning parameter. Rupture distance may be correlated to V/H ratios and should be investigated in the future.

All sites were then binned based on peak ground acceleration (PGA), short period spectral acceleration ($S_s$) and 1.0-second period spectral acceleration ($S_1$), see Figure 6. The geometric mean of the V/H ratio for each data bin was graphed verses period. The results are shown in Figure 9 for the investigated Japan and Chile recorded data at non-basin sites

| Group | PGA min | PGA max |
|---|---|---|
| 1 | 0.0 | 0.25 |
| 2 | 0.25 | 0.50 |
| 3 | 0.50 | 0.75 |
| 4 | 0.75 | 1.00 |
| 5 | 1.00 | 2.00 |

| Group | Ss min | Ss max |
|---|---|---|
| 1 | 0.0 | 0.75 |
| 2 | 0.75 | 1.50 |
| 3 | 1.50 | 2.25 |
| 4 | 2.25 | 3.00 |

| Group | S1 min | S1 max |
|---|---|---|
| 1 | 0 | 0.1 |
| 2 | 0.1 | 0.2 |
| 3 | 0.2 | 0.3 |
| 4 | 0.3 | 0.5 |
| 5 | 0.5 | 0.7 |

**Figure 6: Data bins used for PGA (left), Ss(middle) and S1 right.**

Results in Figure 7 indicate that for non-basin sites recorded V/H ratios were greatest at short periods less than 0.2 seconds. V/H ratios were greater than 1.0 at sites where the PGA was between 0.5-0.75g between 0-0.2s periods. V/H ratios were also greater than 1.0 at sites where PGA was between 1.0-2.0g and between 0.6-0.8g. In general for sites with PGAs below 1.0g, V/H ratios decreased as period increased.

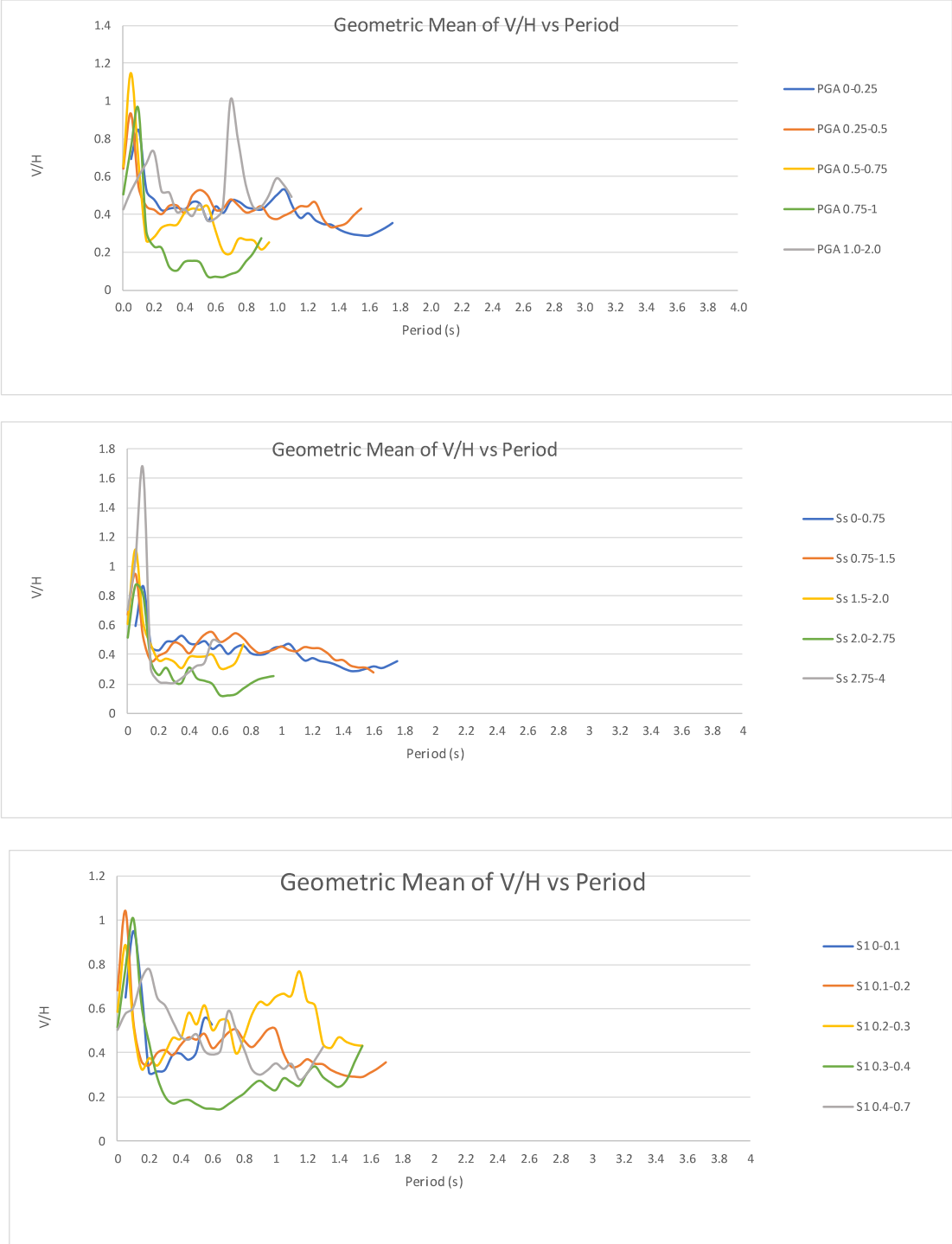


**Figure 7: Geometric Mean of V/H vs. Period for Recorded Time History Data of Japan and Chile Subduction Zone Earthquakes, Non-basin Sites.**
**Binned by: PGA (top), $S_s$ (middle), $S_1$ (bottom).**

Figure 7 also indicates that V/H ratios were greatest at sites with $S_s$ between 1.5-2.0g and 2.75-4.0g; V/H ratios were greater than 1.0 for both of these bins between 0-0.2s periods. Overall V/H ratios decreased as period increased.

Results binned by $S_1$ showed no clear trends other than V/H ratios being greatest between 0-0.2s periods and decreasing as period increases, similar to results binned by PGA and $S_1$.

The geometric mean of V/H ratios are graphed for periods ranging from 0.0-1.8 seconds. This is because accelerations beyond 1.8 second periods decayed to a value of less than 0.5*PGA, and were therefore not included, as they would have less significant effects on structures.

## 8 Data Analysis: CSZ M9 Tool, Non-Basin Sites

The M9 CSZ Tool is being developed to provide data in a visualization format for a full rupture 9.0 Mw earthquakes along the Cascadia Subduction Zone. The tool currently includes 30 different CSZ full rupture scenarios and provides 5% critically damped spectral accelerations for locations across the Pacific Northwest. All of the predicted CSZ ground motion data used for this study was the geometric mean response of the 30 different rupture scenarios. Three general Pacific Northwest (PNW) locations were reviewed in the M9 Tool for comparison with the event data presented in Section 7 above from Japan and Chile. The sites selected in the Seattle, Portland and Medford regions were located onshore and outside of deep sediment basins, See Figure 8.

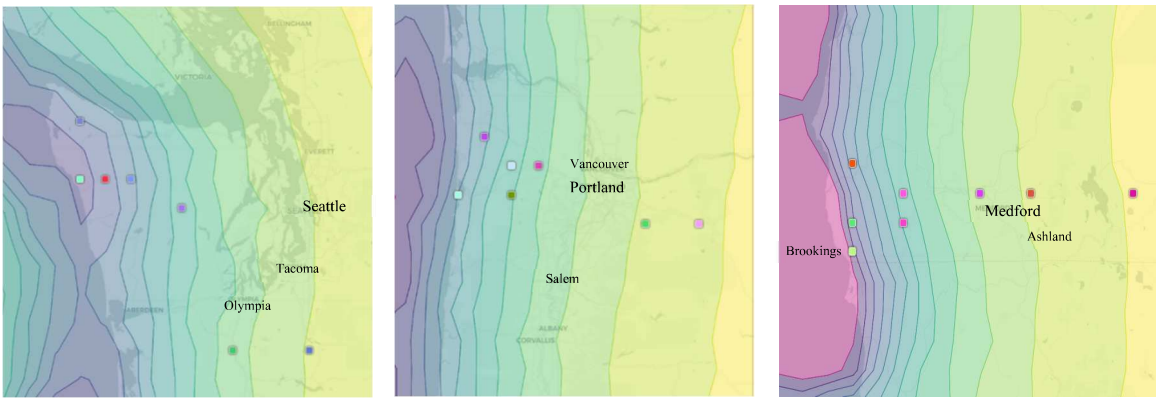


**Figure 8: M9 CSZ Tool Non-Basin Sites Reviewed, Seattle (left), Portland (middle), Medford (right)**

All M9 Tool acceleration data is for Site Class B soil conditions. The maximum predicted vertical spectral acceleration at the reviewed CSZ non-basin stations ranged from 0.20g to 1.76g. The maximum V/H spectral acceleration ratios at the reviewed non-basin CSZ stations ranged from 0.46 to 2.2. See Figure 9 for examples of RSA curves developed and Appendix B for all data.

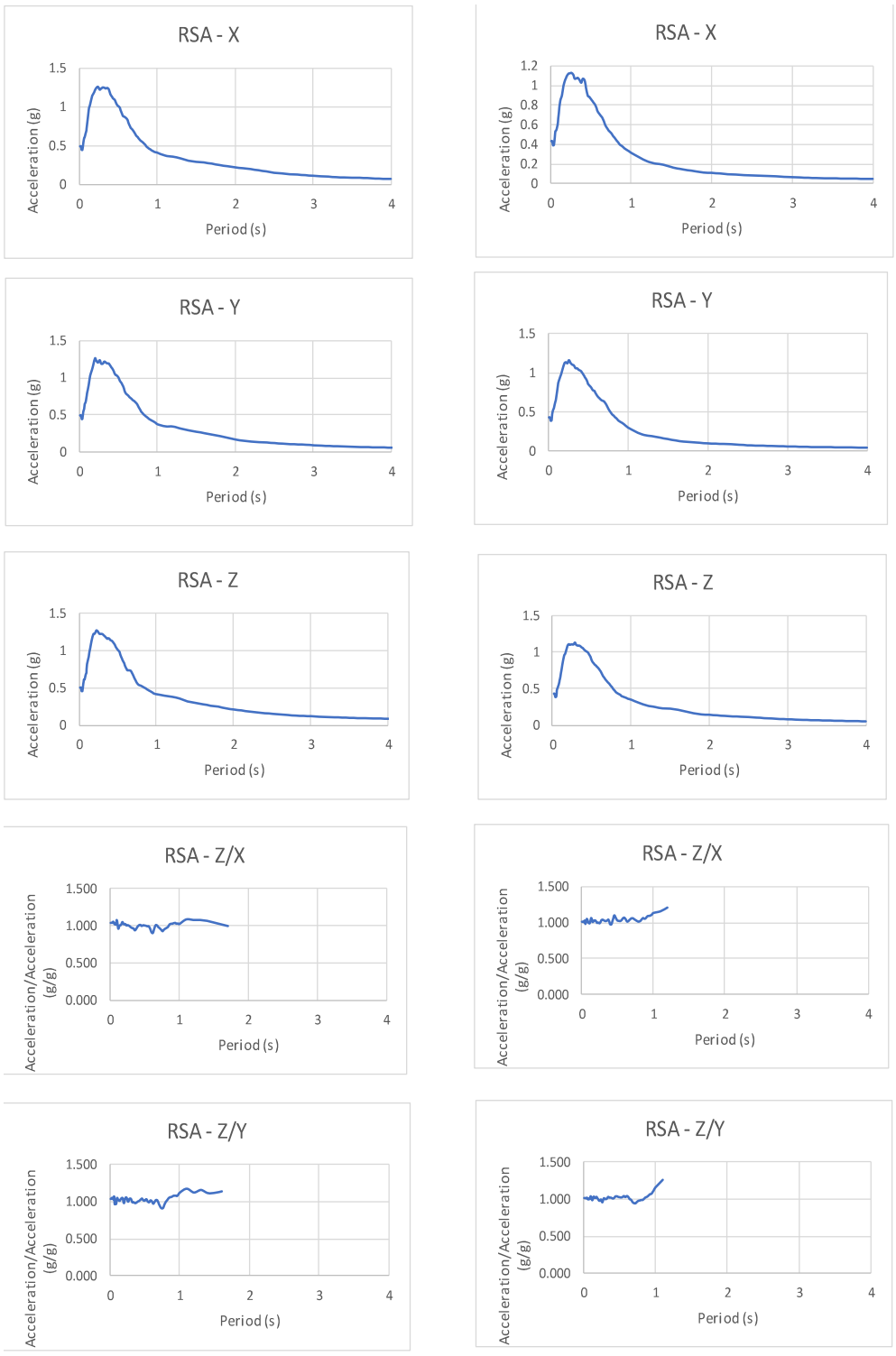


**Figure 9: Examples of RSA and V/H Ratio Curves Developed. M9 CSZ Tool. Stations Puget Sound Region (Seattle 8 )(left) and Northern Oregon (Portland 8) (right). In order from top to bottom: X-direction RSA, Y-direction RSA, Z-direction RSA, X/Z RSA ratio, Y/Z RSA ratio. See Appendix B for RSA curves for all reviewed sites.**

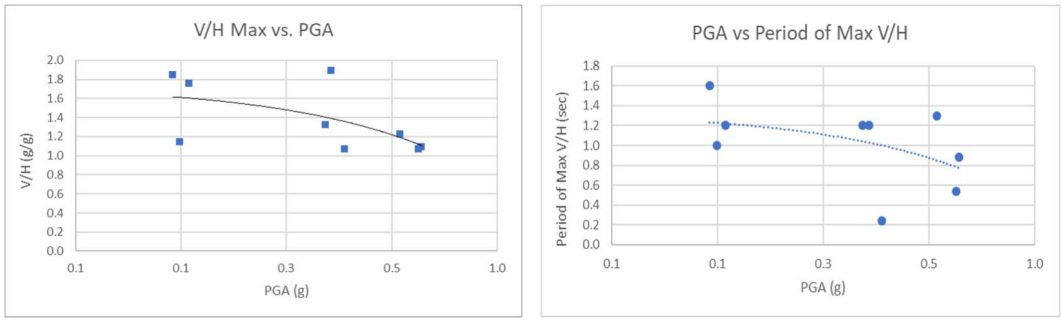


**Figure 10: CSZ M9 Tool Non-basin sites, V/H Max vs PGA (left), PGA vs Period of Max V/H (right)**

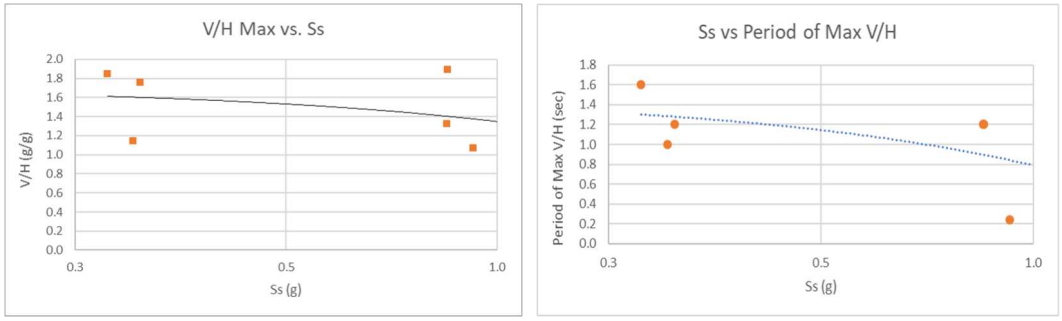


**Figure 11: CSZ M9 Tool Non-basin Sites, V/H Max vs $S_S$ (left), $S_S$ vs Period of Max V/H (right)**

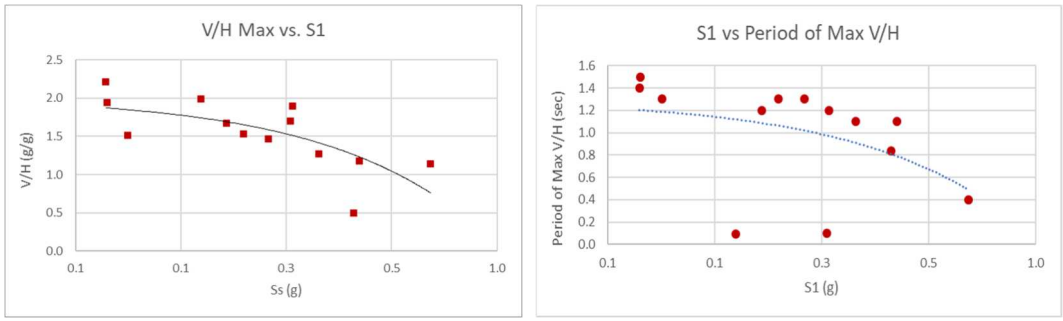


**Figure 12: CSZ M9 Tool Non-basin Sites, V/H Max vs $S_1$ (left), $S_1$ vs Period of Max V/H (right)**

Figure 10, Figure 11 and Figure 12 (left) show the PGA, $S_s$, and $S_1$ respectively for each M9 CSZ non-basin site investigated versus the maximum spectral V/H ratio at that site. This figure indicates that most investigated M9 CSZ sites had max V/H ratios between 1.0-2.0. It also shows that there is a slight correlation between increasing PGA and $S_s$ and decreasing V/H ratio. There is not a strong correlation between $S_s$ values and V/H ratios.

Figure 10, Figure 11 and Figure 12 (right) show the PGA, $S_s$, and $S_1$ respectively for each M9 CSZ site investigated versus the spectral period that the maximum spectral V/H ratio occurred. This figure indicates that most sites' max V/H ratio occurred at periods greater than 0.8 seconds. It also indicated that there is not a strong correlation between the magnitude of PGA, $S_S$ or $S_1$ and the period where the max V/H ratio occurs.

RSA data was reviewed and binned for non-basin CSZ sites similarly to the steps outlined in Section 7.

Results in Figure 13 indicate that for non-basin CSZ sites V/H ratios were consistently near 1.0 for periods up to 1.0 seconds for all PGA bins. V/H ratios increased after 1.0 second periods. V/H ratios were greatest for smaller PGAs of 0.1-0.25g.

V/H ratios were consistently near 1.0 for periods up to 1.0 seconds for all $S_s$ bins. Sites with $S_s$ values between 0.1-1.5g V/H ratios increased for periods greater than 1.0 seconds, while site with $S_s$ values greater than 1.5g V/H ratios decreased.

V/H ratios were consistently between 0.75 – 1.25 for all $S_1$ bins at periods between 0-0.8s. As periods increased greater than 1.0 seconds, V/H ratios increased for all sites with $S_1$ less than 0.5g and decreased for sites with $S_1$ greater than 0.5g.

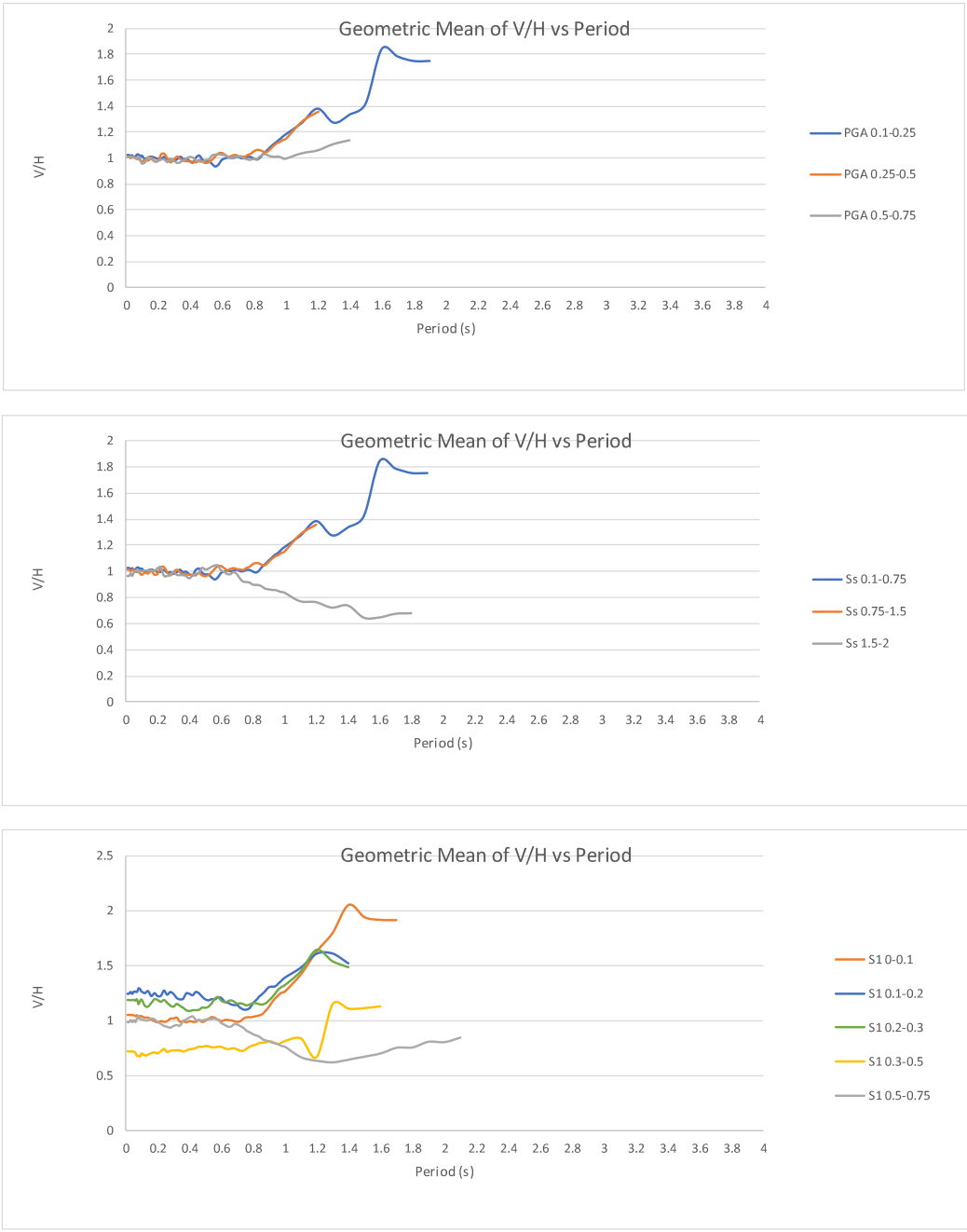


**Figure 13: Geometric Mean of V/H vs. Period for CSZ M9 Tool Data, Non-basin Sites. Binned by: PGA (top), $S_s$ (middle), $S_1$ (bottom).**

Geometric mean of V/H ratios are graphed for periods ranging from 0.0-2.2 seconds. This is because accelerations beyond approximately 2.2 second periods decayed to a value of less than 0.5*PGA, and were therefore not included, as they would have less significant effects on structures. This range is similar to the range of significant accelerations for the Japan and Chile stations investigated.

## 9 Non-Basin Discussion, Japan & Chile Time History Data vs. CSZ M9 Tool Data

Predicted CSZ V/H ratios are on average larger than V/H ratios from the Japan and Chile events. Recorded event data from the reviewed Japan and Chile subduction zone earthquakes indicates that V/H ratios peak at short periods between 0-0.2s and then taper to a V/H ratio of approximately 0.6 and remain consistent as period increases. The predicted CSZ M9 Tool data trends vary from the recorded Japan and Chile subduction earthquake data as the M9 Tool data predicts that the V/H ratios will remain consistently near 1.0 for periods between 0-1.0 seconds and then increase for sites with lower PGA and $S_s$, while decreasing for sites with higher PGA and $S_s$. This suggests that the predicted V/H ground motion behavior in a CSZ earthquake has inverse trends when compared to the recorded Japan and Chile even data.

While recorded data sees vertical acceleration ratios decaying at longer periods, the predicted CSZ data anticipates that vertical acceleration ratios will not decay as rapidly, but instead increase at longer periods. The M9 CSZ V/H ratios for periods between 0.0-1.0 seconds are almost consistently 1.0, this is the portion of the RSA

curve that contains the bulk of the higher magnitude accelerations, only when the curve starts to decay after 1.0 seconds, do the V/H ratios sharply increase.

The M9 CSZ synthetic seismograms were created using stochastic synthetic seismograms for periods less than 1.0 seconds and an assumed V/H ratio of 1.0. For periods greater than 1.0 seconds, deterministic synthetic seismograms were used from 3D physics based simulations. These assumptions explain why the CSZ predicted V/H ratios are consistently near 1.0 for periods less than 1.0 seconds. The initial 3D model that was used to develop the predicted M9 CSZ synthetic seismograms was limited by the grid size that could be used in the model given the computational resources that were available. This limited the period range that deterministic results could be determined for. A refined 3D model using smaller grid sizing is currently being developed and will allow for deterministic results for periods between 0.0 seconds and 1.0 second. This study recommends re-evaluating and comparing trends between the recorded data and predicted data when refined predicted data becomes available. If the current approach of using stochastic results for periods below 1.0 and using a set V/H ratio, further consideration could be given to the assumed V/H ratio value; this study has shown that the M9 CSZ assumed V/H ratio may be conservative in comparison to V/H ratios observed during other subduction zone earthquakes, but the maximum magnitudes of the vertical accelerations for the M9 CSZ are comparable to the maximum magnitudes of reviewed vertical accelerations from recorded subduction events.

Similarly to the recorded data, the M9 CSZ data also contains sites that are predicted to experience vertical spectral accelerations greater than 1.0g. These large vertical response accelerations could have a significant impact on structures during and event. The predicted M9 CSZ responses reviewed and discussed in this study are the geometric mean of the 30 possible rupture scenarios, so there could be singular rupture scenarios and sites that have larger or smaller maximum responses than what is reported here.

## 10 Deep Sediment Basins

Basin amplification is a phenomenon in which deep sedimentary basins increase earthquake ground motions. These deep sedimentary basins consist of soils that do not reach a layer of very hard rock for many kilometers depth. Within the Puget Sound Region and the Portland Metro Area there are deep sedimentary basins that could amplify ground shaking during a CSZ event and increase damage to structures. For this study the Portland Metro and Puget Sound Basins were characterized by the depth until soils reached a $V_{S30}$ equal to 2500m/s ($Z_{2.5}$). CSZ V/H ratios in the Portland and Puget Sound Basins were investigated and compared to V/H ratios in the Kanto and Nagata Basins in Japan during the Great Tohoku Earthquake.

Sites in the Kanto and Nigata basins were selected for analysis if they were onshore, with soil $V_{S30}$ greater than 180m/s, and at locations that showed no evidence of liquefaction. Site selection criteria was set to reduce the effects of soft soil

amplifications but also to provide a sufficient number of review sites for each basin. Basin depth at selected sites range between 2-5km.

| Kanto Basin : Z2.5 = 2.5-5km | | | | | Niigata Basin: Z2.5 = 2.5-5km | | | |
|---|---|---|---|---|---|---|---|---|
| Station | $V_{S30}$ | Max UD (g) | Max V/H (g/) | | Station | $V_{S30}$ | Max UD (g) | Max V/H (g/) |
| CHB012 | 300 | 0.39 | 0.89 | | NIG010 | 200 | 0.05 | 0.75 |
| CHB015 | 200 | 0.23 | 0.97 | | NIG013 | 200 | 0.04 | 0.72 |
| CHB017 | 300 | 0.14 | 1.08 | | NIG016 | 200 | 0.03 | 1.63 |
| CHB026 | 400 | 0.15 | 0.92 | | NIG024 | 500 | 0.04 | 1.62 |
| CHB013 | 300 | 0.11 | 0.81 | | NIG025 | 200 | 0.04 | 1.04 |
| CHBH10 | 300 | 0.29 | 1 | | NIG026 | 300 | 0.03 | 1.39 |
| TKY007 | 300 | 0.24 | 0.84 | | NIG028 | 400 | 0.06 | 1.17 |

**Table 3: Japan Basin Sites Reviewed**

For the Portland and Puget Sound Basins, PGA, $S_S$ and $S_1$ values were not varied enough to bin data based on these values. Instead, each basin is binned together. Puget Sound sites were selected to have similar $Z_{2.5}$ values as the Kanto and Nigata Basins. Portland Basin has a maximum $Z_{2.5}$ value of approximately 2.2km; Portland sites were chosen that had $Z_{2.5}$ values near or greater than 2km.

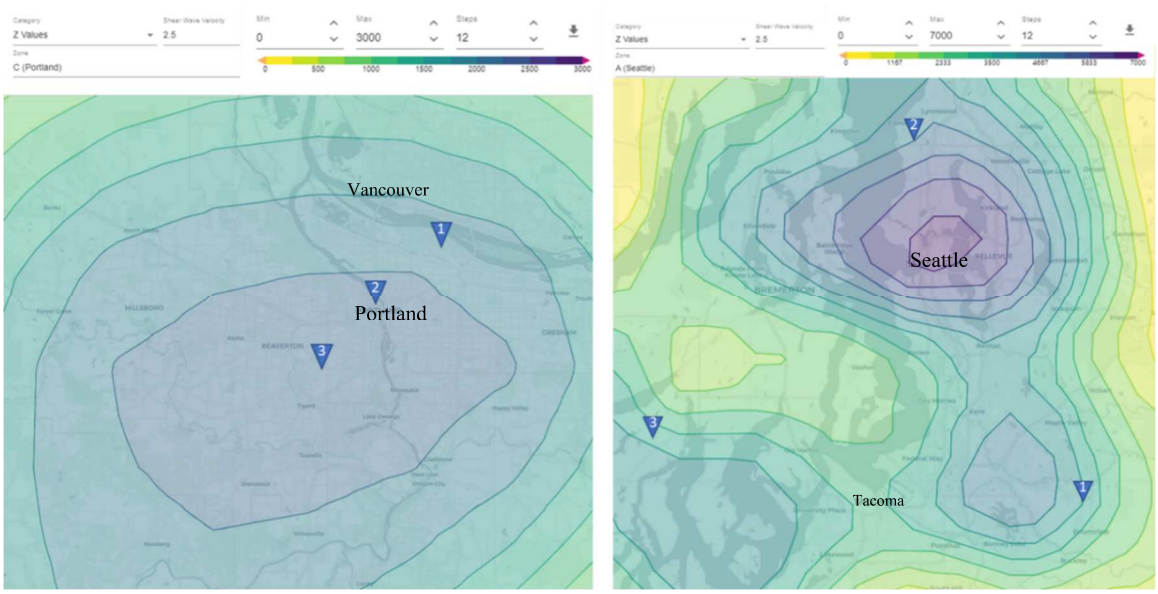


**Figure 14: Deep Sedimentary Basin Sites: Portland (left), Seattle (right)**

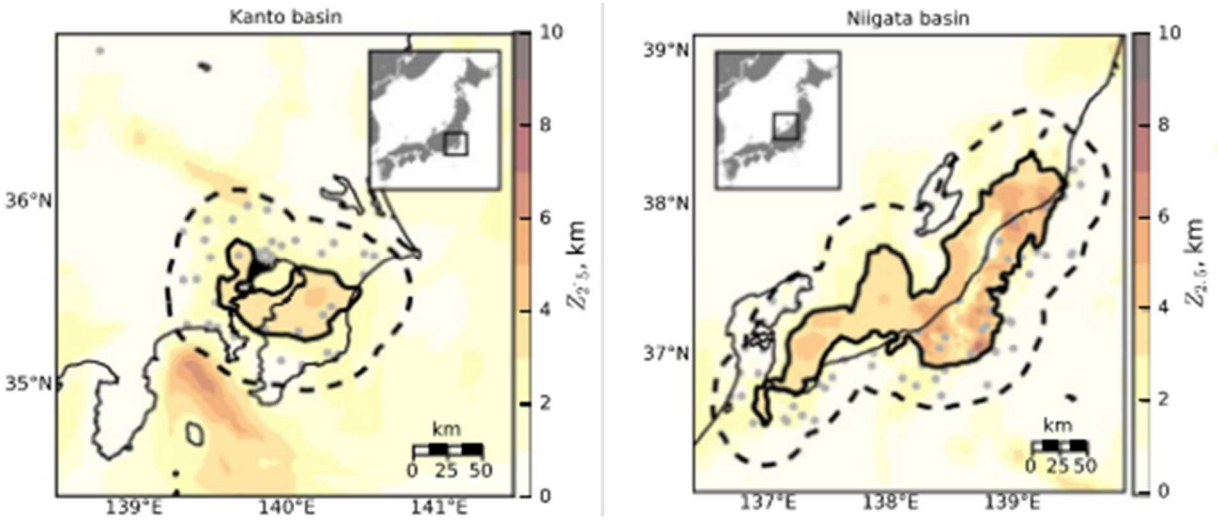


**Figure 15: Deep sedimentary Basins in Japan: Kanto (left), Nigata (right)**

RSA data for basin sites was reviewed and binned similarly to the steps outlined for non-basin sites in Section 7 and Section 8.

## 11 Data Analysis: Japan, Kanto and Nigata Basin Sites

The maximum recorded vertical spectral acceleration at the reviewed basin stations ranged from 0.03g to 0.39g. The maximum V/H spectral acceleration ratios at the reviewed basin stations ranged from 0.69 to 1.6.


**Figure 16: Examples of RSA and V/H Ratio Curves Developed. Kanto & Nigata Basins**

**Stations:TKY007 (left) and CBH012 (right). In order from top to bottom: X-direction RSA, Y-direction RSA, Z-direction RSA, X/Z RSA ratio, Y/Z RSA ratio. See Appendix C for RSA curves for all reviewed sites.**

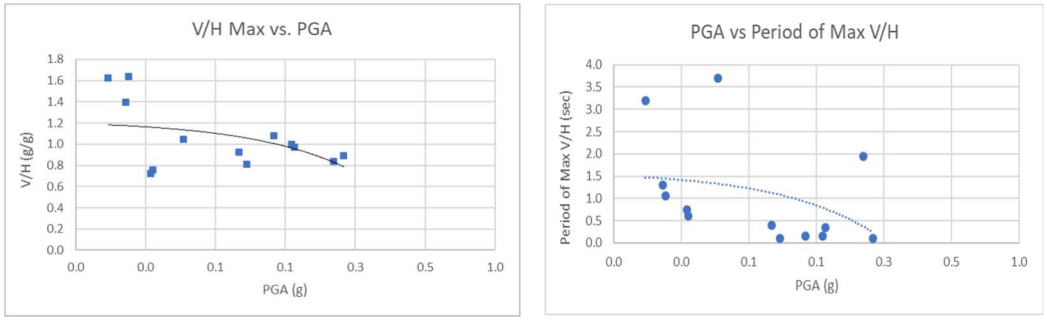


**Figure 17: Kanto and Nigata basin sites, V/H Max vs PGA (left), PGA vs Period of Max V/H (right)**

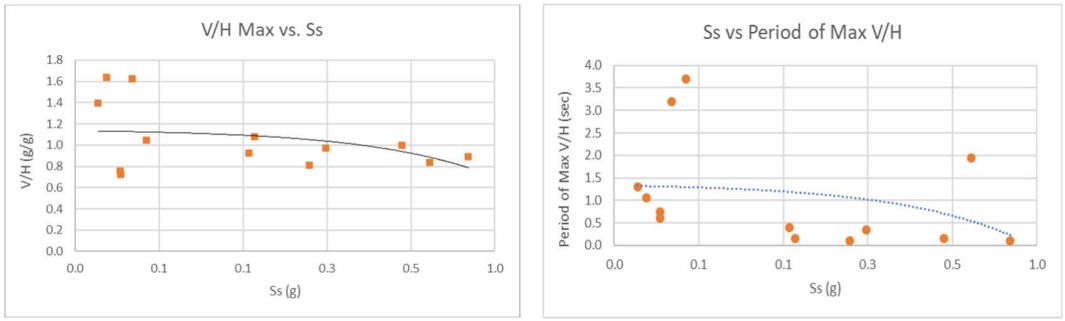


**Figure 18: Kanto and Nigata Basin Sites, V/H Max vs SS (left), SS vs Period of Max V/H (right)**

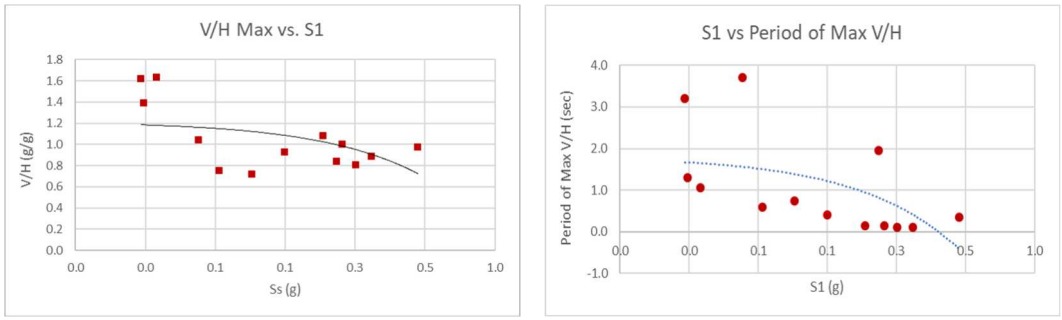


**Figure 19: Kanto and Nigata basin sites, V/H Max vs S1 (left), S1 vs Period of Max V/H (right)**

Figure 17, Figure 18 and Figure 19 (left) show the PGA, $S_s$, and $S_1$ respectively for each basin site investigated versus the maximum spectral V/H ratio at that site. This figure indicates that all investigated basin sites had max V/H ratios greater than 0.6. It also shows that there is a slight correlation between increasing PGA, $S_s$ and $S_1$ and decreasing V/H ratio.

Figure 17, Figure 18 and Figure 19 (right) show the PGA, $S_s$, and $S_1$ respectively for each basin site investigated versus the spectral period that the maximum spectral V/H ratio occurred. This figure indicates that the max V/H ratios occurred at periods of 0-4.0 seconds across sites, with many sites experiencing a maximum V/H ratio at periods below 1.0. This figure also indicated that there is not a strong correlation between the magnitude of PGA, $S_S$ or $S_1$ and the period where the max V/H ratio occurs.

Results in Figure 20 indicate that for the Kanto and Nigata Basin sites V/H ratios for PGA less than 0.1g were between 0.45-0.65 for all periods. For PGA between 0.1g-0.2g V/H ratios peaked at 0.77 at short periods less than 0.2s and long period greater than 3.6s. For other periods V/H ratios were between 0.3-0.6.

V/H ratios were consistently between 0.5-0.7 for $S_s$ values below 0.1g. Sites with $S_s$ values between 0.1-1.1g V/H ratios peaked at 0.75 at period 0.2s and were between 0.35 and 0.55 for other periods.

V/H ratios were consistently between 0.5 – 0.65 for sites with $S_1$ less than 0.1g. For sites with values of $S_1$ between 0.1-1.0g, V/H ratios peaked at 0.2s periods and then were consistently between 0.35-0.5.

On average V/H ratios were larger for lower PGA, $S_s$ and $S_1$ bins.

Kanto and Nigato Basin V/H ratios were on average smaller for short periods and larger for longer periods than the non-basin Japan and Chile data in Figure 7.

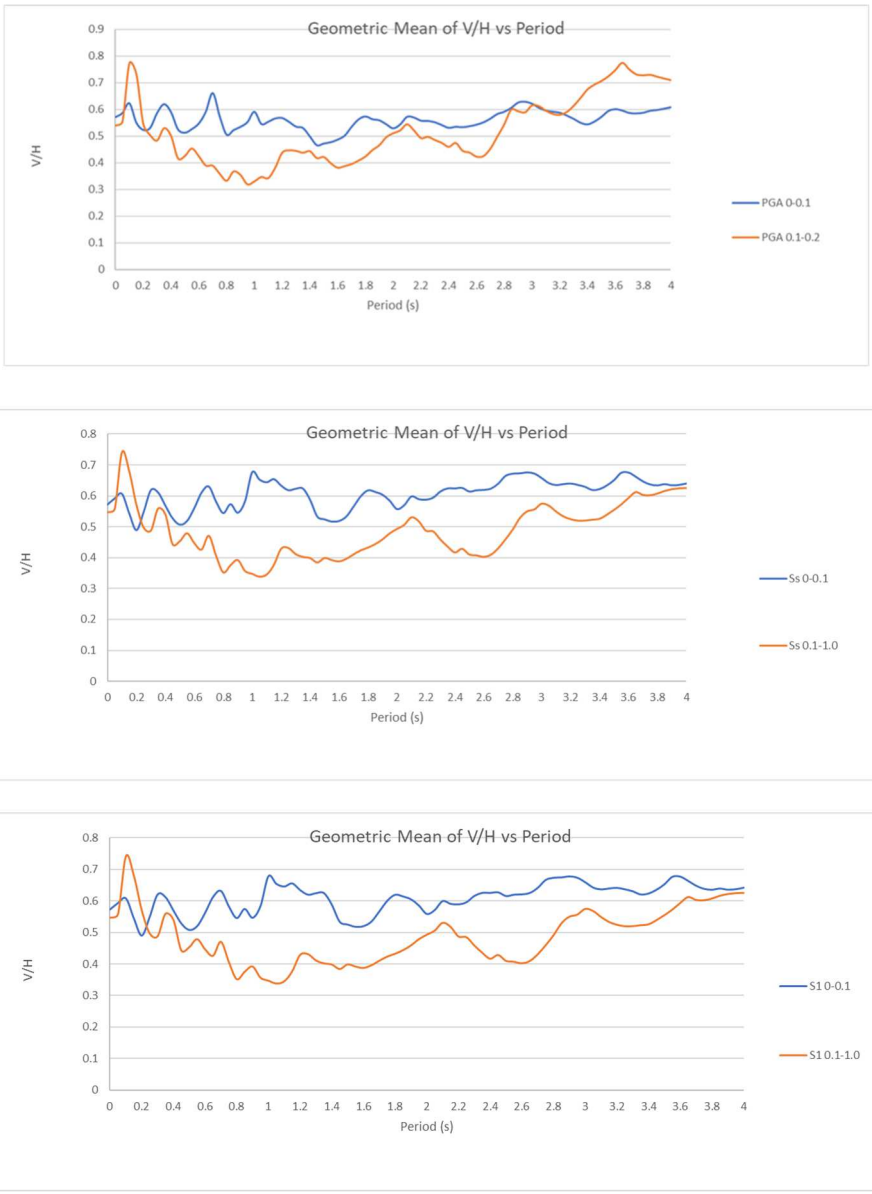


**Figure 20: Geometric Mean of V/H vs. Period for Recorded Time History Data of The Great Tohoku Earthquake in the Kanto and Nigata Basins.**
**Binned by: PGA (top), Ss (middle), S1 (bottom).**

The Geometric mean of V/H vs Period plots for the basin sites are graphed into longer periods than the non-basin sites. This means that at the Kanto and Nigata basin sites, the accelerations remained at or above 0.5*PGA for longer periods. This indicates that basin site accelerations did not decay as quickly at longer periods like they did at non-basin sites.

## 12 Data Analysis: CSZ M9 Tool, Basin Sites

The maximum predicted vertical spectral acceleration at the reviewed CSZ basin stations ranged from 0.34g to 0.60g. See Example CSZ Tool Spectra in Figure 21.

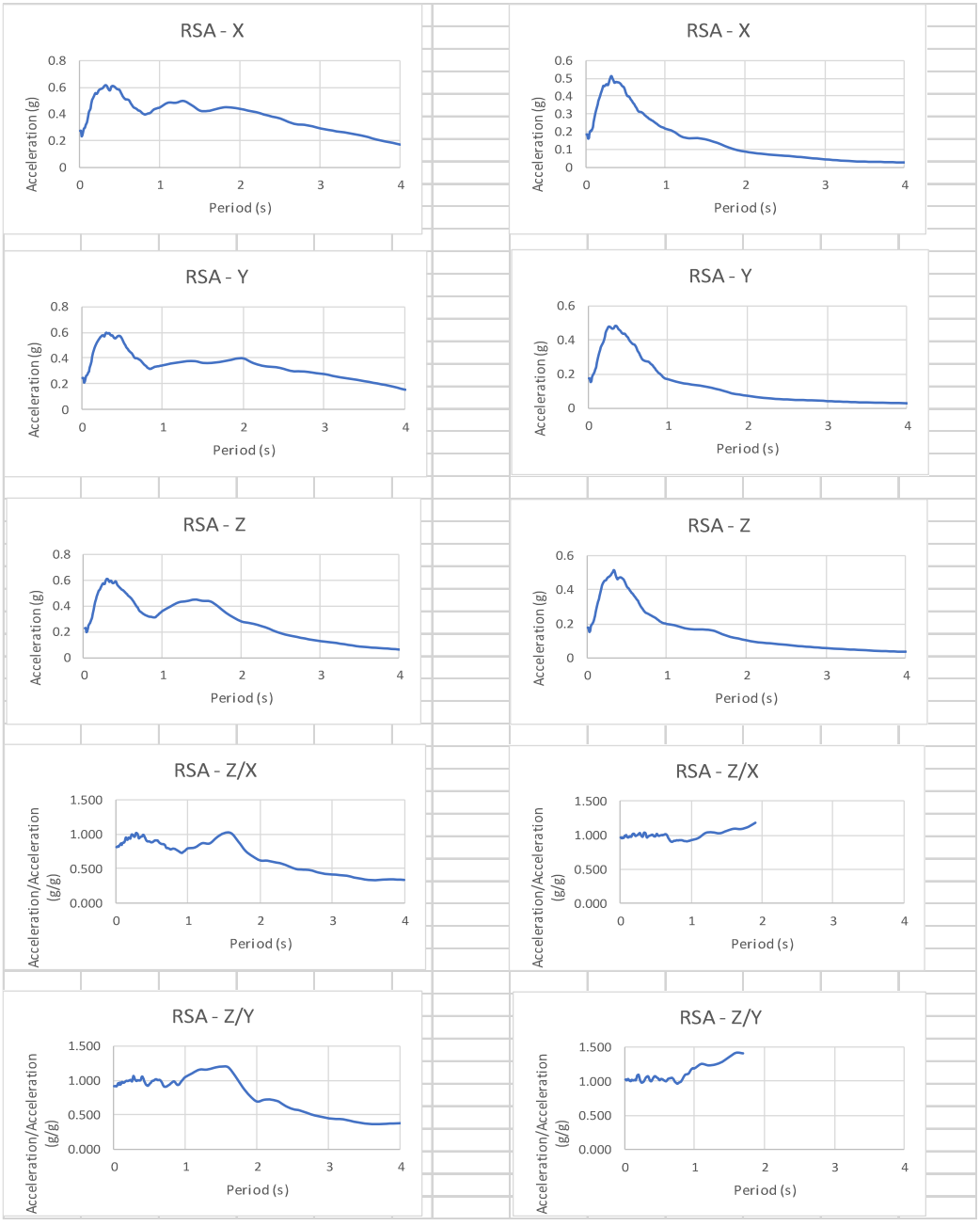


**Figure 21: Examples of RSA and V/H Ratio Curves Developed. M9 CSZ Tool Basin Sites Stations Puget Sound Region (Seattle 3)(left) and Northern Oregon (Portland 1) (right). In order from top to bottom: X-direction RSA, Y-direction RSA, Z-direction RSA, X/Z RSA ratio, Y/Z RSA ratio. See Appendix D for RSA curves for all reviewed sites.**

For the M9 CSZ predicted ground motions at basin sites, again the results reviewed and reported here were for the geometric mean of the 30 different M9 CSZ rupture scenarios.

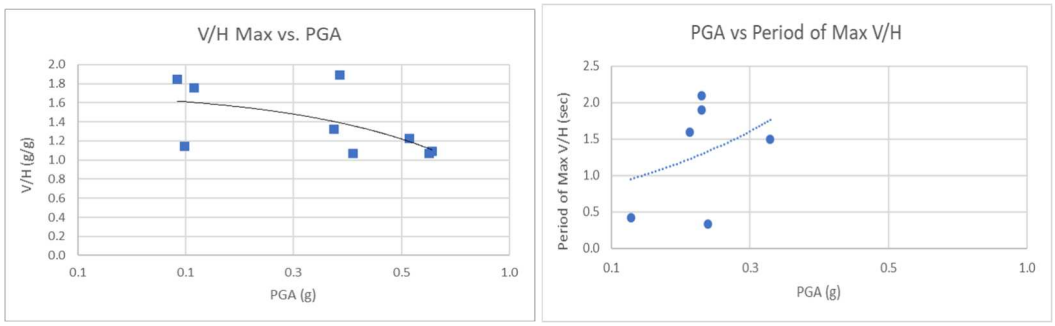


**Figure 22: Portland and Puget Sound Basin Sites, V/H Max vs PGA (left), PGA vs Period of Max V/H (right)**

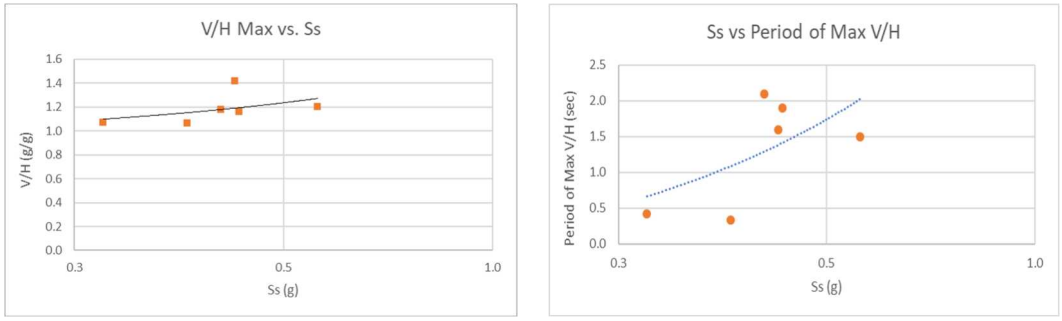


**Figure 23: Portland and Puget Sound Basin Sites, V/H Max vs $S_S$ (left), PGA vs Period of Max V/H (right)**

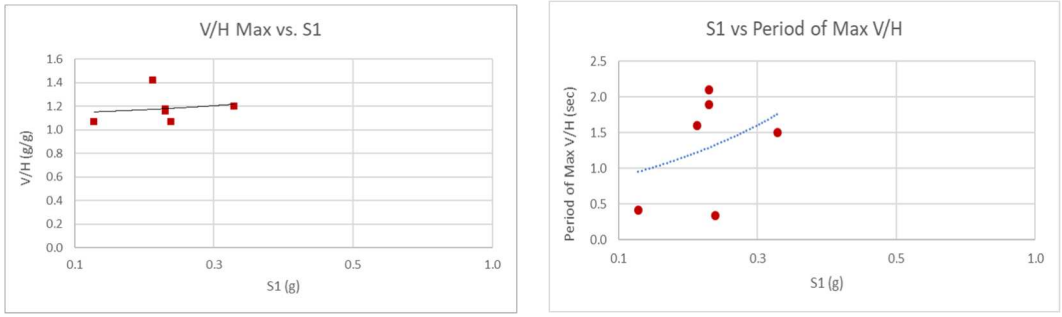


**Figure 24: Portland and Puget Sound Basin Sites, V/H Max vs $S_1$ (left), PGA vs Period of Max V/H (right)**

Figure 22, Figure 23 and Figure 24 (left) show the PGA, $S_s$, and $S_1$ respectively for each M9 CSZ basin site investigated versus the maximum spectral V/H ratio at that site. This figure indicates that all investigated M9 CSZ basin sites had max V/H ratios greater than 1.0.

Figure 22, Figure 23 and Figure 24 (right) show the PGA, $S_s$, and $S_1$ respectively for each basin site investigated versus the spectral period that the maximum spectral V/H ratio occurred. This figure indicates that the max V/H ratios occurred at periods of 0-1.6 seconds across sites. This figure also indicated that there is not a strong correlation between the magnitude of PGA, $S_S$ or $S_1$ and the period where the max V/H ratio occurs.

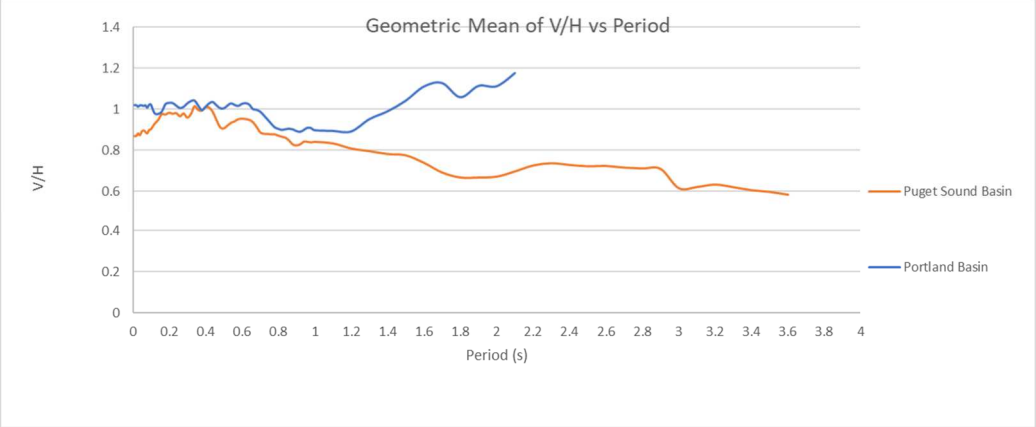


**Figure 25: Geometric Mean of V/H vs. Period for CSZ M9 Tool Data, Basin Sites**

Results in Figure 25 show that overall Portland V/H ratios are higher than Puget Sound Basin V/H ratios. Between periods 0-1.0 seconds both Puget Sound and Portland basin V/H ratios are near 1.0. At periods greater than 1.0 seconds Portland Basin V/H ratios increase, while Puget Sound Basin V/H ratios decrease.

CSZ Basin site V/H ratios are similar to non-basin CSZ V/H ratios for periods between 0-1.0 seconds. CSZ Basin site V/H ratios are smaller than non-basin site V/H ratios for periods greater than 1.0 seconds.

The Geometric mean of V/H vs Period plots for the M9 CSZ basin sites are graphed for periods ranging from 0-2.0 seconds for the Portland Basin and 0-3.6 seconds for the Puget Sound Basin. These ranges are slightly shorter than the Nigata and Kanto basin sites, but still much longer than the non-basin site ranges. This indicates that M9 CSZ basin site accelerations decayed slightly faster than the Nigata and Kanto basins, but still did not decay as quickly at longer periods as the non-basin sites did.

## 13 Basin Discussion: Japan Basin Time History Data vs. CSZ M9 Tool Basin Data

On average the CSZ M9 Tool predicts that the Portland and Puget Sound Basins will have higher V/H ratios than the recorded Kanto and Nigata Basin V/H ratios. Portland Basin V/H ratios are larger than the Kanto and Nigata Basin V/H ratios at all periods. Puget Sound Basin V/H ratios are on average larger than the Kanto and Nigata Basin V/H ratios for periods between 0-3.2 seconds. These findings suggest that basin amplification effects during a CSZ earthquake could have more significant impact on vertical ground accelerations and therefore a more significant impact on structures in the Pacific Northwest Basins than what was observed during the Great Tohoku Earthquake. CSZ Basin sites are predicted to experience V/H ratios 30-60% higher for periods between 0-1.0 seconds than recorded basin site

data. The maximum predicted magnitude of vertical accelerations at reviewed CSZ sites was approximately 50% larger than the maximum magnitude of vertical accelerations recorded in the Kanto and Nigata basins. This maximum magnitude of predicted vertical spectral accelerations was approximately 0.6g, which is still below 1.0g acceleration.

The predicted CSZ basin data also anticipates a decay in vertical spectral accelerations, but at some sites reviewed, not as quickly. At some CSZ basin sites it is predicted that vertical spectral accelerations will begin to decay as periods increase, but then increase again between periods of 1.0-2.0 seconds. This trend is not seen at the recorded data basin sites where vertical accelerations steadily decay at longer periods.

The geometric mean of V/H ratios show similar trends between both recorded data basin sites and the predicted data sites; V/H ratios remain mostly a consistent value between period ranges of 0.0-1.4 seconds. At periods greater than 1.4 seconds, the predicted CSZ basin sites in the Puget Sound Region decrease, while those in Portland increase. These longer periods will likely not impact most structures significantly though.

The M9 CSZ synthetic seismograms were created using stochastic synthetic seismograms for periods less than 1.0 seconds and an assumed V/H ratio of 1.0. For periods greater than 1.0 seconds, deterministic synthetic seismograms were used from 3D physics based simulations. These assumptions explain why the CSZ predicted V/H ratios are consistently near 1.0 for periods less than 1.0 seconds. The

initial 3D model that was used to develop the predicted M9 CSZ seismograms was limited by the grid size that could be used given the computational resources that were available, which limited the period range that deterministic results could be determined for. A refined 3D model using a smaller grid size is currently being developed and will allow for deterministic results for periods between 0.0 seconds and 1.0 second. This study recommends re-evaluating and comparing trends between the recorded data and predicted data when refined predicted CSZ data becomes available. If the current approach of using stochastic results for periods below 1.0 and using a set V/H ratios remains, further consideration could be given to the assumed V/H ratio value; this study has shown that the CSZ assumed V/H ratio may be conservative in magnitude at basin sites in comparison to V/H ratios observed at basin sites during other subduction zone earthquakes, but the CSZ basin sites' vertical accelerations decay faster than recorded basin sites.

## 14 Conclusions

Review of subduction zone ground motion records has highlighted differences in response spectra trends between recorded data from Japan and Chile and the M9 CSZ predicted ground motions.

Magnitudes of maximum vertical acceleration response across the individual sites were comparable between the M9 CSZ non-basin sites and the recorded data non-basin sites. Recorded data from non-basin sites mostly had maximum vertical acceleration peaks at short periods and then rapid decay of vertical acceleration as periods increased. Conversely, the M9 CSZ non-basin sites are predicted to have

higher vertical accelerations for a longer range of periods and then decay less quickly.

All of the predicted M9 CSZ acceleration responses that were reviewed and discussed for this study were the geometric mean of the 30 different predicted M9 CSZ rupture scenarios. This means that there is likely singular rupture scenarios and sites that could have larger or smaller responses than what has been discussed in this study.

Maximum magnitudes of predicted and recorded vertical acceleration response for non-basin sites exceeds 1.0g and could have significant impact on structural response during an M9 CSZ earthquake. Based on this prediction vertical acceleration effects of a Cascadia Subduction Zone earthquake should likely be accounted for in design of earthquake resistant structures in the Pacific Northwest.

The V/H ratios for the M9 CSZ are predicted to be about 30-60% higher than the Nigata and Kanto basin data reviewed. Basin sites in the PNW are predicted to experience maximum vertical spectral accelerations up to 50% greater than the Nigata and Kanto basin site data reviewed. The maximum magnitude of vertical spectral acceleration predicted in the PNW was approximately 2.1g at M9 CSZ sites reviewed. This is a significant response, indicating that vertical acceleration effects should likely be considered for design of earthquake resistant structures in the Pacific Northwest.

The M9 CSZ synthetic seismograms were created using stochastic synthetic seismograms for periods less than 1.0 seconds and an assumed V/H ratio of 1.0.

For periods greater than 1.0 seconds, deterministic synthetic seismograms were used from 3D physics based simulations. These assumptions explain why the CSZ predicted V/H ratios are consistently near 1.0 for periods less than 1.0 seconds. This study has shown that the CSZ assumed V/H ratio may be conservative in comparison to V/H ratios observed during other subduction zone earthquakes, but at non-basin sites the maximum magnitudes of the vertical accelerations for the M9 CSZ are comparable to the maximum magnitudes of reviewed vertical accelerations from recorded subduction events. This study also found that CSZ basin sites' vertical accelerations decay more quickly than reviewed recorded data at Japanese basin sites. If the current approach of using stochastically determined M9 CSZ ground motions for periods less than 1.0 seconds remains, this study would suggest considering a different set V/H ratio equal to 1.0 for periods less than 0.2 seconds and a V/H ratio equal to 0.6 for periods greater than 0.2 seconds.

## 15 Suggestions for Future Study

Suggested further study for this topic includes re-assessing trends of the M9 CSZ predicted ground motions when the refined 3D geophysics model is available and re-comparing trends with the recorded ground motions trends from Japan and Chile. Additional suggestions include: further investigating subduction zone earthquake vertical accelerations' relation to site variables including rupture distance and site soil classifications and review of case studies of bridges subjected to significant subduction zone vertical seismic accelerations with consideration of the impact of combined vertical and horizontal ground motions.

## 16 References


AASHTO. (2015). Guide specifications for LRFD seismic bridge design, Washington, DC.

Button, M. R., Cronin, C. J., & Mayes, R. L. (2002). Effect of vertical motions on seismic response of highway bridges. Journal of structural engineering, 128(12), 1551-1564.

Bozorgnia, Y., & Campbell, K. W. (2004). The vertical-to-horizontal response spectral ratio and tentative procedures for developing simplified V/H and vertical design spectra. Journal of Earthquake Engineering, 8(02), 175-207.

Bozorgnia, Y., & Stewart, J. P. (2019, April). PEER 2020/02 - Data Resources for NGA- Subduction Project Electronic Supplement. Retrieved August 1, 2020, from ttps://apps.peer.berkeley.edu/publications/peer_reports/reports_2020/NGA-Sub_flatfile_PSA5perc_2019-Apr.xlsx

Castro, S., Benavente, R., Crempien, J., Candia, G., de la Llera, J.C. (2021). A Consistently Processed Strong Motion Database for Chilean Earthquakes. Submitted.

Dusicka, P. (in progress: 2022), Portland State University, M9 CSZ Online Tool, https://m9csz.cee.pdx.edu/

Elgamal, A., & He, L. (2004). Vertical earthquake ground motion records: an overview. Journal of Earthquake Engineering, 8(05), 663-697.

Frankel, A., & Grant, A. (2021). Site Response, Basin Amplification, and Earthquake Stress Drops in the Portland, Oregon Area. Bulletin of the Seismological Society of America, 111(2), 671-685.

Frankel, A., Wirth, E., Marafi, N., Vidale, J., & Stephenson, W. (2018). Broadband Synthetic Seismograms for Magnitude 9 Earthquakes on the Cascadia Megathrust Based on 3D Simulations and Stochastic Synthetics, Part 1: Methodology and Overall Results. Bulletin of the Seismological Society of America, 108(5A), 2347-2369.

Kim, S. J., Holub, C. J., & Elnashai, A. S. (2011). Analytical assessment of the effect of vertical earthquake motion on RC bridge piers. Journal of Structural Engineering, 137(2), 252-260.

Kim, S. J., Holub, C. J., & Elnashai, A. S. (2011). Experimental investigation of the behavior of RC bridge piers subjected to horizontal and vertical earthquake motion. Engineering Structures, 33(7), 2221-2235.

Kunnath S.K., Erduran E, Chai YH, Yashinsky M. Effect of near–fault vertical ground motions on seismic response of highway overcrossings. J Bridge Eng, ASCE 2008;13(3):282–90.

Kunnath, S. K., Abrahamson, N., Chai, Y.H. (2008). Development of guidelines for incorporation of vertical ground motion effects in seismic design of highway bridges. California Department of Transportation, Sacramento, California.

Marafi, N. A., Eberhard, M. O., Berman, J. W., Wirth, E. A., & Frankel, A. D. (2017). Effects of deep basins on structural collapse during large subduction earthquakes. Earthquake Spectra, 33(3), 963-997.

Midorikawa, S., Miura, H., & Si, H. (2012). Preliminary analysis for characteristics of strong ground motion from gigantic earthquakes. In Proceedings of the 15th World Conference on Earthquake Engineering. Tokyo, Japan: International Association for Earthquake Engineering.

National Research Institute for Earth Science and Disaster Resilience (2019), NIED K-NET, KiK-net, National Research Institute for Earth Science and Disaster Resilience, doi:10.17598/NIED.0004

Oregon Department of Transportation. (2020). Bridge Design Manual, Salem, Oregon.

Papazoglou, A. J., & Elnashai, A. S. (1996). Analytical and field evidence of the damaging effect of vertical earthquake ground motion. Earthquake Engineering & Structural Dynamics, 25(10), 1109-1137.

SeismoSignal (2021). Strong Motion Data Signal Processor [Computer software]. https://seismosoft.com/

State of California Department of Transportation, Caltrans Seismic Design Criteria Version 2.0, April 2019

Washington Department of Transportation. (2019). Bridge Design Manual (LRFD), Olympia, Washington.

# APPENDIX A:

## NON-BASIN RECORDED RSA DATA
## JAPAN & CHILE

| EQ | Station |
|---|---|
| Illapel 8.4 | 2051 |

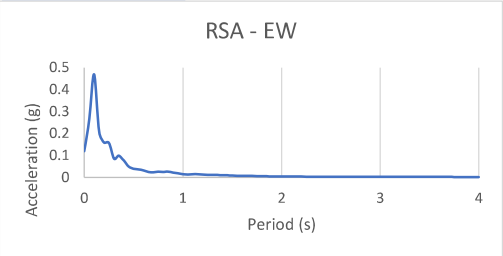


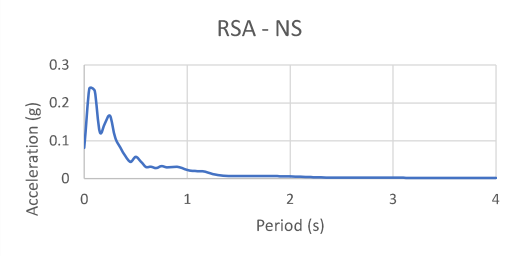


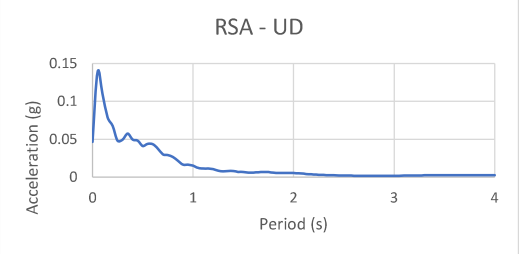


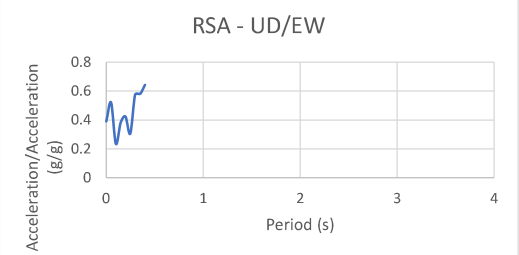


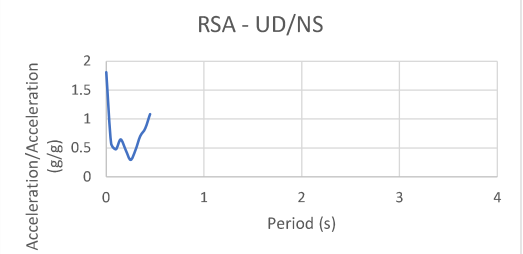


| | |
|---|---|
| Max UD (g) | 0.139 |
| Per Max UD (s) | 0.05 |
| Max UD/EW (g) | 0.643 |
| Per Max UD/EW (s) | 0.40 |
| Max UD/NS (g) | 1.807 |
| Per Max UD/NS (s) | 0.00 |

| RSA - EW | | RSA - NS | | MAX( EW, NS) | |
|---|---|---|---|---|---|
| PGA = | 0.119 | PGA = | 0.082 | PGA = | 0.119 |
| Ss = | 0.159 | Ss = | 0.147 | Ss = | 0.159 |
| S1 = | 0.015 | S1 = | 0.023 | S1 = | 0.023 |

| EQ | Station |
|---|---|
| Iquique 7.6 | 480 |

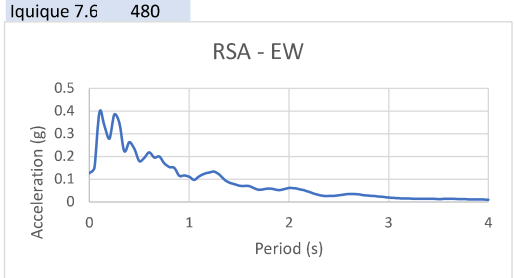


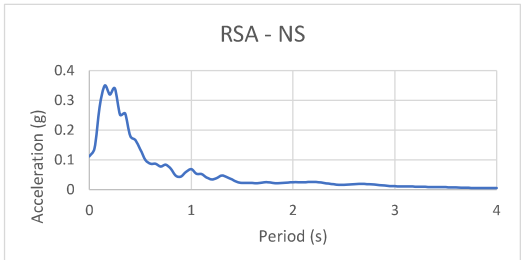


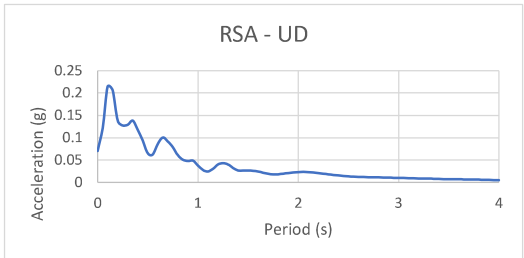


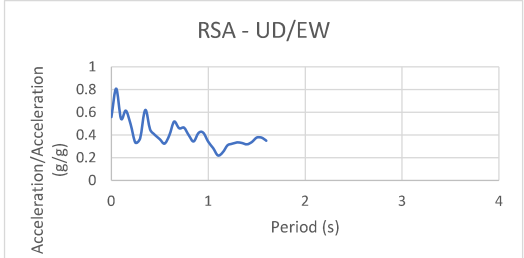


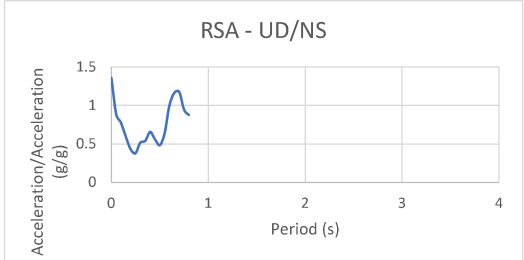


| | |
|---|---|
| Max UD (g) | 0.214 |
| Per Max UD (s) | 0.10 |
| Max UD/EW (g) | 0.808 |
| Per Max UD/EW (s) | 0.05 |
| Max UD/NS (g) | 1.358 |
| Per Max UD/NS (s) | 0.00 |

| RSA - EW | | RSA - NS | | MAX( EW, NS) | |
|---|---|---|---|---|---|
| PGA = | 0.126 | PGA = | 0.112 | PGA = | 0.126 |
| Ss = | 0.279 | Ss = | 0.320 | Ss = | 0.320 |
| S1 = | 0.111 | S1 = | 0.069 | S1 = | 0.111 |

| EQ | Station |
|---|---|
| Iquique 7.6 | 494 |

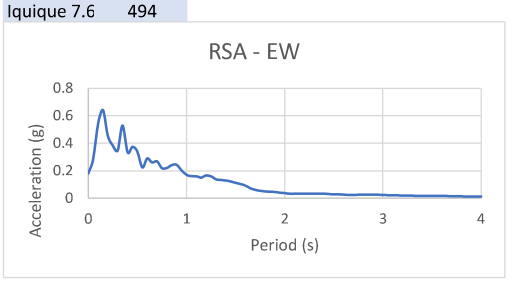


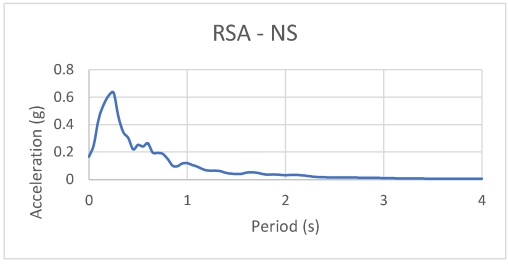


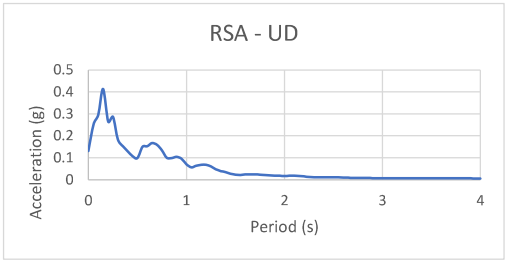


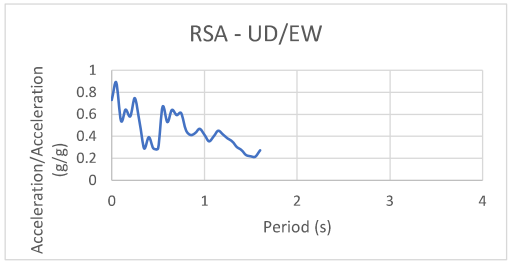


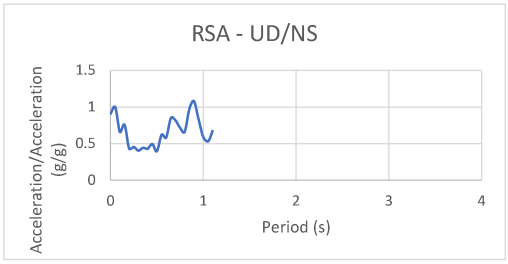


| | |
|---|---|
| Max UD (g) | 0.413 |
| Per Max UD (s) | 0.15 |
| Max UD/EW (g) | 0.890 |
| Per Max UD/EW (s) | 0.05 |
| Max UD/NS (g) | 0.996 |
| Per Max UD/NS (s) | 0.05 |

| RSA - EW | | RSA - NS | | MAX( EW, NS) | |
|---|---|---|---|---|---|
| PGA = | 0.180 | PGA = | 0.167 | PGA = | 0.180 |
| Ss = | 0.455 | Ss = | 0.609 | Ss = | 0.609 |
| S1 = | 0.171 | S1 = | 0.120 | S1 = | 0.171 |

| EQ | Station |
|---|---|
| Iquique 8.2 | 337 |

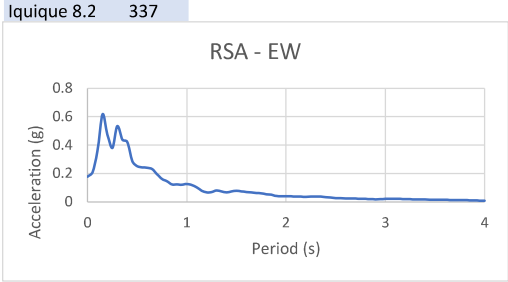


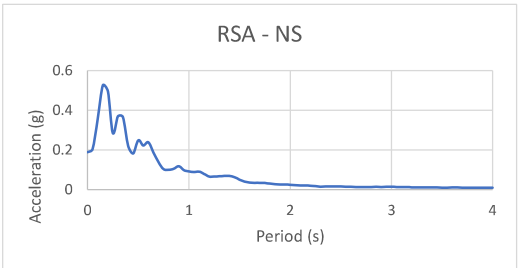


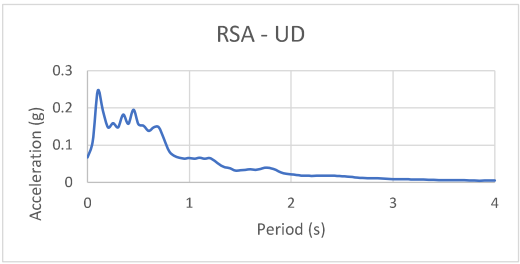


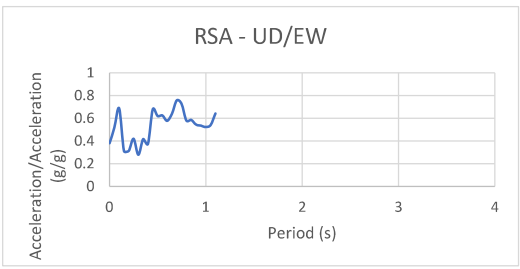


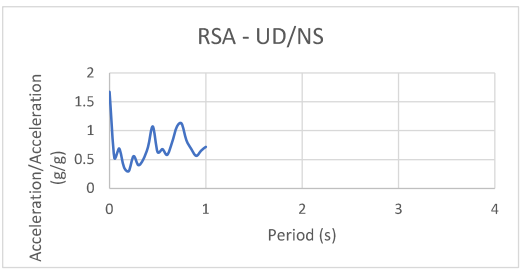


| | |
|---|---|
| Max UD (g) | 0.246 |
| Per Max UD (s) | 0.10 |
| Max UD/EW (g) | 0.758 |
| Per Max UD/EW (s) | 0.70 |
| Max UD/NS (g) | 1.673 |
| Per Max UD/NS (s) | 0.00 |

| RSA - EW | | RSA - NS | | MAX( EW, NS) | |
|---|---|---|---|---|---|
| PGA = | 0.177 | PGA = | 0.189 | PGA = | 0.189 |
| Ss = | 0.475 | Ss = | 0.495 | Ss = | 0.495 |
| S1 = | 0.126 | S1 = | 0.092 | S1 = | 0.126 |

| EQ | Station |
|---|---|
| Iquique 7.6 | 481 |

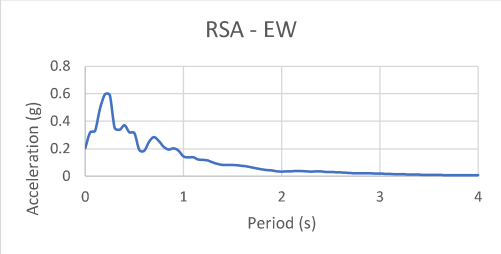


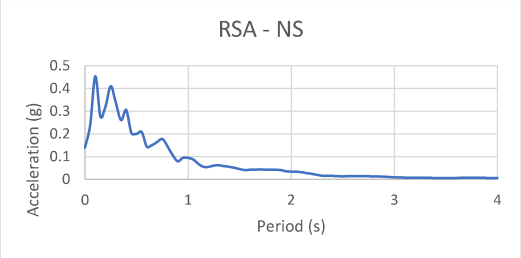


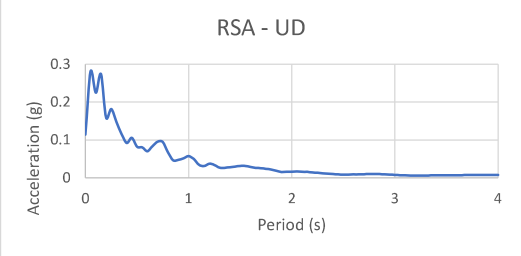


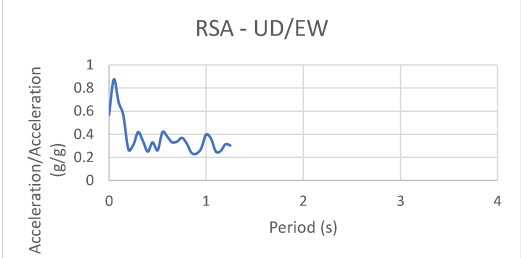


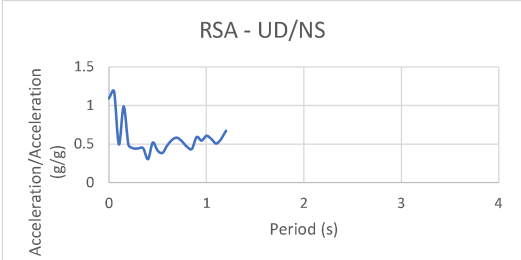


| | |
|---|---|
| Max UD (g) | 0.281 |
| Per Max UD (s) | 0.05 |
| Max UD/EW (g) | 0.877 |
| Per Max UD/EW (s) | 0.05 |
| Max UD/NS (g) | 1.183 |
| Per Max UD/NS (s) | 0.05 |

| RSA - EW | | RSA - NS | | MAX( EW, NS) | |
|---|---|---|---|---|---|
| PGA = | 0.202 | PGA = | 0.139 | PGA = | 0.202 |
| Ss = | 0.597 | Ss = | 0.325 | Ss = | 0.597 |
| S1 = | 0.144 | S1 = | 0.094 | S1 = | 0.144 |

| EQ | Station |
|---|---|
| Iquique 7.6 | 472 |

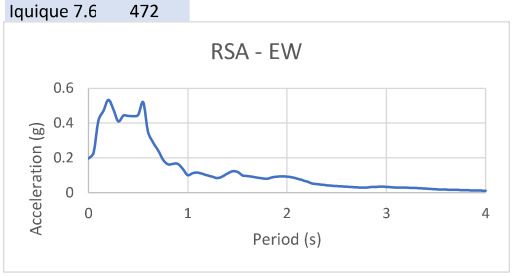


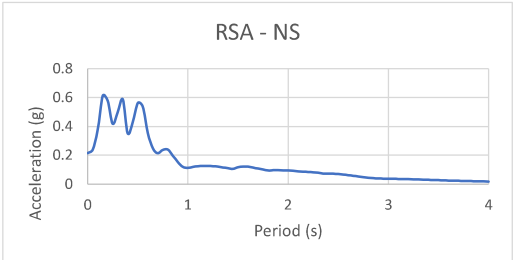


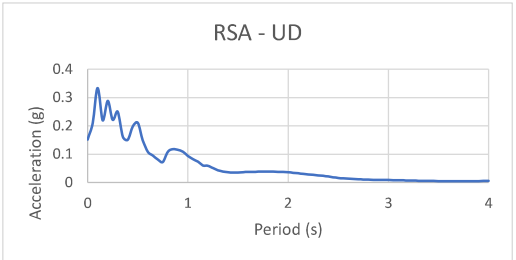


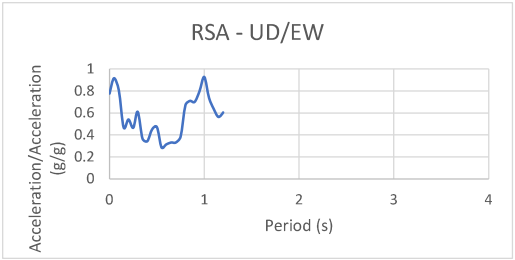


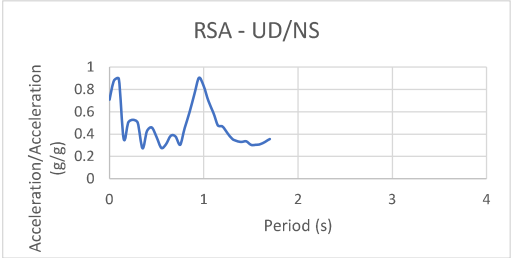


| | |
|---|---|
| Max UD (g) | 0.333 |
| Per Max UD (s) | 0.10 |
| Max UD/EW (g) | 0.927 |
| Per Max UD/EW (s) | 1.00 |
| Max UD/NS (g) | 0.904 |
| Per Max UD/NS (s) | 0.95 |

| RSA - EW | | RSA - NS | | MAX( EW, NS) | |
|---|---|---|---|---|---|
| PGA = | 0.196 | PGA = | 0.214 | PGA = | 0.214 |
| Ss = | 0.534 | Ss = | 0.576 | Ss = | 0.576 |
| S1 = | 0.101 | S1 = | 0.113 | S1 = | 0.113 |

| EQ | Station |
|---|---|
| Tohoku 9.0 | FKS014 |

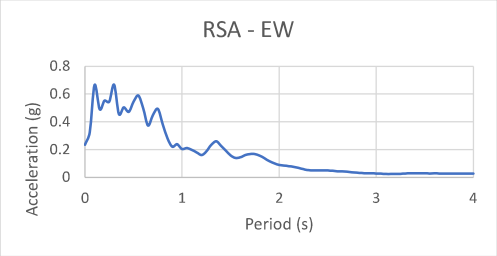


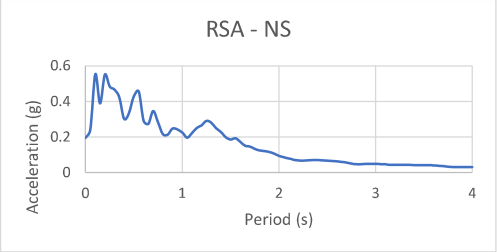


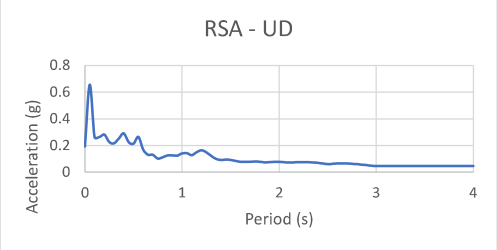


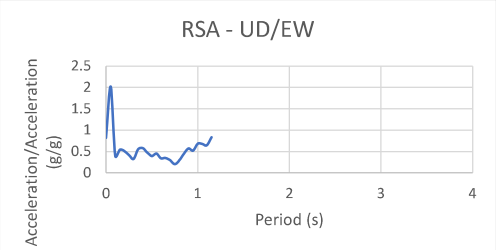


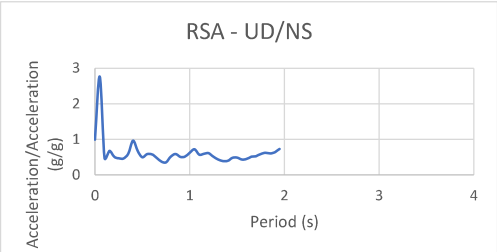


| | |
|---|---|
| Max UD (g) | 0.656 |
| Per Max UD (s) | 0.05 |
| Max UD/EW (g) | 2.020 |
| Per Max UD/EW (s) | 0.05 |
| Max UD/NS (g) | 2.765 |
| Per Max UD/NS (s) | 0.05 |

| RSA - EW | | RSA - NS | | MAX( EW, NS) | |
|---|---|---|---|---|---|
| PGA = | 0.235 | PGA = | 0.194 | PGA = | 0.235 |
| Ss = | 0.552 | Ss = | 0.550 | Ss = | 0.552 |
| S1 = | 0.205 | S1 = | 0.225 | S1 = | 0.225 |

| EQ | Station |
|---|---|
| Iquique 7.6 | 478 |

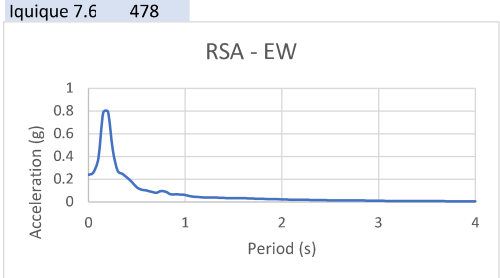


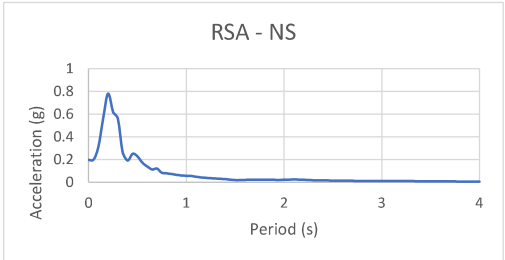


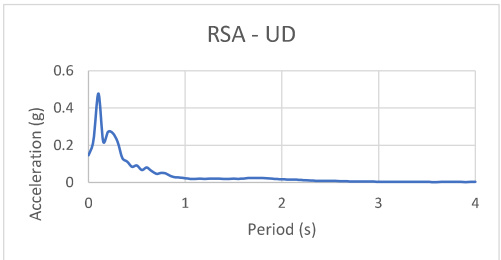


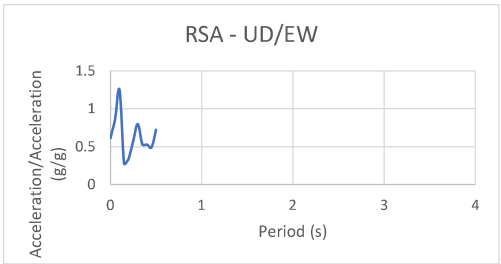


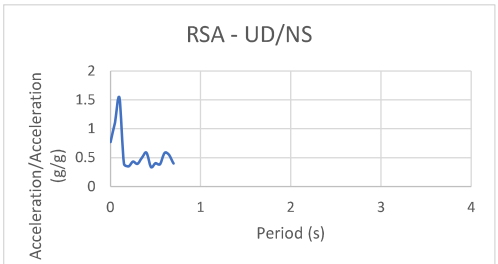


| | |
|---|---|
| Max UD (g) | 0.479 |
| Per Max UD (s) | 0.10 |
| Max UD/EW (g) | 1.251 |
| Per Max UD/EW (s) | 0.10 |
| Max UD/NS (g) | 1.534 |
| Per Max UD/NS (s) | 0.10 |

| RSA - EW | | RSA - NS | | MAX( EW, NS) | |
|---|---|---|---|---|---|
| PGA = | 0.239 | PGA = | 0.197 | PGA = | 0.239 |
| Ss = | 0.794 | Ss = | 0.780 | Ss = | 0.794 |
| S1 = | 0.060 | S1 = | 0.058 | S1 = | 0.060 |

| EQ | Station |
|---|---|
| Iquique 8.2 | 352 |

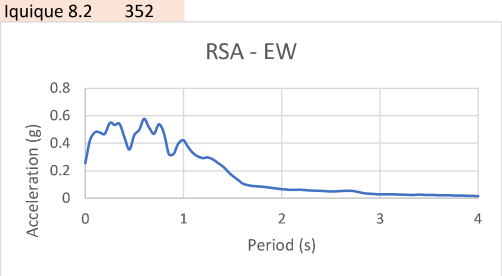


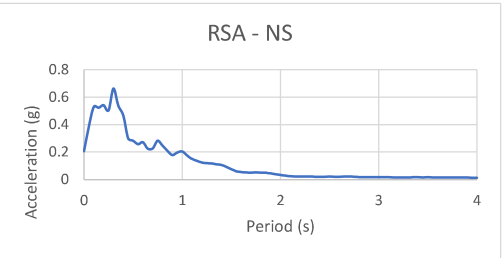


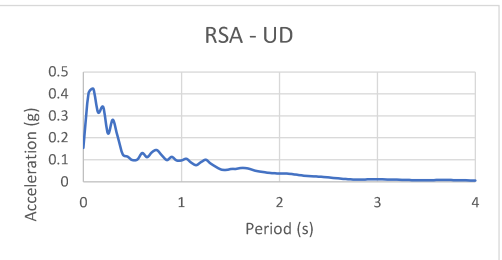


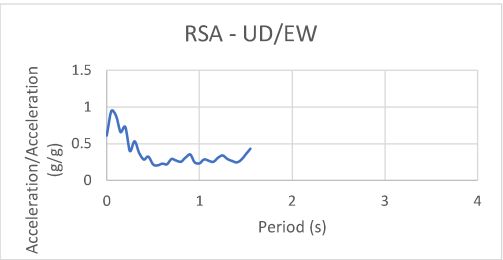


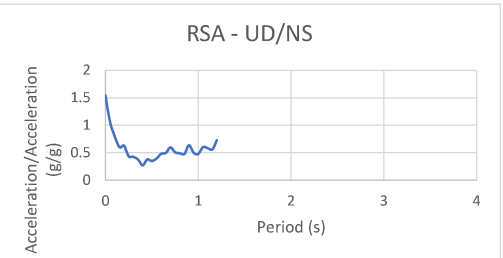


| | |
|---|---|
| Max UD (g) | 0.424 |
| Per Max UD (s) | 0.10 |
| Max UD/EW (g) | 0.944 |
| Per Max UD/EW (s) | 0.05 |
| Max UD/NS (g) | 1.542 |
| Per Max UD/NS (s) | 0.00 |

| RSA - EW | | RSA - NS | | MAX( EW, NS) | |
|---|---|---|---|---|---|
| PGA = | 0.253 | PGA = | 0.205 | PGA = | 0.253 |
| Ss = | 0.468 | Ss = | 0.541 | Ss = | 0.541 |
| S1 = | 0.422 | S1 = | 0.204 | S1 = | 0.422 |

| EQ | Station |
|---|---|
| Iquique 8.2 | 351 |

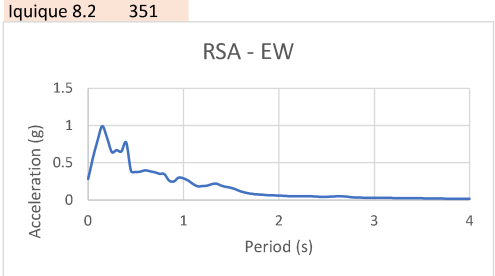


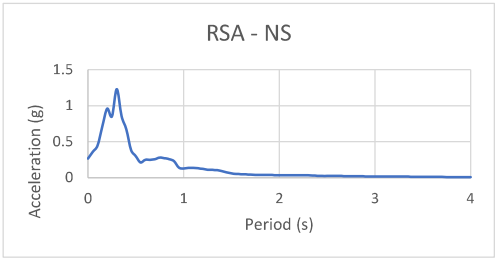


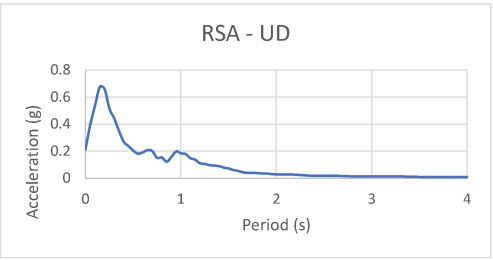


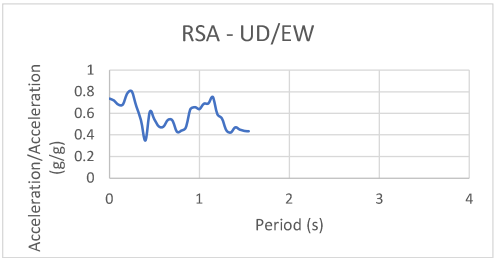


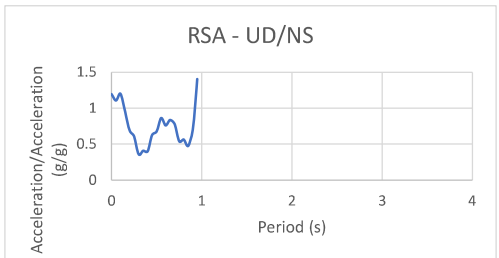


| | |
|---|---|
| Max UD (g) | 0.675 |
| Per Max UD (s) | 0.15 |
| Max UD/EW (g) | 0.800 |
| Per Max UD/EW (s) | 0.25 |
| Max UD/NS (g) | 1.406 |
| Per Max UD/NS (s) | 0.95 |

| RSA - EW | | RSA - NS | | MAX( EW, NS) | |
|---|---|---|---|---|---|
| PGA = | 0.284 | PGA = | 0.265 | PGA = | 0.284 |
| Ss = | 0.838 | Ss = | 0.959 | Ss = | 0.959 |
| S1 = | 0.289 | S1 = | 0.127 | S1 = | 0.289 |

| EQ | Station |
|---|---|
| Illapel 8.4 | 2023 |

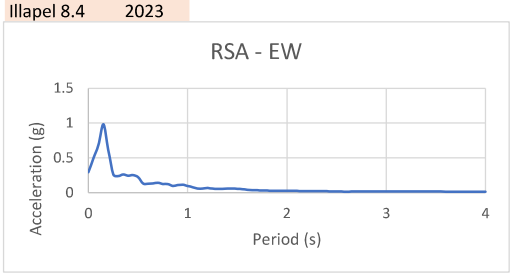


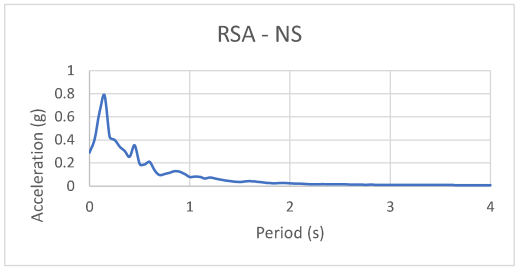


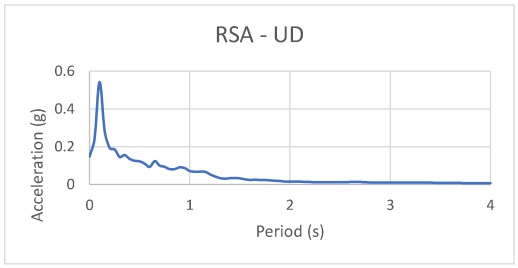


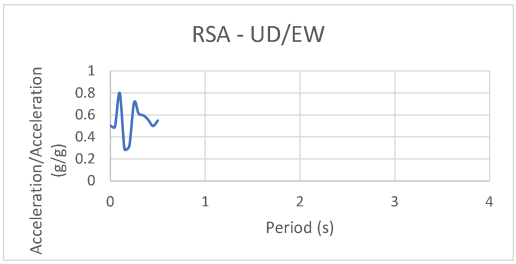


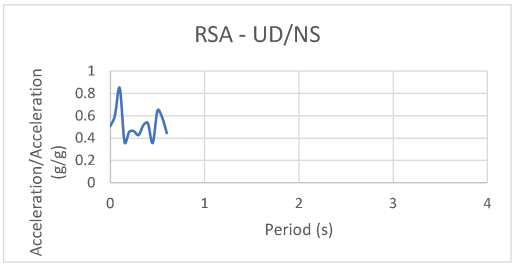


| | |
|---|---|
| Max UD (g) | 0.542 |
| Per Max UD (s) | 0.10 |
| Max UD/EW (g) | 0.798 |
| Per Max UD/EW (s) | 0.10 |
| 0 | 0 |
| Max UD/NS (g) | 0.848 |
| Per Max UD/NS (s) | 0.10 |

| RSA - EW | | RSA - NS | | MAX( EW, NS) | |
|---|---|---|---|---|---|
| PGA = | 0.295 | PGA = | 0.292 | PGA = | 0.295 |
| Ss = | 0.616 | Ss = | 0.428 | Ss = | 0.616 |
| S1 = | 0.096 | S1 = | 0.079 | S1 = | 0.096 |

| EQ | Station |
|---|---|
| Tohoku 9.0 | IWTH22 |

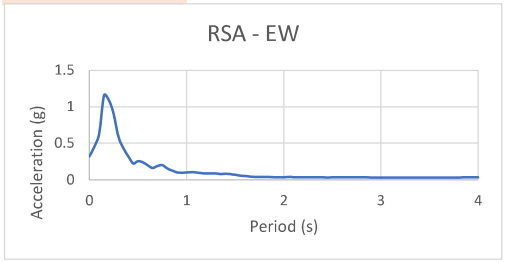


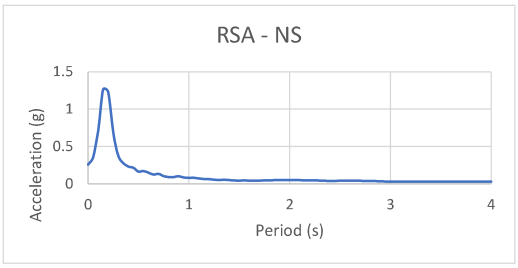


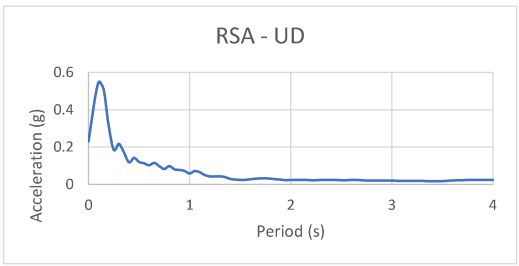


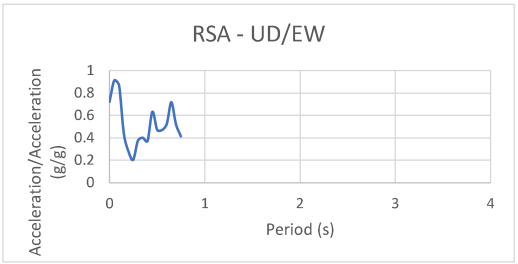


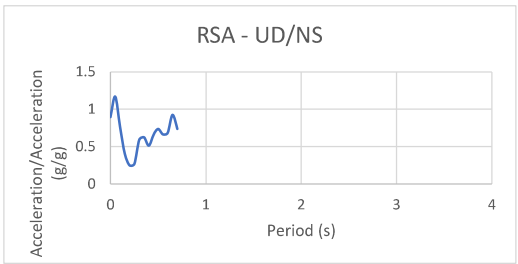


| | |
|---|---|
| Max UD (g) | 0.550 |
| Per Max UD (s) | 0.10 |
| Max UD/EW (g) | 0.914 |
| Per Max UD/EW (s) | 0.05 |
| Max UD/NS (g) | 1.170 |
| Per Max UD/NS (s) | 0.05 |

| RSA - EW | | RSA - NS | | MAX( EW, NS) | |
|---|---|---|---|---|---|
| PGA = | 0.320 | PGA = | 0.257 | PGA = | 0.320 |
| Ss = | 1.092 | Ss = | 1.228 | Ss = | 1.228 |
| S1 = | 0.101 | S1 = | 0.079 | S1 = | 0.101 |

| EQ | Station |
|---|---|
| Illapel 8.4 | 2031 |

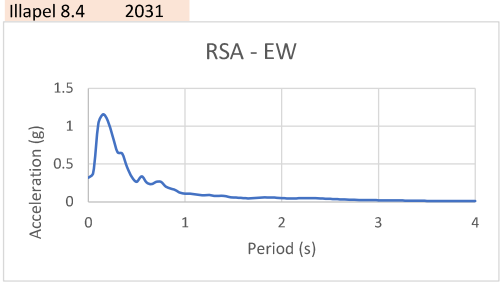


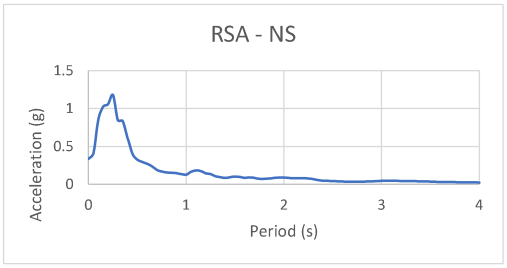


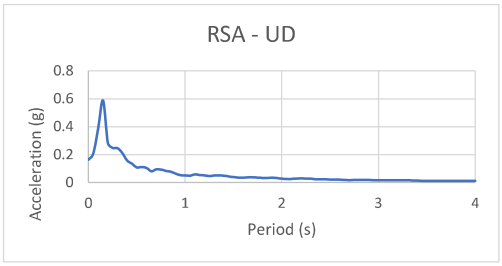


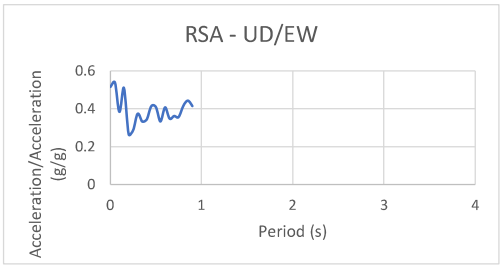


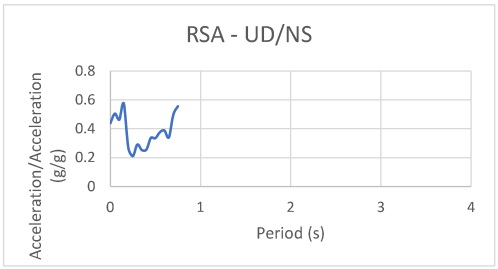


| | |
|---|---|
| Max UD (g) | 0.588 |
| Per Max UD (s) | 0.15 |
| Max UD/EW (g) | 0.539 |
| Per Max UD/EW (s) | 0.05 |
| Max UD/NS (g) | 0.574 |
| Per Max UD/NS (s) | 0.15 |

| RSA - EW | | RSA - NS | | MAX( EW, NS) | |
|---|---|---|---|---|---|
| PGA = | 0.317 | PGA = | 0.336 | PGA = | 0.336 |
| Ss = | 1.068 | Ss = | 1.056 | Ss = | 1.068 |
| S1 = | 0.109 | S1 = | 0.128 | S1 = | 0.128 |

| EQ | Station |
|---|---|
| Tohoku 9.0 | IWT008 |

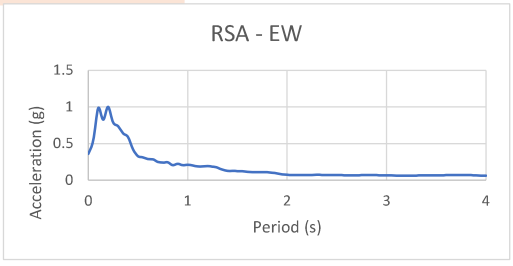


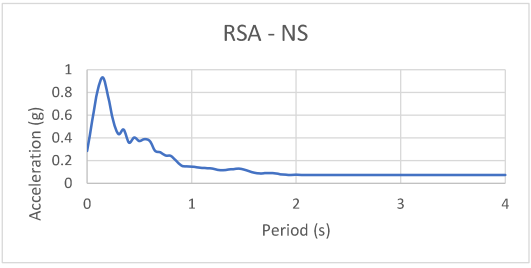


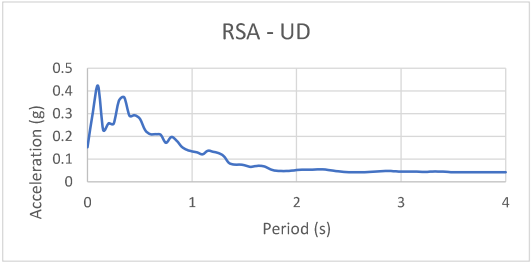


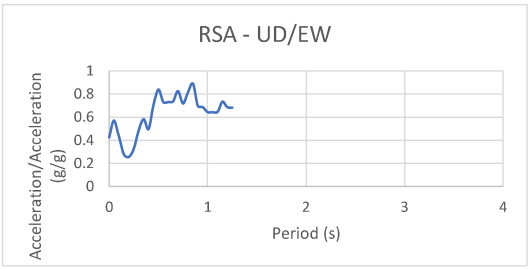


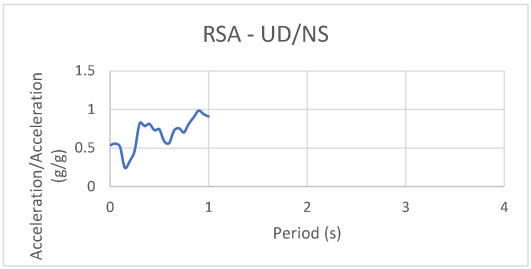


| | |
|---|---|
| Max UD (g) | 0.423 |
| Per Max UD (s) | 0.10 |
| Max UD/EW (g) | 0.890 |
| Per Max UD/EW (s) | 0.85 |
| Max UD/NS (g) | 0.984 |
| Per Max UD/NS (s) | 0.90 |

| RSA - EW | | RSA - NS | | MAX( EW, NS) | |
|---|---|---|---|---|---|
| PGA = | 0.359 | PGA = | 0.286 | PGA = | 0.359 |
| Ss = | 1.002 | Ss = | 0.774 | Ss = | 1.002 |
| S1 = | 0.209 | S1 = | 0.148 | S1 = | 0.209 |

| EQ | Station |
|---|---|
| Tohoku 9.0 | IWTH18 |

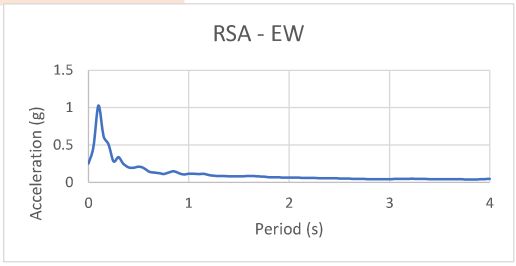


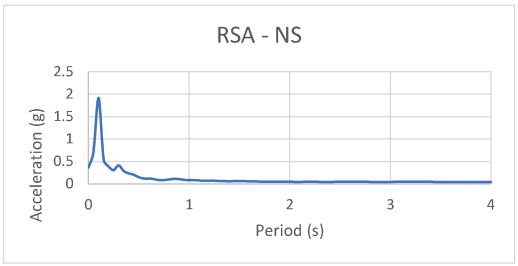


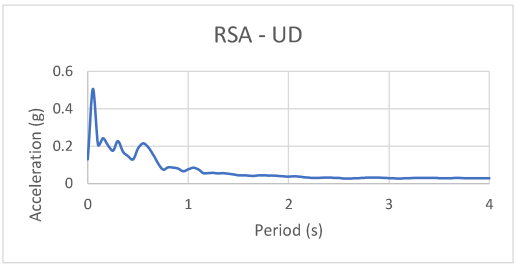


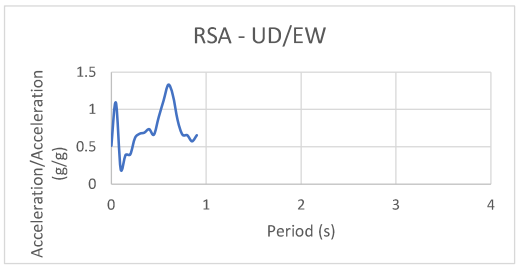


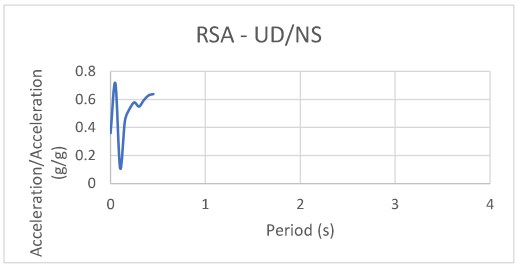


| | |
|---|---|
| Max UD (g) | 0.507 |
| Per Max UD (s) | 0.05 |
| Max UD/EW (g) | 1.332 |
| Per Max UD/EW (s) | 0.60 |
| Max UD/NS (g) | 0.716 |
| Per Max UD/NS (s) | 0.05 |

| RSA - EW | | RSA - NS | | MAX( EW, NS) | |
|---|---|---|---|---|---|
| PGA = | 0.252 | PGA = | 0.361 | PGA = | 0.361 |
| Ss = | 0.514 | Ss = | 0.388 | Ss = | 0.514 |
| S1 = | 0.115 | S1 = | 0.085 | S1 = | 0.115 |

| EQ | Station |
|---|---|
| Iquique 8.2 | 335 |

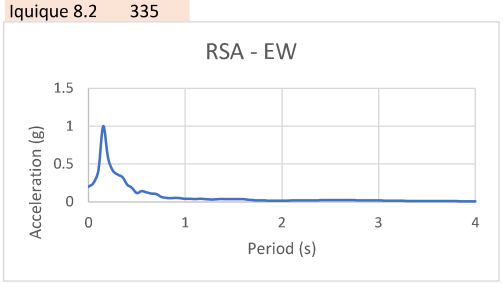


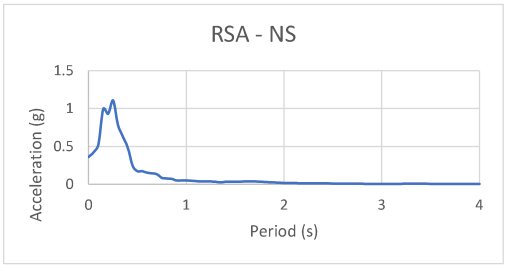


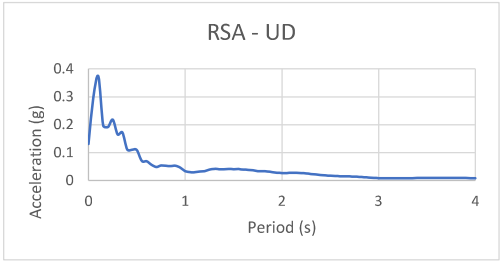


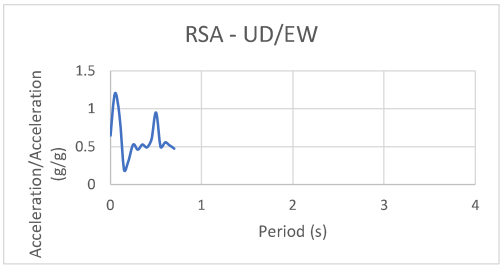


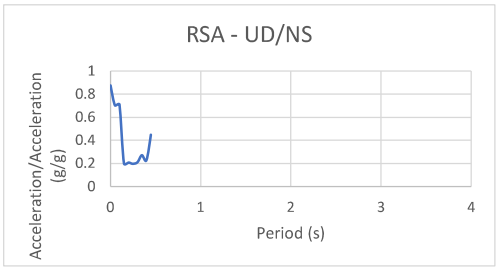


| | |
|---|---|
| Max UD (g) | 0.372 |
| Per Max UD (s) | 0.10 |
| Max UD/EW (g) | 1.204 |
| Per Max UD/EW (s) | 0.05 |
| Max UD/NS (g) | 0.877 |
| Per Max UD/NS (s) | 0.00 |

| RSA - EW | | RSA - NS | | MAX( EW, NS) | |
|---|---|---|---|---|---|
| PGA = | 0.202 | PGA = | 0.361 | PGA = | 0.361 |
| Ss = | 0.587 | Ss = | 0.928 | Ss = | 0.928 |
| S1 = | 0.041 | S1 = | 0.050 | S1 = | 0.050 |

| EQ | Station |
|---|---|
| Iquique 7.6 | 492 |

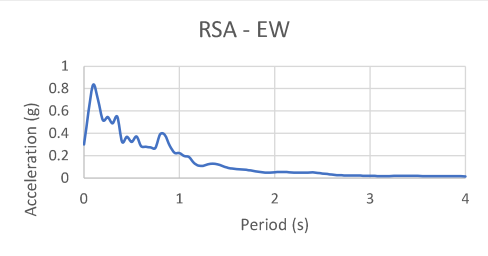


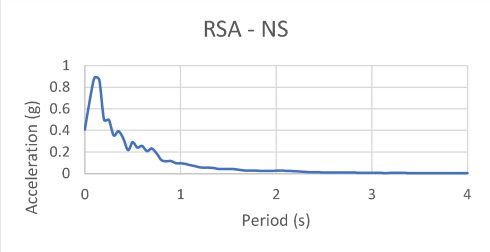


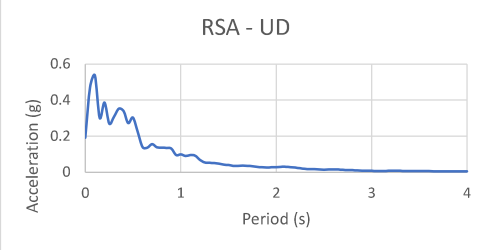


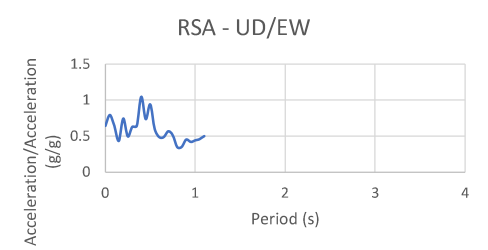


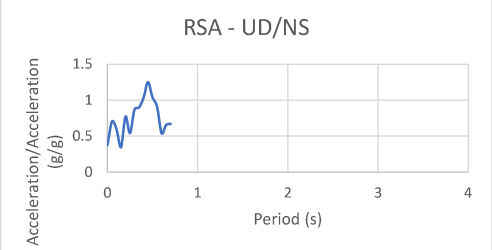


| | |
|---|---|
| Max UD (g) | 0.537 |
| Per Max UD (s) | 0.10 |
| Max UD/EW (g) | 1.044 |
| Per Max UD/EW (s) | 0.40 |
| Max UD/NS (g) | 1.250 |
| Per Max UD/NS (s) | 0.45 |

| RSA - EW | | RSA - NS | | MAX( EW, NS) | |
|---|---|---|---|---|---|
| PGA = | 0.299 | PGA = | 0.408 | PGA = | 0.408 |
| Ss = | 0.518 | Ss = | 0.498 | Ss = | 0.518 |
| S1 = | 0.223 | S1 = | 0.096 | S1 = | 0.223 |

| EQ | Station |
|---|---|
| Miyagi 7.1 | IWTH21 |

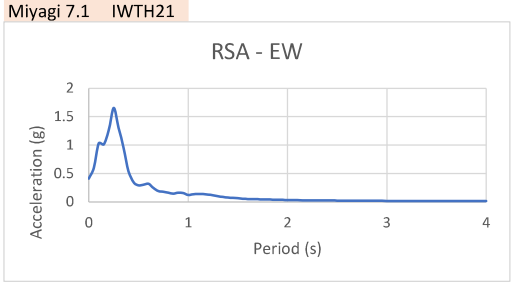


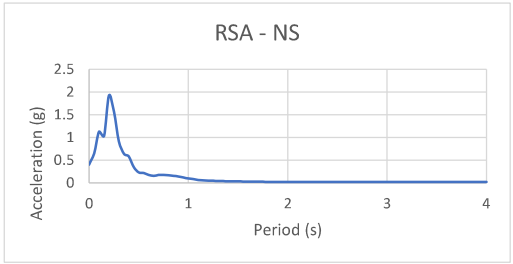


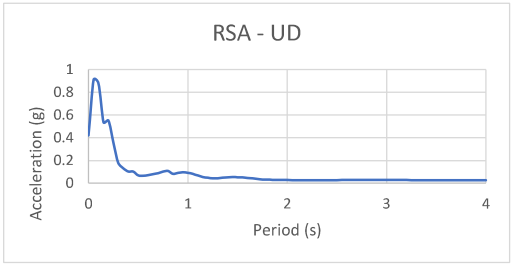


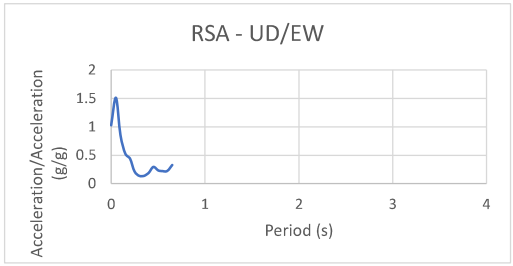


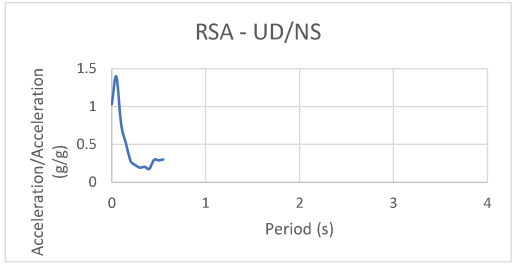


| | |
|---|---|
| Max UD (g) | 0.911 |
| Per Max UD (s) | 0.05 |
| Max UD/EW (g) | 1.512 |
| Per Max UD/EW (s) | 0.05 |
| Max UD/NS (g) | 1.397 |
| Per Max UD/NS (s) | 0.05 |

| RSA - EW | | RSA - NS | | MAX( EW, NS) | |
|---|---|---|---|---|---|
| PGA = | 0.409 | PGA = | 0.408 | PGA = | 0.409 |
| Ss = | 1.256 | Ss = | 1.925 | Ss = | 1.925 |
| S1 = | 0.120 | S1 = | 0.099 | S1 = | 0.120 |

| EQ | Station |
|---|---|
| Tohoku 9.0 | IBRH14 |

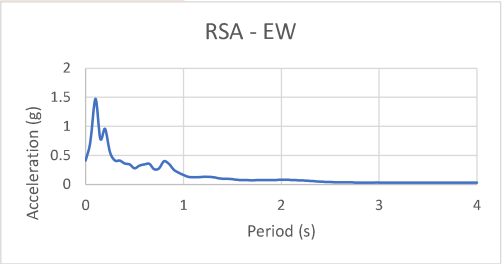


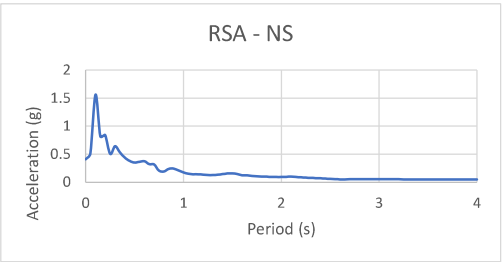


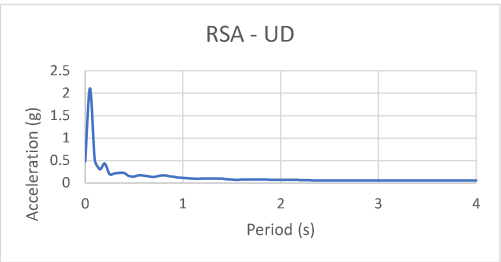


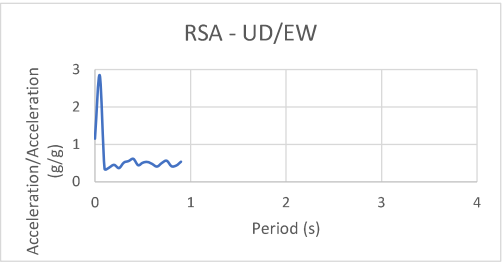


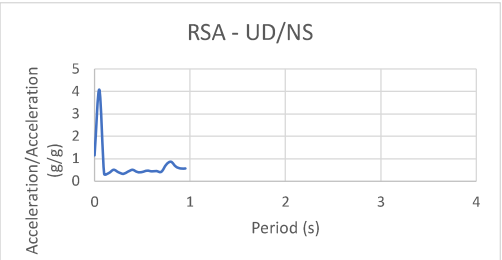


| | |
|---|---|
| Max UD (g) | 2.113 |
| Per Max UD (s) | 0.05 |
| Max UD/EW (g) | 2.845 |
| Per Max UD/EW (s) | 0.05 |
| Max UD/NS (g) | 4.077 |
| Per Max UD/NS (s) | 0.05 |

| RSA - EW | | RSA - NS | | MAX( EW, NS) | |
|---|---|---|---|---|---|
| PGA = | 0.413 | PGA = | 0.412 | PGA = | 0.413 |
| Ss = | 0.954 | Ss = | 0.843 | Ss = | 0.954 |
| S1 = | 0.162 | S1 = | 0.174 | S1 = | 0.174 |

| EQ | Station |
|---|---|
| Iquique 8.2 | 348 |

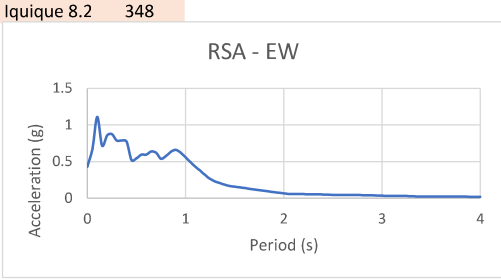


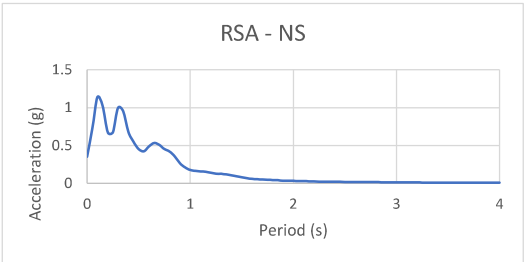


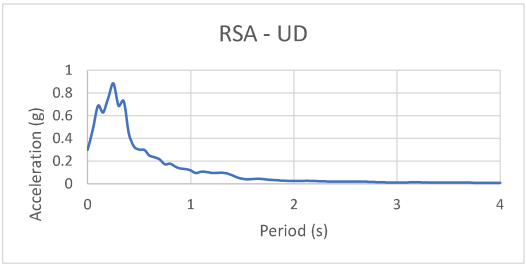


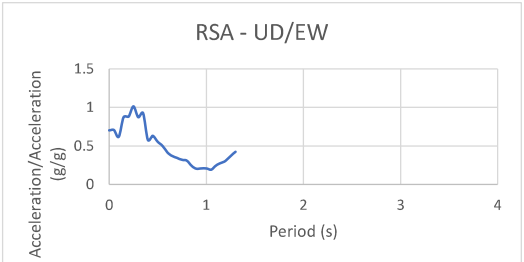


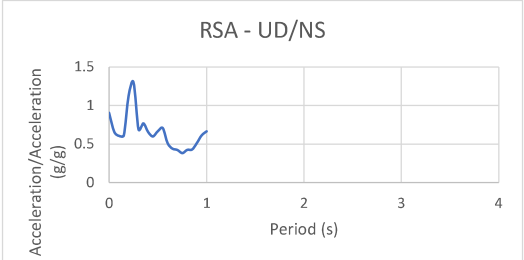


| | |
|---|---|
| Max UD (g) | 0.884 |
| Per Max UD (s) | 0.25 |
| Max UD/EW (g) | 1.014 |
| Per Max UD/EW (s) | 0.25 |
| Max UD/NS (g) | 1.303 |
| Per Max UD/NS (s) | 0.25 |

| RSA - EW | | RSA - NS | | MAX( EW, NS) | |
|---|---|---|---|---|---|
| PGA = | 0.427 | PGA = | 0.350 | PGA = | 0.427 |
| Ss = | 0.857 | Ss = | 0.673 | Ss = | 0.857 |
| S1 = | 0.557 | S1 = | 0.177 | S1 = | 0.557 |

| EQ | Station |
|---|---|
| Tohoku 9.0 | IWTH21 |

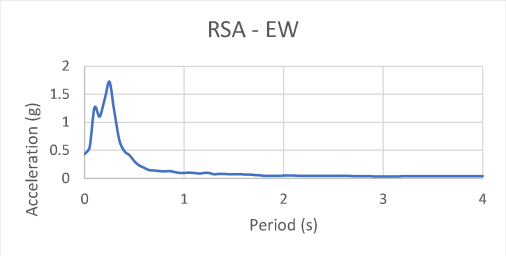


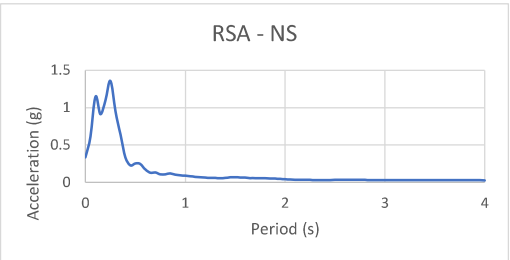


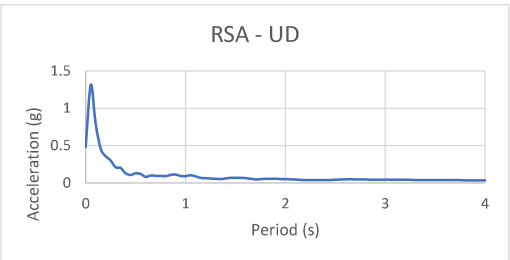


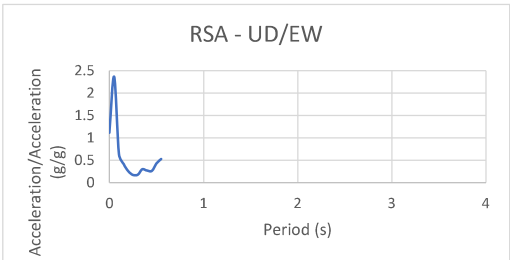


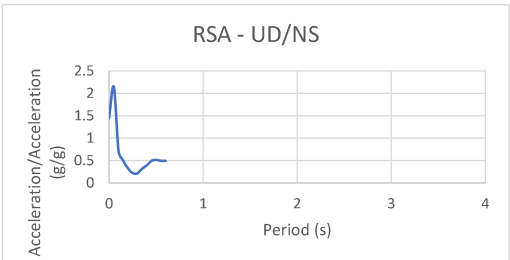


| | |
|---|---|
| Max UD (g) | 1.315 |
| Per Max UD (s) | 0.05 |
| Max UD/EW (g) | 2.362 |
| Per Max UD/EW (s) | 0.05 |
| Max UD/NS (g) | 2.143 |
| Per Max UD/NS (s) | 0.05 |

| RSA - EW | | RSA - NS | | MAX( EW, NS) | |
|---|---|---|---|---|---|
| PGA = | 0.431 | PGA = | 0.334 | PGA = | 0.431 |
| Ss = | 1.394 | Ss = | 1.099 | Ss = | 1.394 |
| S1 = | 0.099 | S1 = | 0.088 | S1 = | 0.099 |

| EQ | Station |
|---|---|
| Miyagi 7.1 | IWTH28 |

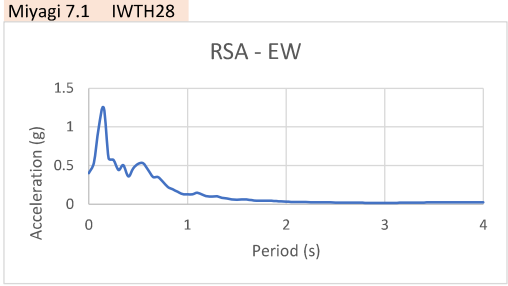


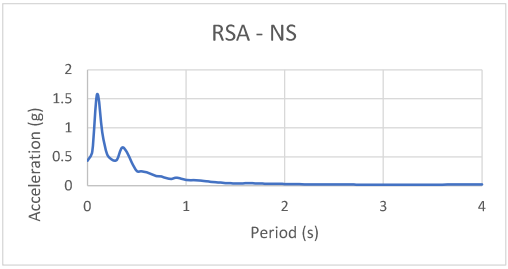


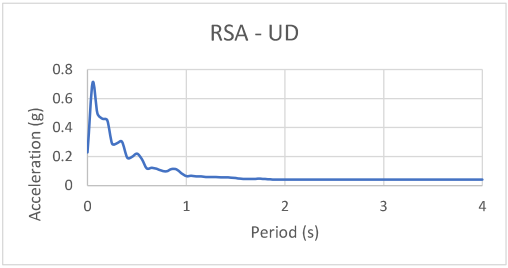


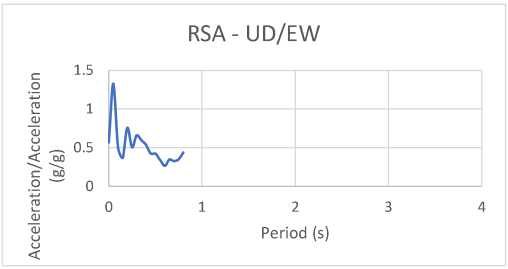


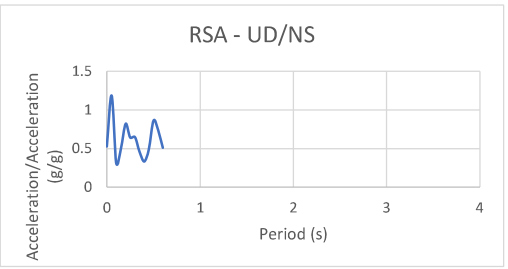


| | |
|---|---|
| Max UD (g) | 0.710 |
| Per Max UD (s) | 0.05 |
| Max UD/EW (g) | 1.328 |
| | |
| Max UD/NS (g) | 1.188 |
| Per Max UD/NS (s) | 0.05 |

| RSA - EW | | RSA - NS | | MAX( EW, NS) | |
|---|---|---|---|---|---|
| PGA = | 0.403 | PGA = | 0.432 | PGA = | 0.432 |
| Ss = | 0.595 | Ss = | 0.548 | Ss = | 0.595 |
| S1 = | 0.127 | S1 = | 0.102 | S1 = | 0.127 |

| EQ | Station |
|---|---|
| Tohoku 9.0 | FKSH09 |

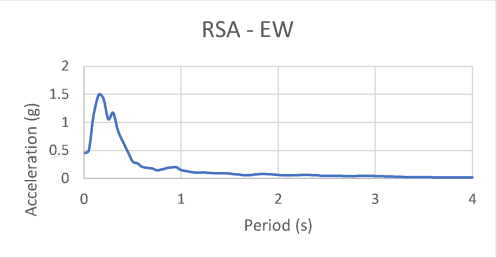


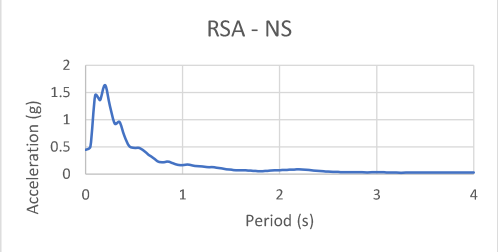


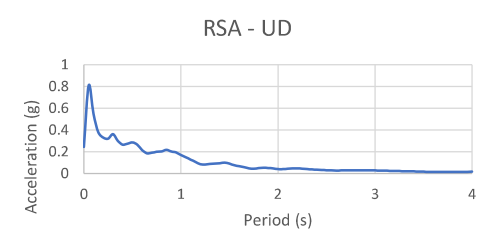


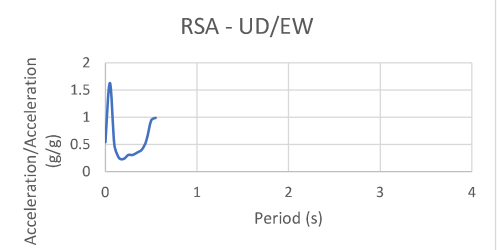


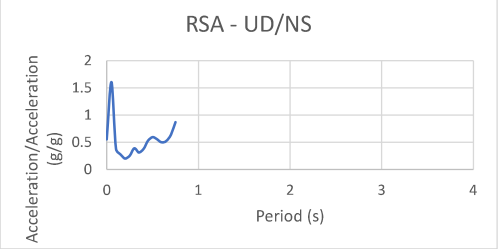


| | |
|---|---|
| Max UD (g) | 0.810 |
| Per Max UD (s) | 0.05 |
| Max UD/EW (g) | 1.630 |
| Per Max UD/EW (s) | 0.05 |
| Max UD/NS (g) | 1.604 |
| Per Max UD/NS (s) | 0.05 |

| RSA - EW | | RSA - NS | | MAX( EW, NS) | |
|---|---|---|---|---|---|
| PGA = | 0.453 | PGA = | 0.444 | PGA = | 0.453 |
| Ss = | 1.419 | Ss = | 1.636 | Ss = | 1.636 |
| S1 = | 0.152 | S1 = | 0.162 | S1 = | 0.162 |

| EQ | Station |
|---|---|
| Tohoku 9.0 | MYGH03 |

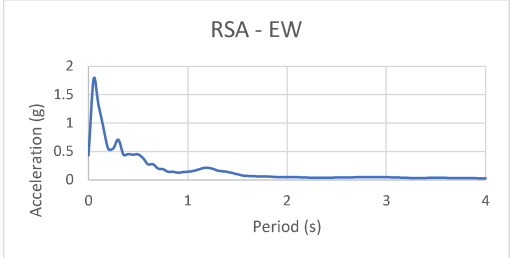


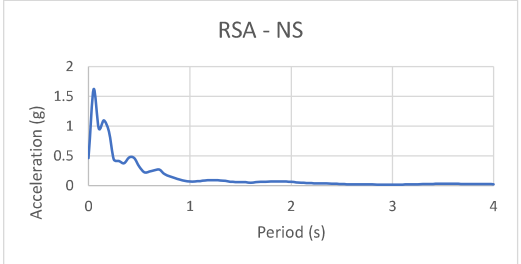


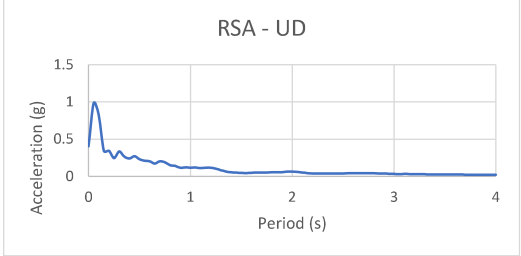


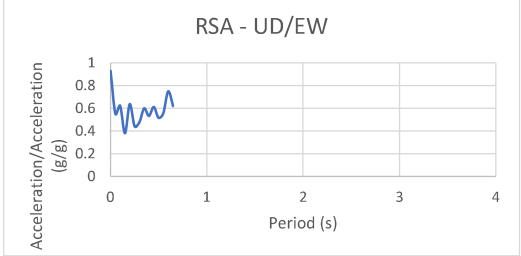


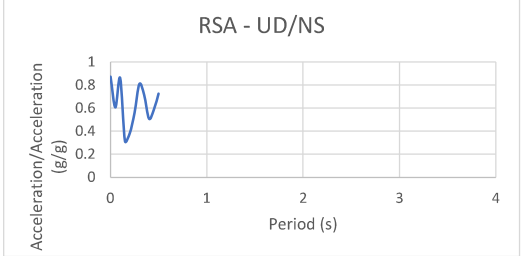


| | |
|---|---|
| Max UD (g) | 0.980 |
| Per Max UD (s) | 0.05 |
| Max UD/EW (g) | 0.930 |
| Per Max UD/EW (s) | 0.00 |
| Max UD/NS (g) | 0.872 |
| Per Max UD/NS (s) | 0.00 |

| RSA - EW | | RSA - NS | | MAX( EW, NS) | |
|---|---|---|---|---|---|
| PGA = | 0.433 | PGA = | 0.462 | PGA = | 0.462 |
| Ss = | 0.542 | Ss = | 0.910 | Ss = | 0.910 |
| S1 = | 0.141 | S1 = | 0.069 | S1 = | 0.141 |

| EQ | Station |
|---|---|
| Iquique 8.2 | 329 |

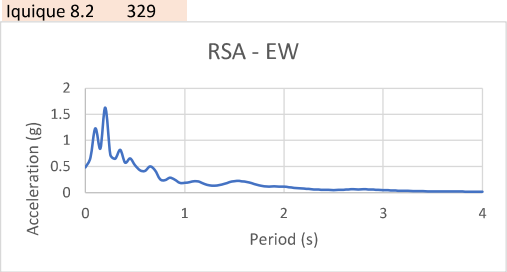


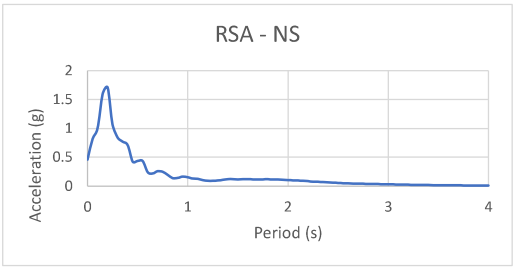


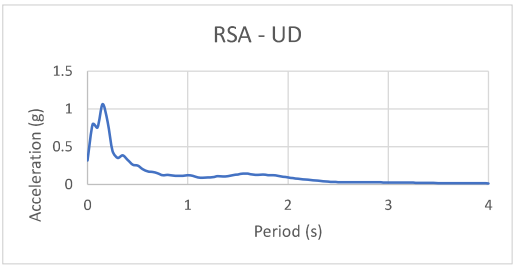


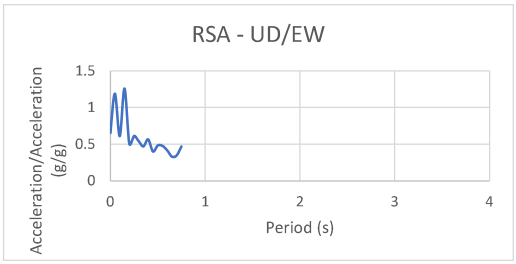


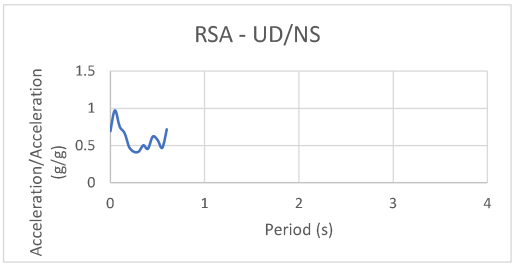


| | |
|---|---|
| Max UD (g) | 1.064 |
| Per Max UD (s) | 0.15 |
| Max UD/EW (g) | 1.259 |
| Per Max UD/EW (s) | 0.15 |
| Max UD/NS (g) | 0.972 |
| Per Max UD/NS (s) | 0.05 |

| RSA - EW | | RSA - NS | | MAX( EW, NS) | |
|---|---|---|---|---|---|
| PGA = | 0.485 | PGA = | 0.458 | PGA = | 0.485 |
| Ss = | 1.631 | Ss = | 1.709 | Ss = | 1.709 |
| S1 = | 0.187 | S1 = | 0.154 | S1 = | 0.187 |

| EQ | Station |
|---|---|
| Tohoku 9.0 | IWTH23 |

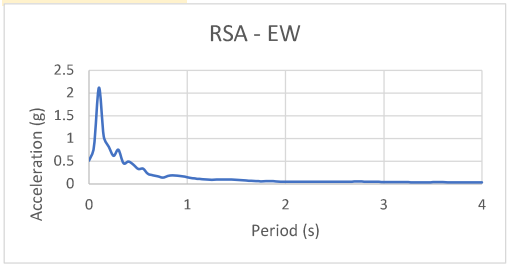


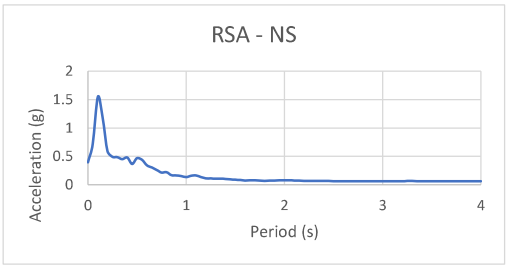


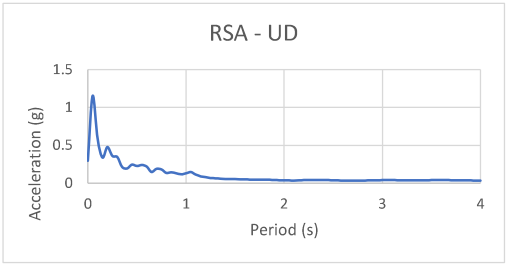


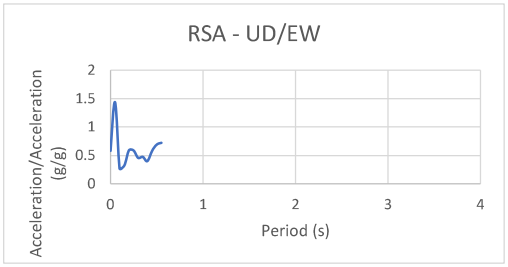


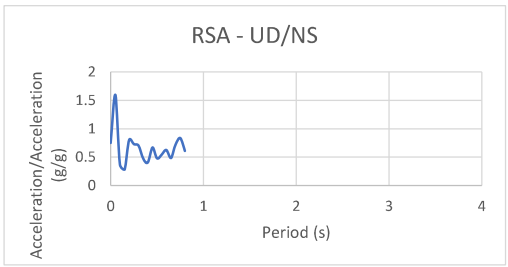


| | |
|---|---|
| Max UD (g) | 1.153 |
| Per Max UD (s) | 0.05 |
| Max UD/EW (g) | 1.437 |
| Per Max UD/EW (s) | 0.05 |
| Max UD/NS (g) | 1.596 |
| Per Max UD/NS (s) | 0.05 |

| RSA - EW | | RSA - NS | | MAX( EW, NS) | |
|---|---|---|---|---|---|
| PGA = | 0.511 | PGA = | 0.397 | PGA = | 0.511 |
| Ss = | 0.812 | Ss = | 0.593 | Ss = | 0.812 |
| S1 = | 0.146 | S1 = | 0.136 | S1 = | 0.146 |

| EQ | Station |
|---|---|
| Tohoku 9.0 | MYGH12 |

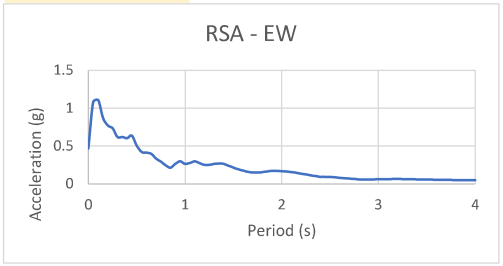


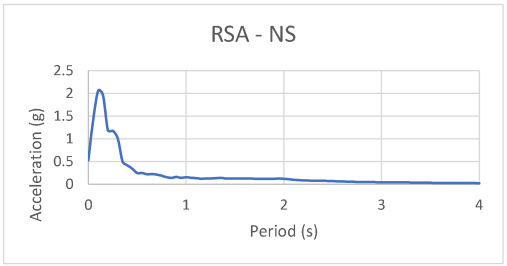


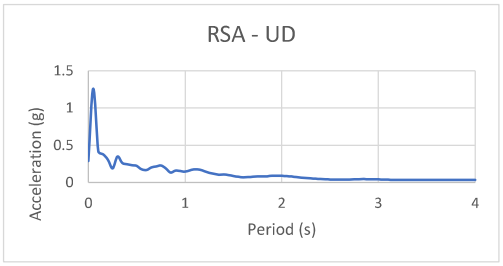


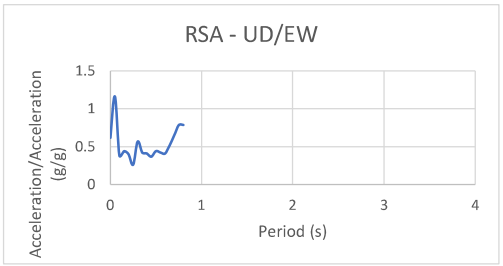


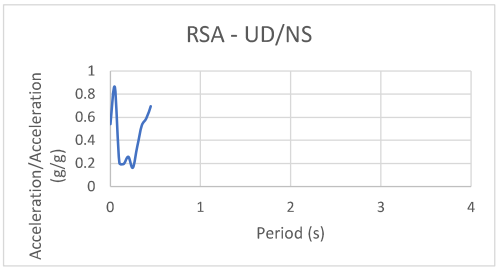


| | |
|---|---|
| Max UD (g) | 1.258 |
| Per Max UD (s) | 0.05 |
| Max UD/EW (g) | 1.164 |
| Per Max UD/EW (s) | 0.05 |
| Max UD/NS (g) | 0.858 |
| Per Max UD/NS (s) | 0.05 |

| RSA - EW | | RSA - NS | | MAX( EW, NS) | |
|---|---|---|---|---|---|
| PGA = | 0.467 | PGA = | 0.531 | PGA = | 0.531 |
| Ss = | 0.770 | Ss = | 1.193 | Ss = | 1.193 |
| S1 = | 0.263 | S1 = | 0.157 | S1 = | 0.263 |

| EQ | Station |
|---|---|
| Miyagi 7.1 | IWTH23 |

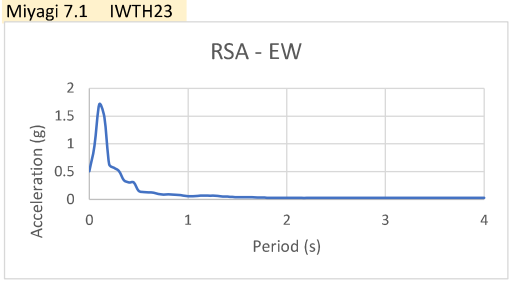


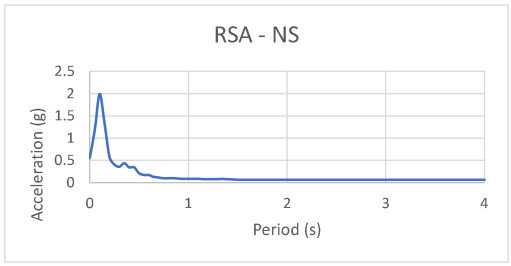


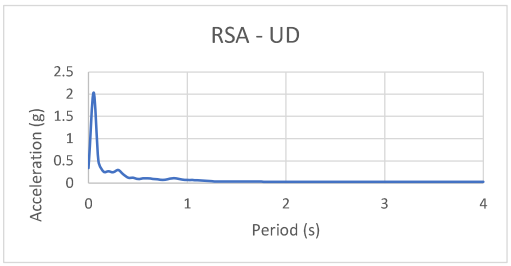


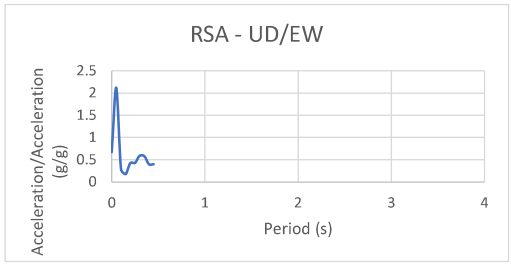


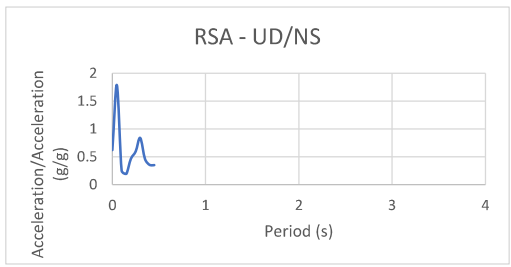


| | |
|---|---|
| Max UD (g) | 2.038 |
| Per Max UD (s) | 0.05 |
| Max UD/EW (g) | 2.115 |
| Per Max UD/EW (s) | 0.05 |
| Max UD/NS (g) | 1.791 |
| Per Max UD/NS (s) | 0.05 |

| RSA - EW | | RSA - NS | | MAX( EW, NS) | |
|---|---|---|---|---|---|
| PGA = | 0.508 | PGA = | 0.553 | PGA = | 0.553 |
| Ss = | 0.634 | Ss = | 0.579 | Ss = | 0.634 |
| S1 = | 0.062 | S1 = | 0.087 | S1 = | 0.087 |

| EQ | Station |
|---|---|
| Tohoku 9.0 | MYGH04 |

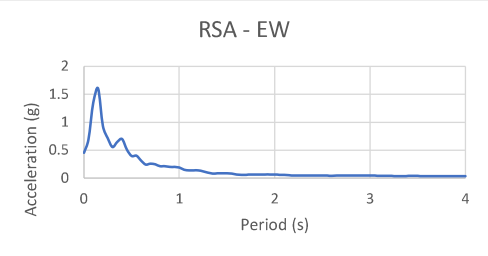


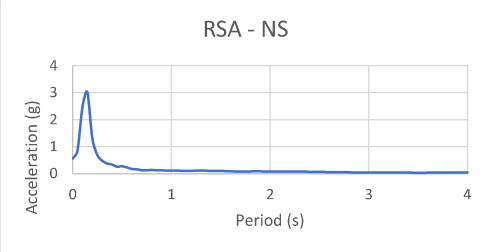


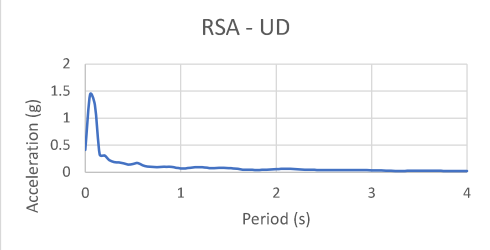


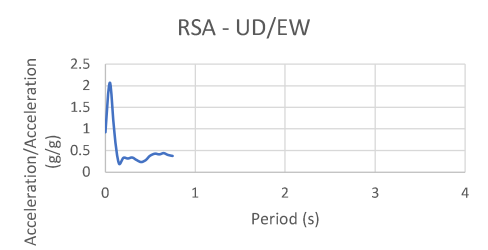


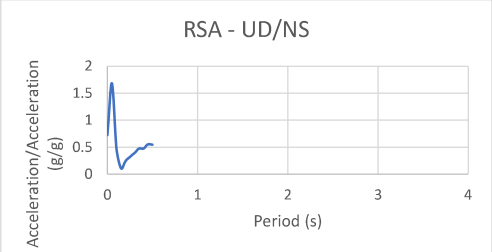


| | |
|---|---|
| Max UD (g) | 1.437 |
| Per Max UD (s) | 0.05 |
| Max UD/EW (g) | 2.071 |
| Per Max UD/EW (s) | 0.05 |
| Max UD/NS (g) | 1.686 |
| Per Max UD/NS (s) | 0.05 |

| RSA - EW | | RSA - NS | | MAX( EW, NS) | |
|---|---|---|---|---|---|
| PGA = | 0.449 | PGA = | 0.569 | PGA = | 0.569 |
| Ss = | 0.930 | Ss = | 1.273 | Ss = | 1.273 |
| S1 = | 0.185 | S1 = | 0.113 | S1 = | 0.185 |

| EQ | Station |
|---|---|
| Tohoku 9.0 | IWT009 |

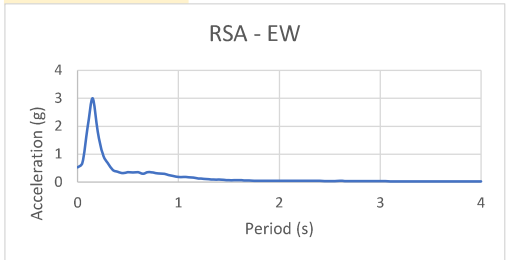


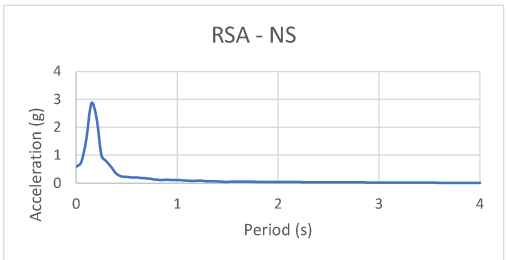


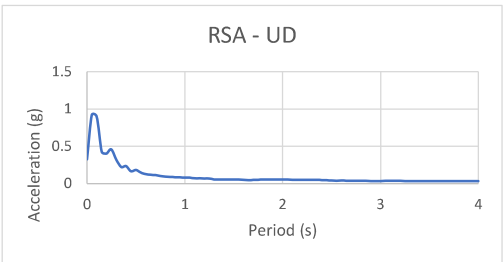


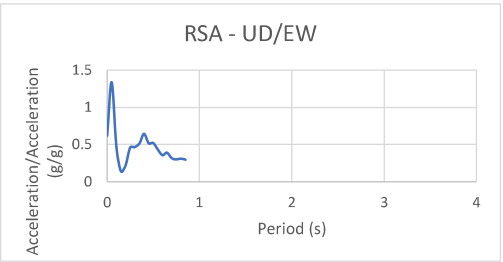


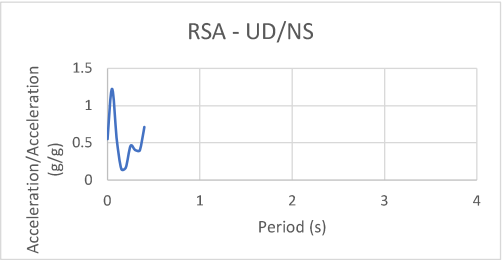


| | |
|---|---|
| Max UD (g) | 0.920 |
| Per Max UD (s) | 0.05 |
| Max UD/EW (g) | 1.338 |
| Per Max UD/EW (s) | 0.05 |
| Max UD/NS (g) | 1.225 |
| Per Max UD/NS (s) | 0.05 |

| RSA - EW | | RSA - NS | | MAX( EW, NS) | |
|---|---|---|---|---|---|
| PGA = | 0.521 | PGA = | 0.587 | PGA = | 0.587 |
| Ss = | 1.806 | Ss = | 2.385 | Ss = | 2.385 |
| S1 = | 0.180 | S1 = | 0.113 | S1 = | 0.180 |

| EQ | Station |
|---|---|
| Tohoku 9.0 | IBRH16 |

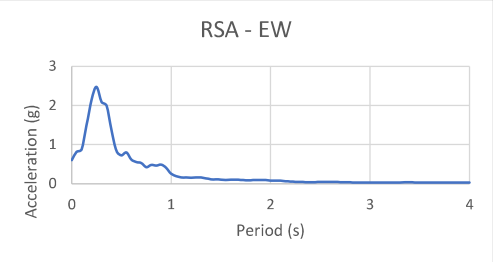


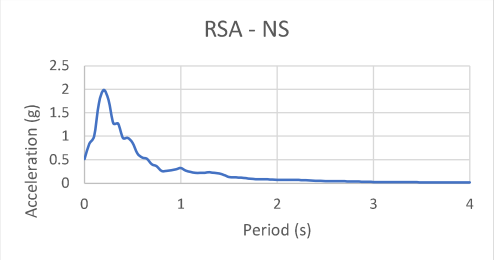


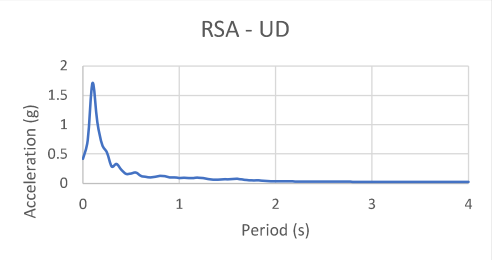


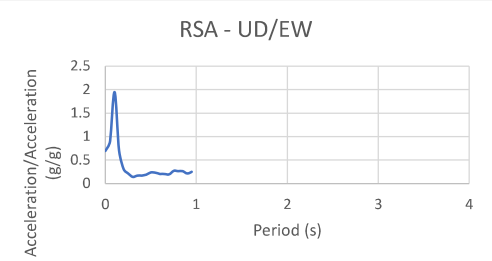


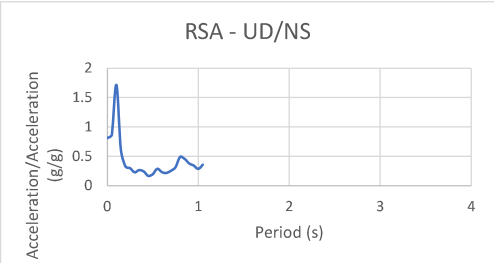


| | |
|---|---|
| Max UD (g) | 1.709 |
| Per Max UD (s) | 0.10 |
| Max UD/EW (g) | 1.944 |
| Per Max UD/EW (s) | 0.10 |
| Max UD/NS (g) | 1.713 |
| Per Max UD/NS (s) | 0.10 |

| RSA - EW | | RSA - NS | | MAX( EW, NS) | |
|---|---|---|---|---|---|
| PGA = | 0.602 | PGA = | 0.514 | PGA = | 0.602 |
| Ss = | 2.150 | Ss = | 1.985 | Ss = | 2.150 |
| S1 = | 0.258 | S1 = | 0.324 | S1 = | 0.324 |

| EQ | Station |
|---|---|
| Tohoku 9.0 | IWTH02 |

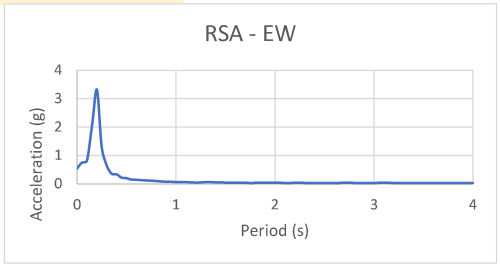


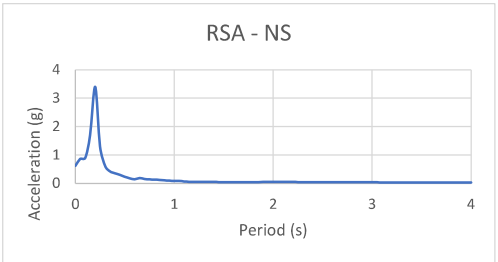


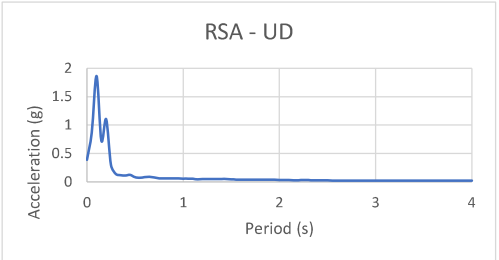


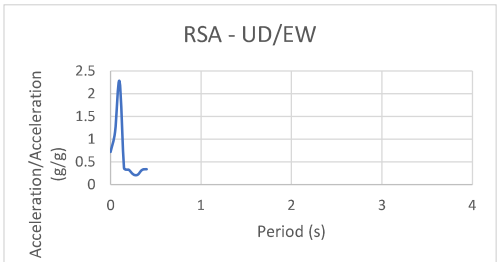


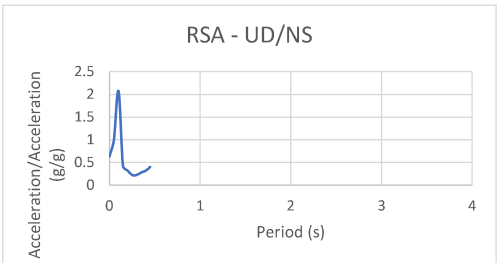


| | |
|---|---|
| Max UD (g) | 1.862 |
| Per Max UD (s) | 0.10 |
| Max UD/EW (g) | 2.277 |
| Per Max UD/EW (s) | 0.10 |
| Max UD/NS (g) | 2.071 |
| Per Max UD/NS (s) | 0.10 |

| RSA - EW | | RSA - NS | | MAX( EW, NS) | |
|---|---|---|---|---|---|
| PGA = | 0.540 | PGA = | 0.613 | PGA = | 0.613 |
| Ss = | 3.318 | Ss = | 3.396 | Ss = | 3.396 |
| S1 = | 0.061 | S1 = | 0.086 | S1 = | 0.086 |

| EQ | Station |
|---|---|
| Miyagi 7.1 | MYGH04 |

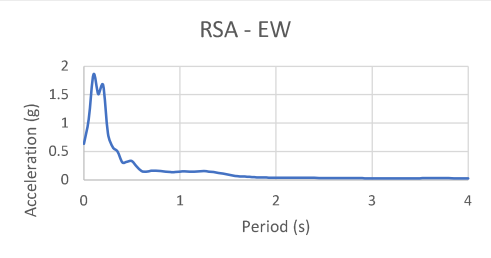


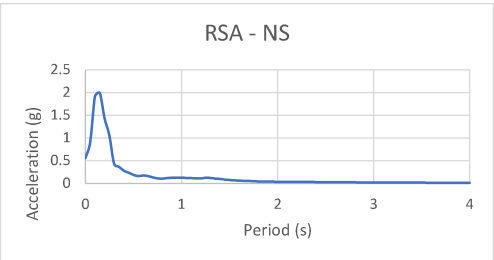


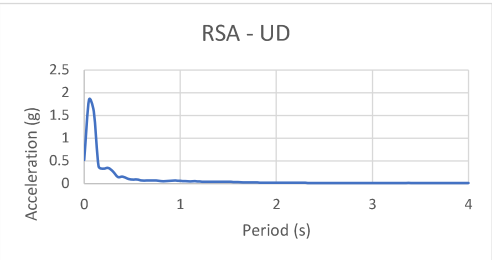


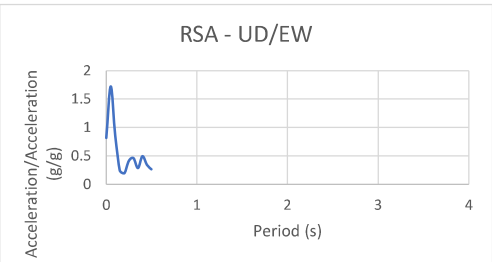


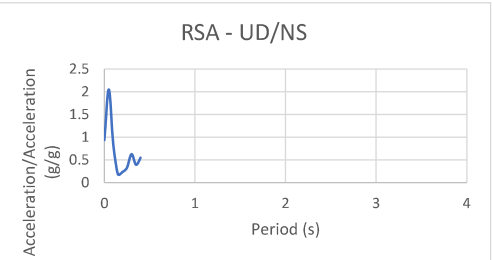


| | |
|---|---|
| Max UD (g) | 1.843 |
| Per Max UD (s) | 0.05 |
| Max UD/EW (g) | 1.725 |
| Per Max UD/EW (s) | 0.05 |
| Max UD/NS (g) | 2.051 |
| Per Max UD/NS (s) | 0.05 |

| RSA - EW | | RSA - NS | | MAX( EW, NS) | |
|---|---|---|---|---|---|
| PGA = | 0.631 | PGA = | 0.552 | PGA = | 0.631 |
| Ss = | 1.668 | Ss = | 1.437 | Ss = | 1.668 |
| S1 = | 0.145 | S1 = | 0.125 | S1 = | 0.145 |

| EQ | Station |
|---|---|
| Miyagi 7.1 | IWTH02 |

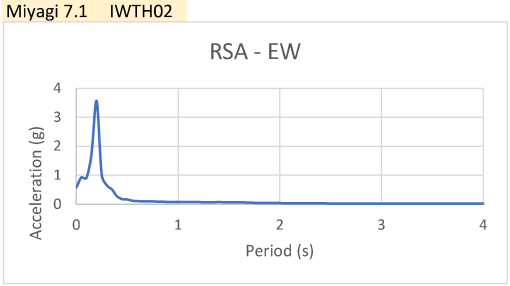


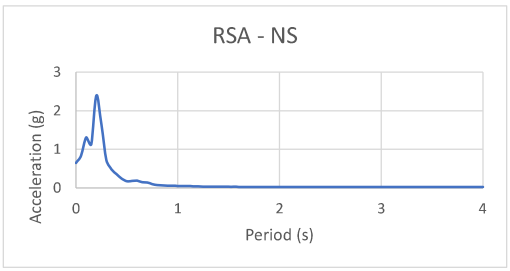


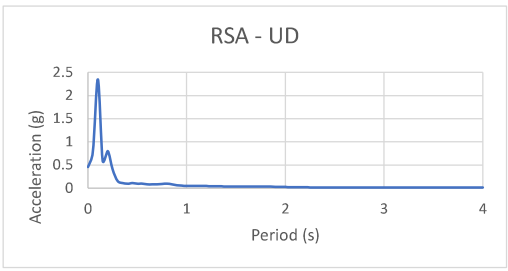


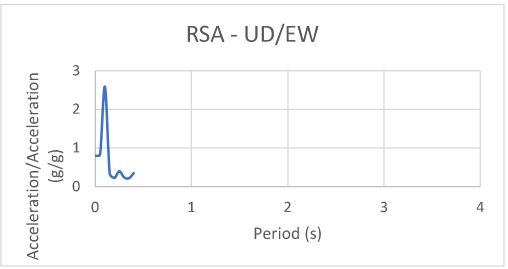


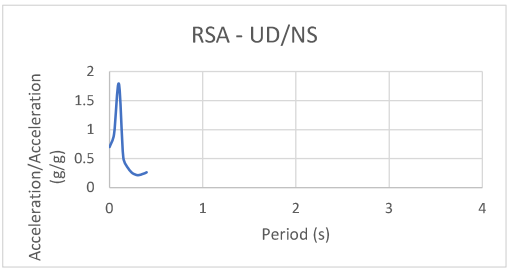


| | |
|---|---|
| Max UD (g) | 2.346 |
| Per Max UD (s) | 0.10 |
| Max UD/EW (g) | 2.589 |
| Per Max UD/EW (s) | 0.10 |
| Max UD/NS (g) | 1.793 |
| Per Max UD/NS (s) | 0.10 |

| RSA - EW | | RSA - NS | | MAX( EW, NS) | |
|---|---|---|---|---|---|
| PGA = | 0.569 | PGA = | 0.649 | PGA = | 0.649 |
| Ss = | 3.559 | Ss = | 2.399 | Ss = | 3.559 |
| S1 = | 0.080 | S1 = | 0.056 | S1 = | 0.080 |

| EQ | Station |
|---|---|
| Tohoku 9.0 | MYG002 |

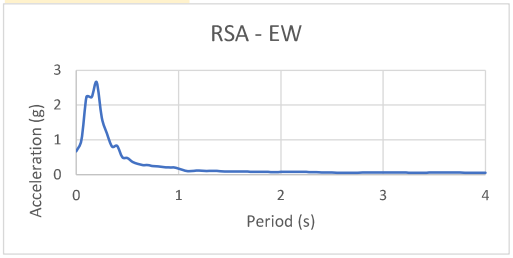


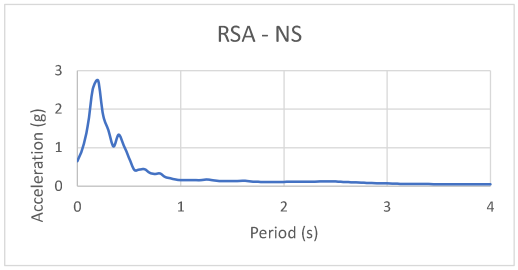


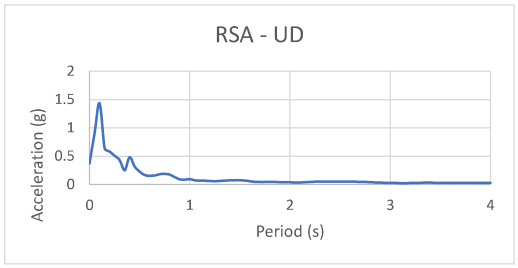


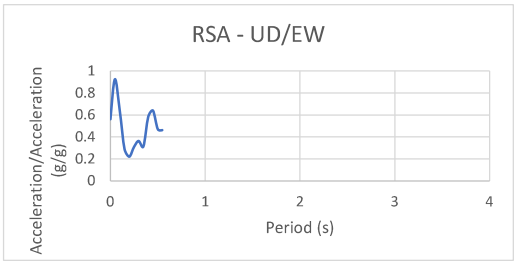


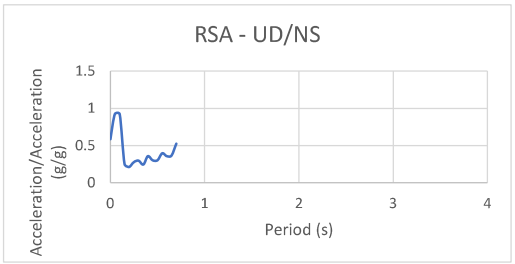


| | |
|---|---|
| Max UD (g) | 1.435 |
| Per Max UD (s) | 0.10 |
| Max UD/EW (g) | 0.924 |
| Per Max UD/EW (s) | 0.05 |
| Max UD/NS (g) | 0.926 |
| Per Max UD/NS (s) | 0.05 |

| RSA - EW | | RSA - NS | | MAX( EW, NS) | |
|---|---|---|---|---|---|
| PGA = | 0.671 | PGA = | 0.645 | PGA = | 0.671 |
| Ss = | 2.657 | Ss = | 2.744 | Ss = | 2.744 |
| S1 = | 0.176 | S1 = | 0.157 | S1 = | 0.176 |

| EQ | Station |
|---|---|
| Miyagi 7.1 | IWT009 |

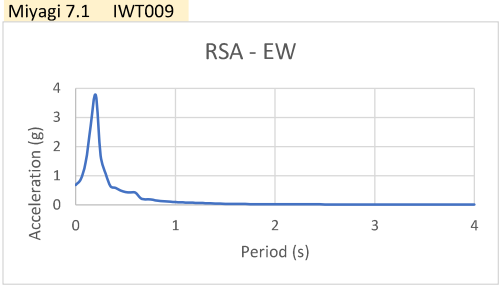


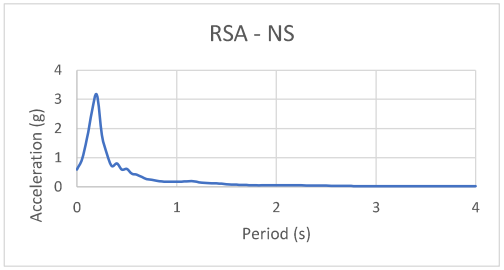


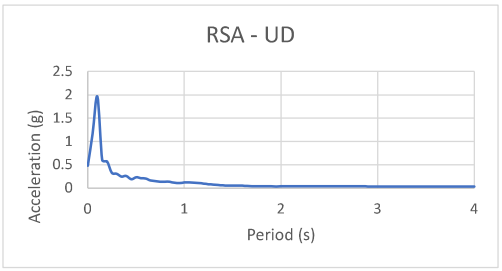


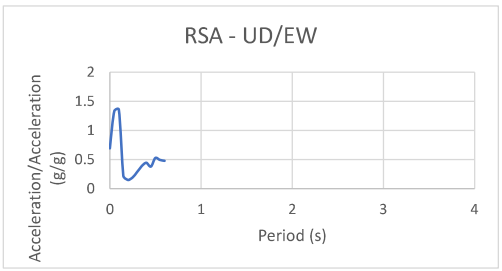


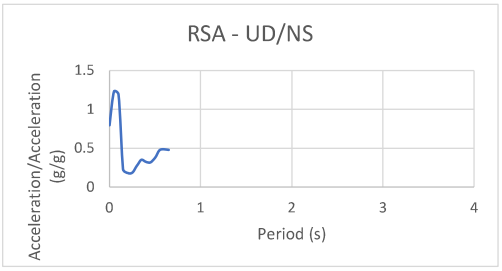


| | |
|---|---|
| Max UD (g) | 1.960 |
| Per Max UD (s) | 0.10 |
| Max UD/EW (g) | 1.355 |
| Per Max UD/EW (s) | 0.10 |
| Max UD/NS (g) | 1.232 |
| Per Max UD/NS (s) | 0.05 |

| RSA - EW | | RSA - NS | | MAX( EW, NS) | |
|---|---|---|---|---|---|
| PGA = | 0.685 | PGA = | 0.598 | PGA = | 0.685 |
| Ss = | 3.761 | Ss = | 3.158 | Ss = | 3.761 |
| S1 = | 0.096 | S1 = | 0.179 | S1 = | 0.179 |

| EQ | Station |
|---|---|
| Miyagi 7.1 | MYGH03 |

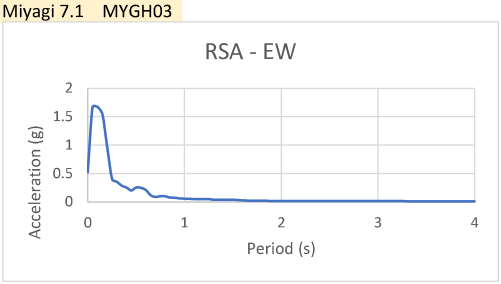


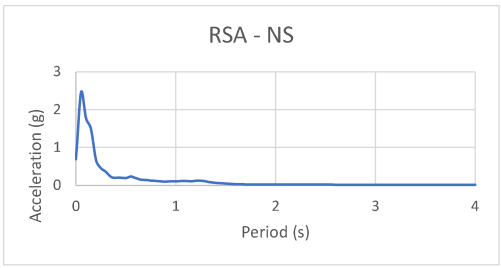


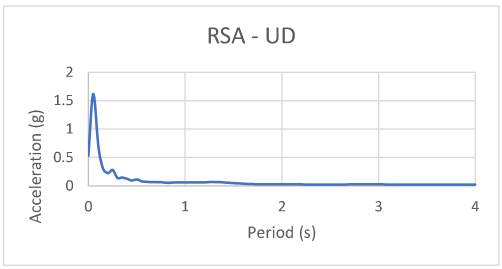


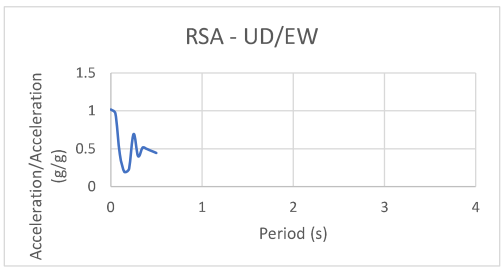


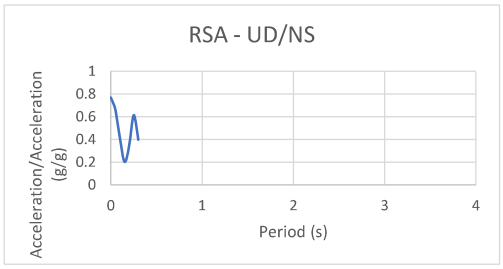


| | |
|---|---|
| Max UD (g) | 1.616 |
| Per Max UD (s) | 0.05 |
| Max UD/EW (g) | 1.018 |
| Per Max UD/EW (s) | 0.00 |
| Max UD/NS (g) | 0.771 |
| Per Max UD/NS (s) | 0.00 |

| RSA - EW | | RSA - NS | | MAX( EW, NS) | |
|---|---|---|---|---|---|
| PGA = | 0.521 | PGA = | 0.688 | PGA = | 0.688 |
| Ss = | 0.955 | Ss = | 0.666 | Ss = | 0.955 |
| S1 = | 0.057 | S1 = | 0.109 | S1 = | 0.109 |

| EQ | Station |
|---|---|
| Tohoku 9.0 | IWTH27 |

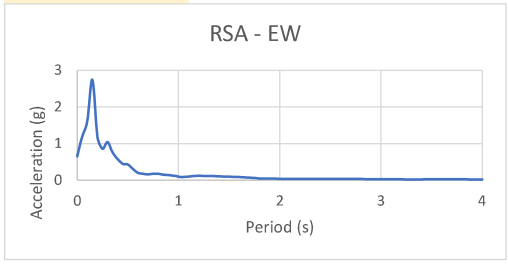


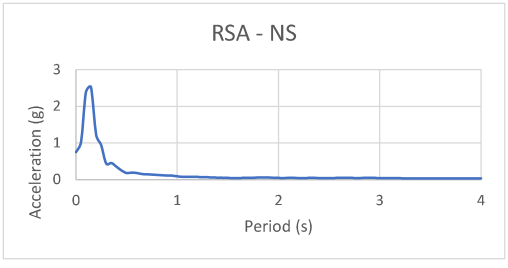


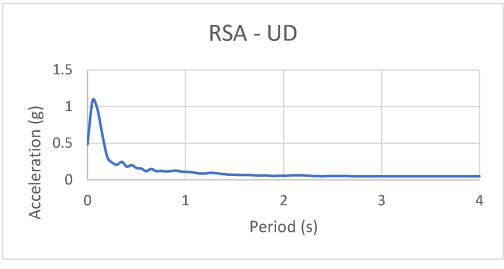


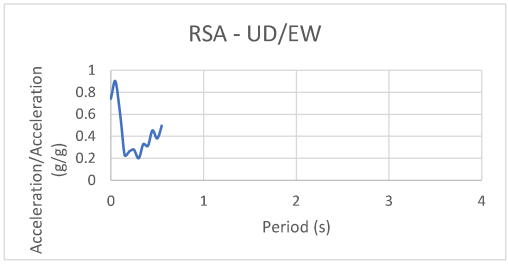


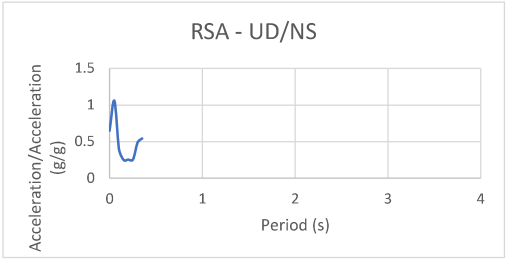


| | |
|---|---|
| Max UD (g) | 1.084 |
| Per Max UD (s) | 0.05 |
| Max UD/EW (g) | 0.902 |
| Per Max UD/EW (s) | 0.05 |
| Max UD/NS (g) | 1.056 |
| Per Max UD/NS (s) | 0.05 |

| RSA - EW | | RSA - NS | | MAX( EW, NS) | |
|---|---|---|---|---|---|
| PGA = | 0.647 | PGA = | 0.744 | PGA = | 0.744 |
| Ss = | 1.185 | Ss = | 1.224 | Ss = | 1.224 |
| S1 = | 0.096 | S1 = | 0.089 | S1 = | 0.096 |

| EQ | Station |
|---|---|
| Tohoku 9.0 | IBRH15 |

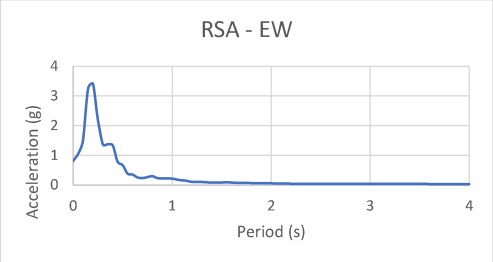


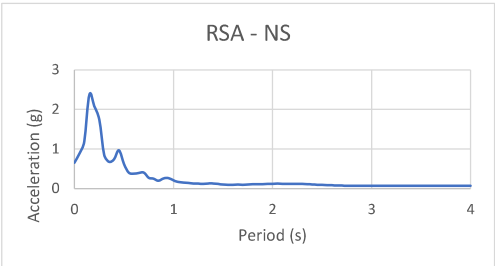


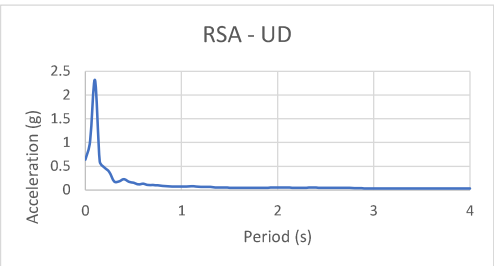


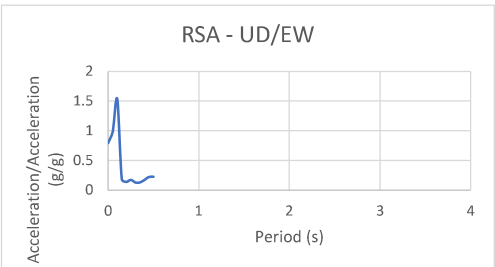


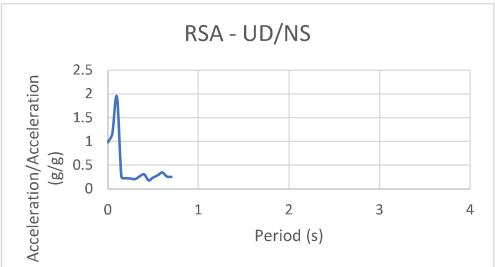


| | |
|---|---|
| Max UD (g) | 2.316 |
| Per Max UD (s) | 0.10 |
| Max UD/EW (g) | 1.528 |
| Per Max UD/EW (s) | 0.10 |
| Max UD/NS (g) | 1.939 |
| Per Max UD/NS (s) | 0.10 |

| RSA - EW | | RSA - NS | | MAX( EW, NS) | |
|---|---|---|---|---|---|
| PGA = | 0.808 | PGA = | 0.649 | PGA = | 0.808 |
| Ss = | 3.410 | Ss = | 2.086 | Ss = | 3.410 |
| S1 = | 0.215 | S1 = | 0.203 | S1 = | 0.215 |

| EQ | Station |
|---|---|
| Tohoku 9.0 | TCGH13 |

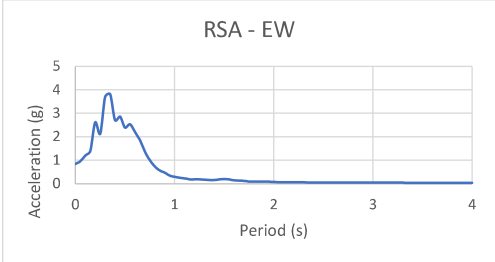


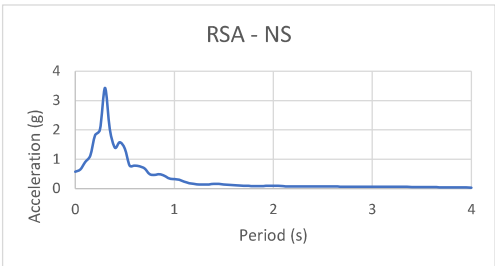


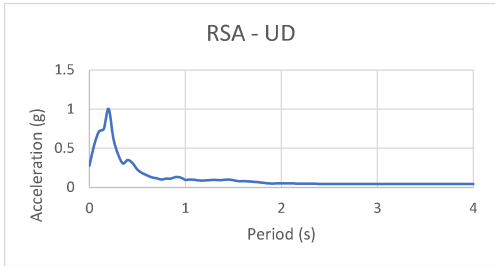


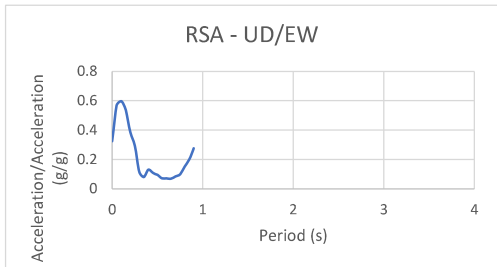


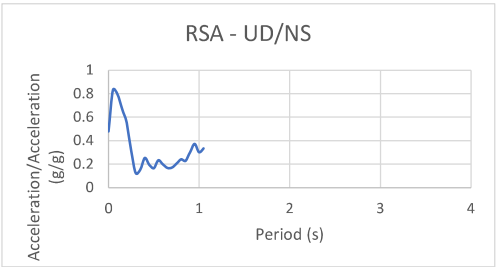


| | |
|---|---|
| Max UD (g) | 1.004 |
| Per Max UD (s) | 0.20 |
| Max UD/EW (g) | 0.597 |
| Per Max UD/EW (s) | 0.10 |
| Max UD/NS (g) | 0.833 |
| Per Max UD/NS (s) | 0.05 |

| RSA - EW | | RSA - NS | | MAX( EW, NS) | |
|---|---|---|---|---|---|
| PGA = | 0.844 | PGA = | 0.572 | PGA = | 0.844 |
| Ss = | 2.606 | Ss = | 1.820 | Ss = | 2.606 |
| S1 = | 0.296 | S1 = | 0.319 | S1 = | 0.319 |

| EQ | Station |
|---|---|
| Miyagi 7.1 | MYG012 |

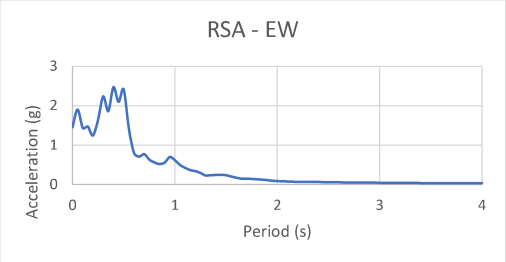


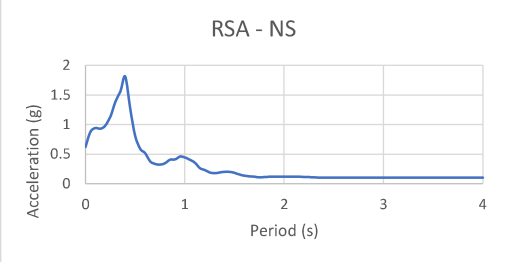


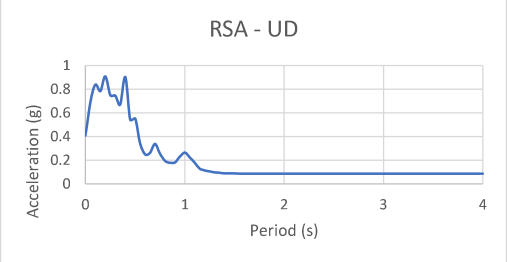


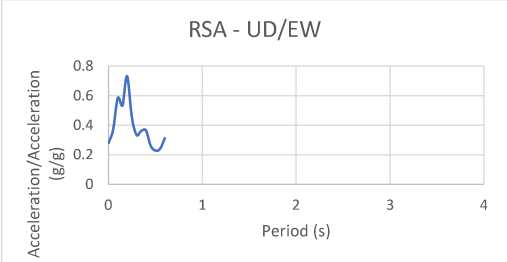


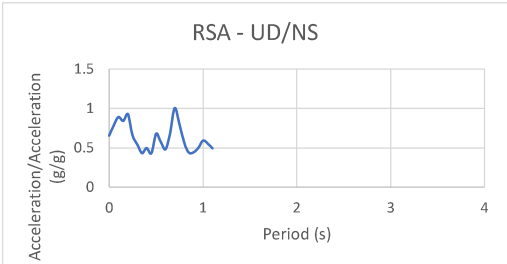


| | |
|---|---|
| Max UD (g) | 0.910 |
| Per Max UD (s) | 0.20 |
| Max UD/EW (g) | 0.731 |
| Per Max UD/EW (s) | 0.20 |
| Max UD/NS (g) | 1.004 |
| Per Max UD/NS (s) | 0.70 |

| RSA - EW | | RSA - NS | | MAX( EW, NS) | |
|---|---|---|---|---|---|
| PGA = | 1.457 | PGA = | 0.622 | PGA = | 1.457 |
| Ss = | 1.244 | Ss = | 0.983 | Ss = | 1.244 |
| S1 = | 0.620 | S1 = | 0.445 | S1 = | 0.620 |

| EQ | Station |
|---|---|
| Tohoku 9.0 | MYG012 |

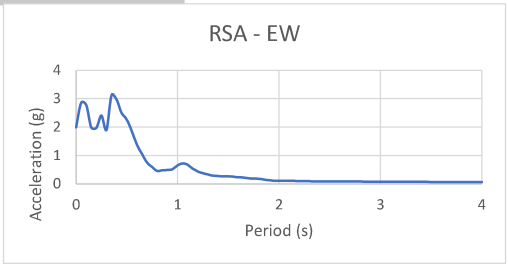


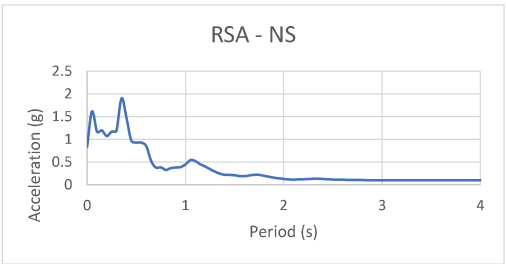


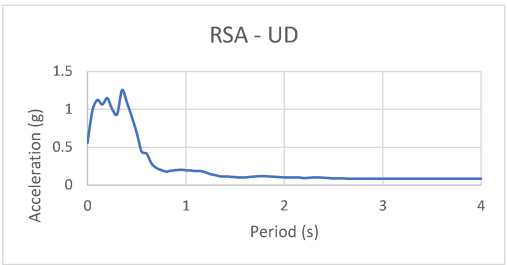


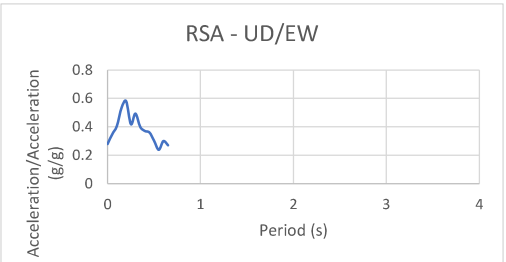


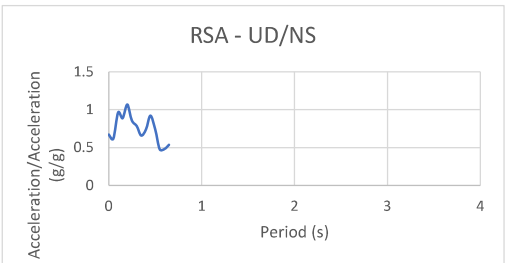


| | |
|---|---|
| Max UD (g) | 1.255 |
| Per Max UD (s) | 0.35 |
| Max UD/EW (g) | 0.582 |
| Per Max UD/EW (s) | 0.20 |
| Max UD/NS (g) | 1.068 |
| Per Max UD/NS (s) | 0.20 |

| RSA - EW | | RSA - NS | | MAX( EW, NS) | |
|---|---|---|---|---|---|
| PGA = | 1.986 | PGA = | 0.830 | PGA = | 1.986 |
| Ss = | 1.970 | Ss = | 1.074 | Ss = | 1.970 |
| S1 = | 0.649 | S1 = | 0.448 | S1 = | 0.649 |

# APPENDIX B:

# NON-BASIN M9 CSZ RSA DATA

Site: Seattle 1

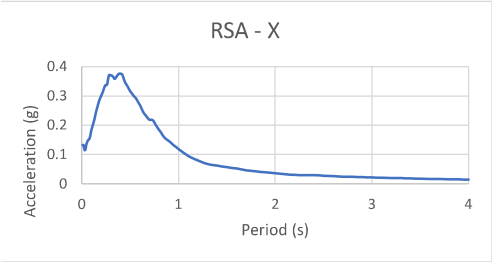


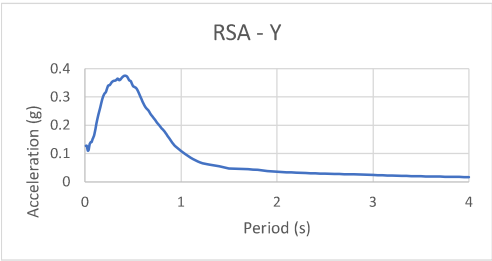


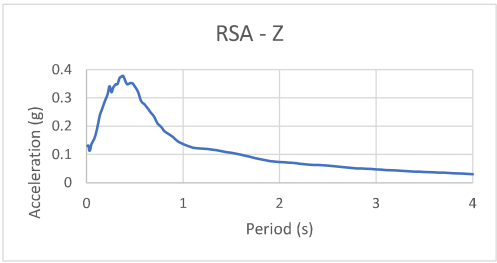


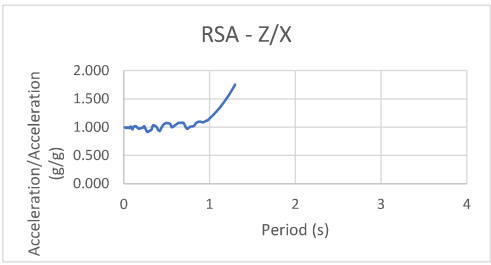


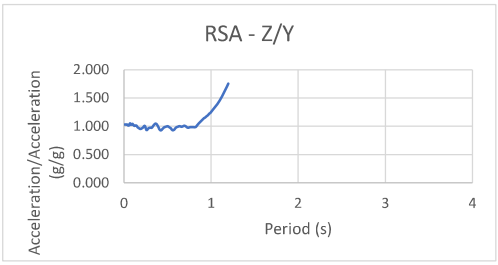


| | |
|---|---|
| Max UD (g) | 0.37778 |
| Per Max UD (s) | 0.38 |
| Max UD/EW (g) | 1.750 |
| Per Max UD/EW (s) | 1.30 |
| Max UD/NS (g) | 1.755 |
| Per Max UD/NS (s) | 1.20 |

| RSA - X | | RSA - Y | | MAX( X, Y) | |
|---|---|---|---|---|---|
| PGA = | 0.132 | PGA = | 0.127 | PGA = | 0.132 |
| Ss = | 0.301 | Ss = | 0.310 | Ss = | 0.310 |
| S1 = | 0.119 | S1 = | 0.110 | S1 = | 0.119 |

Site: Portland 1

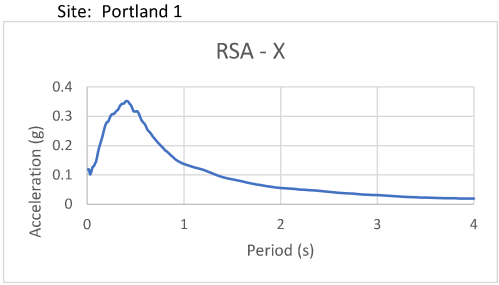


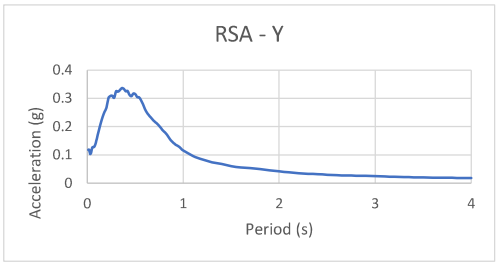


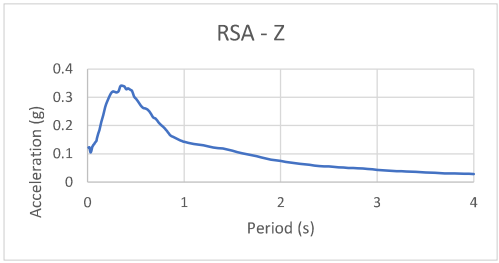


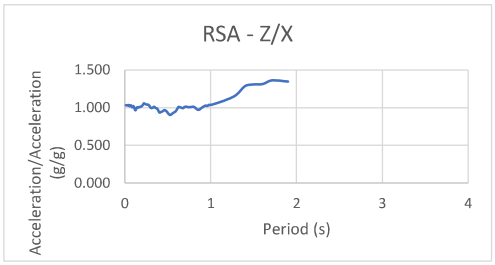


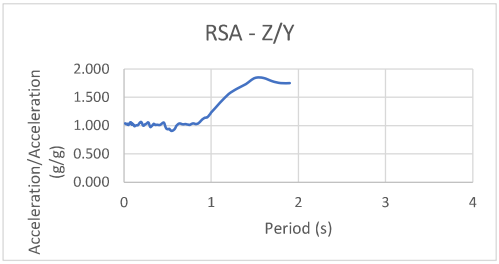


| | |
|---|---|
| Max UD (g) | 0.340197 |
| Per Max UD (s) | 0.36 |
| Max UD/EW (g) | 1.358 |
| Per Max UD/EW (s) | 1.70 |
| Max UD/NS (g) | 1.843 |
| Per Max UD/NS (s) | 1.60 |

| RSA - X | | RSA - Y | | MAX( X, Y) | |
|---|---|---|---|---|---|
| PGA = | 0.119 | PGA = | 0.118 | PGA = | 0.119 |
| Ss = | 0.278 | Ss = | 0.268 | Ss = | 0.278 |
| S1 = | 0.137 | S1 = | 0.116 | S1 = | 0.137 |

Station: Medford 1

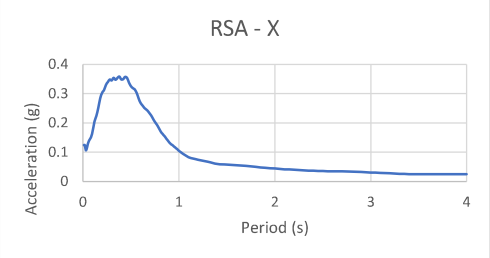


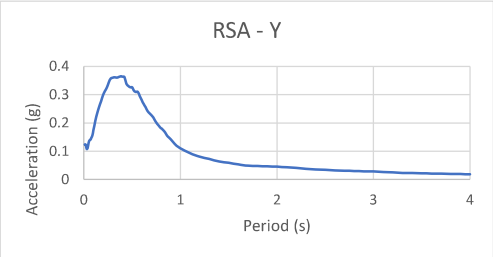


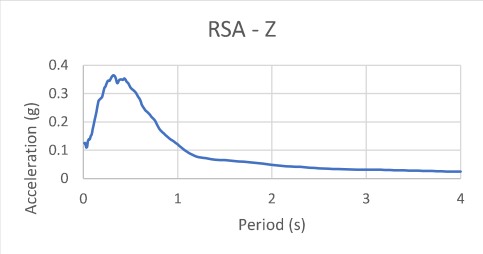


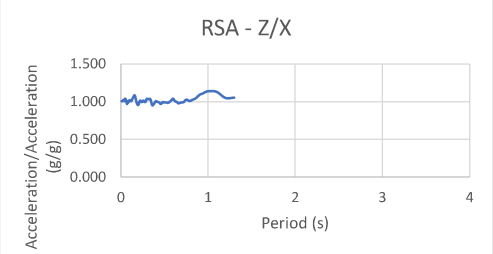


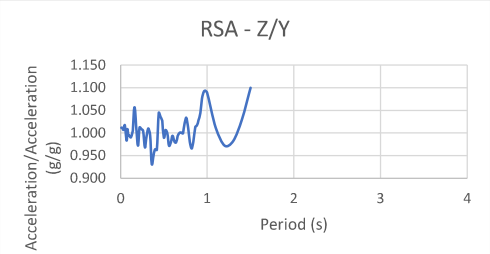


| | |
|---|---|
| Max UD (g) | 0.365323 |
| Per Max UD (s) | 0.32 |
| Max UD/EW (g) | 1.140 |
| Per Max UD/EW (s) | 1.00 |
| Max UD/NS (g) | 1.100 |
| Per Max UD/NS (s) | 1.50 |

| RSA - X | | RSA - Y | | MAX( X, Y) | |
|---|---|---|---|---|---|
| PGA = | 0.124 | PGA = | 0.123 | PGA = | 0.124 |
| Ss = | 0.303 | Ss = | 0.298 | Ss = | 0.303 |
| S1 = | 0.105 | S1 = | 0.110 | S1 = | 0.110 |

Station: Seattle 2

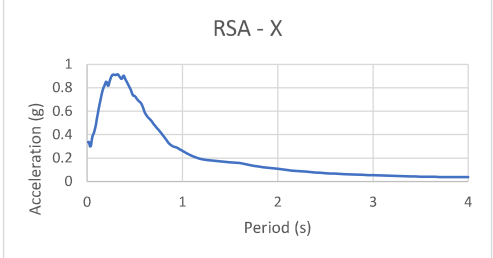


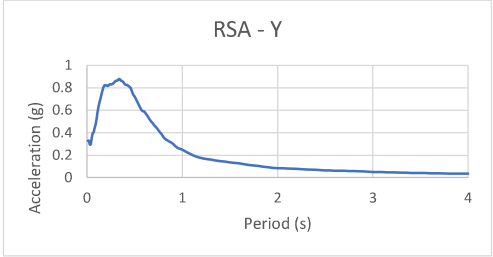


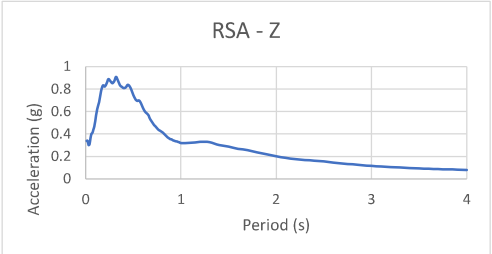


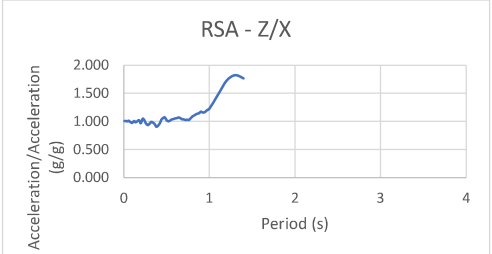


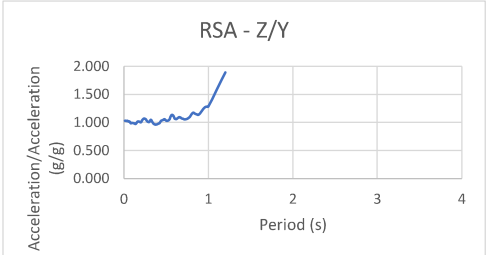


| | |
|---|---|
| Max UD (g) | 0.908856 |
| Per Max UD (s) | 0.32 |
| Max UD/EW (g) | 1.824 |
| Per Max UD/EW (s) | 1.30 |
| Max UD/NS (g) | 1.893 |
| Per Max UD/NS (s) | 1.20 |

| RSA - X | | RSA - Y | | MAX( X, Y) | |
|---|---|---|---|---|---|
| PGA = | 0.337 | PGA = | 0.329 | PGA = | 0.337 |
| Ss = | 0.851 | Ss = | 0.821 | Ss = | 0.851 |
| S1 = | 0.262 | S1 = | 0.249 | S1 = | 0.262 |

Station: Portland 2

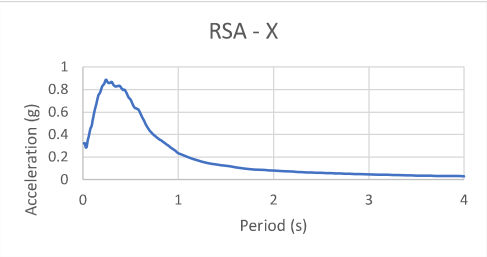


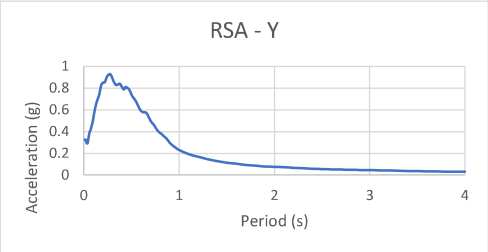


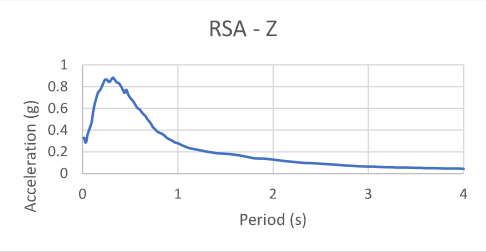


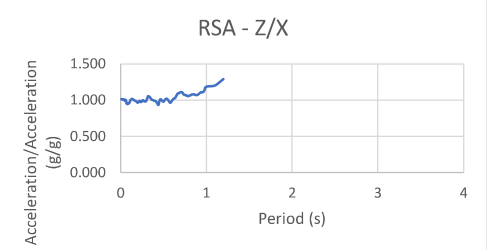


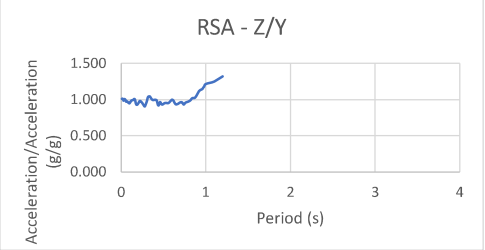


| | |
|---|---|
| Max UD (g) | 0.881793 |
| Per Max UD (s) | 0.32 |
| Max UD/EW (g) | 1.292 |
| Per Max UD/EW (s) | 1.20 |
| Max UD/NS (g) | 1.321 |
| Per Max UD/NS (s) | 1.20 |

| RSA - X | | RSA - Y | | MAX( X, Y) | |
|---|---|---|---|---|---|
| PGA = | 0.322 | PGA = | 0.324 | PGA = | 0.324 |
| Ss = | 0.828 | Ss = | 0.848 | Ss = | 0.848 |
| S1 = | 0.235 | S1 = | 0.230 | S1 = | 0.235 |

Station: Medford 2

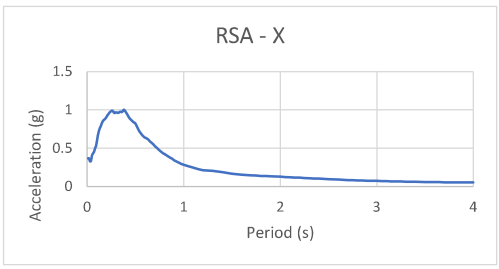


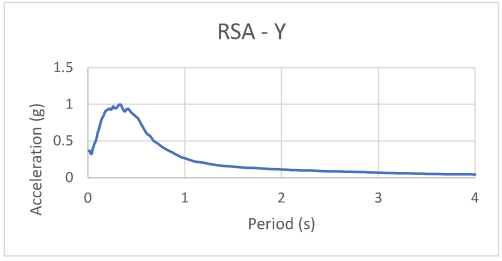


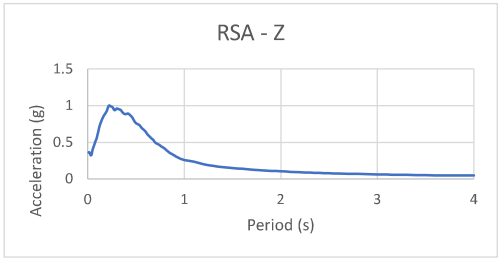


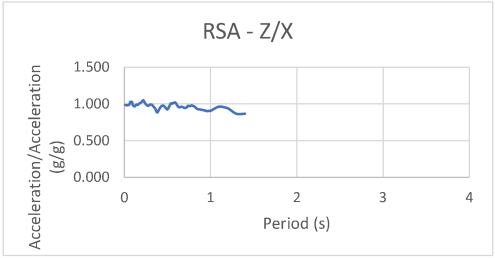


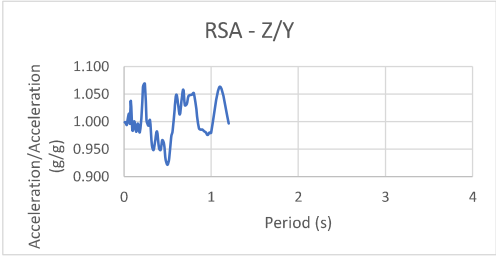


| | |
|---|---|
| Max UD (g) | 0.998091 |
| Per Max UD (s) | 0.22 |
| Max UD/EW (g) | 1.052 |
| Per Max UD/EW (s) | 0.22 |
| Max UD/NS (g) | 1.069 |
| Per Max UD/NS (s) | 0.24 |

| RSA - X | | RSA - Y | | MAX( X, Y) | |
|---|---|---|---|---|---|
| PGA = | 0.367 | PGA = | 0.363 | PGA = | 0.367 |
| Ss = | 0.910 | Ss = | 0.925 | Ss = | 0.925 |
| S1 = | 0.285 | S1 = | 0.264 | S1 = | 0.285 |

Station: Seattle 3

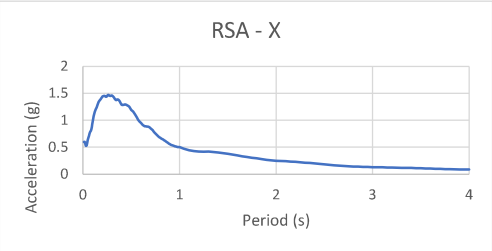


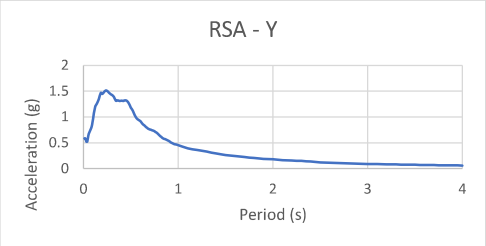


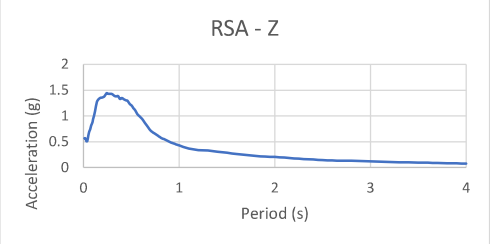


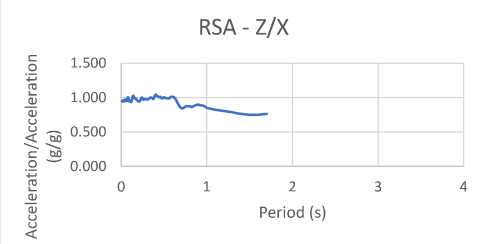


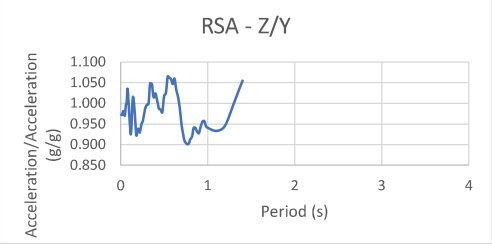


| | |
|---|---|
| Max UD (g) | 1.438564 |
| Per Max UD (s) | 0.24 |
| Max UD/EW (g) | 1.045 |
| Per Max UD/EW (s) | 0.40 |
| Max UD/NS (g) | 1.065 |
| Per Max UD/NS (s) | 0.54 |

| RSA - X | | RSA - Y | | MAX( X, Y) | |
|---|---|---|---|---|---|
| PGA = | 0.598 | PGA = | 0.582 | PGA = | 0.598 |
| Ss = | 1.438 | Ss = | 1.447 | Ss = | 1.447 |
| S1 = | 0.501 | S1 = | 0.454 | S1 = | 0.501 |

Station: Portland 3

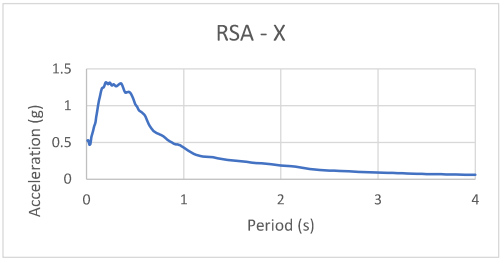


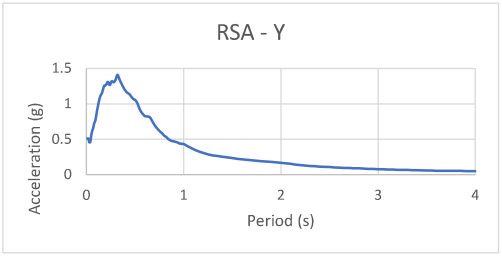


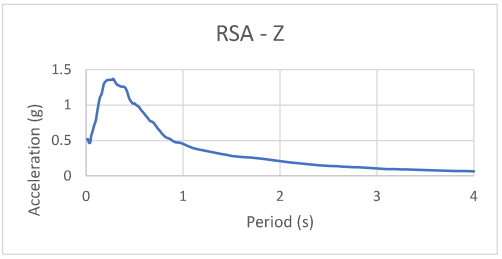


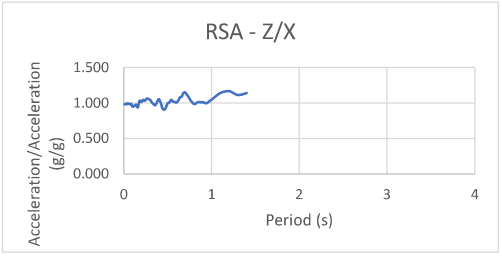


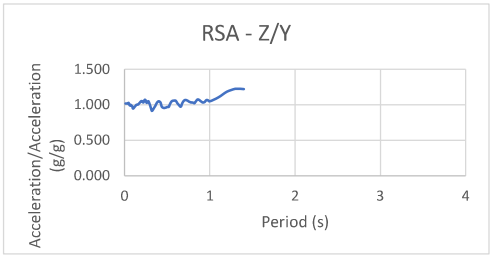


| | |
|---|---|
| Max UD (g) | 1.369607 |
| Per Max UD (s) | 0.28 |
| Max UD/EW (g) | 1.170 |
| Per Max UD/EW (s) | 1.20 |
| Max UD/NS (g) | 1.225 |
| Per Max UD/NS (s) | 1.30 |

| RSA - X | | RSA - Y | | MAX( X, Y) | |
|---|---|---|---|---|---|
| PGA = | 0.528 | PGA = | 0.508 | PGA = | 0.528 |
| Ss = | 1.318 | Ss = | 1.264 | Ss = | 1.318 |
| S1 = | 0.433 | S1 = | 0.432 | S1 = | 0.433 |

Station: Medford 3

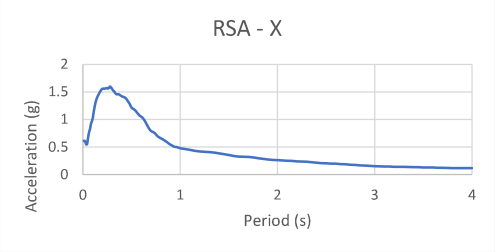


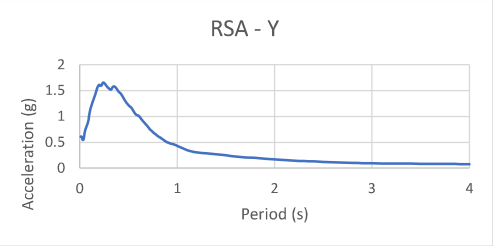


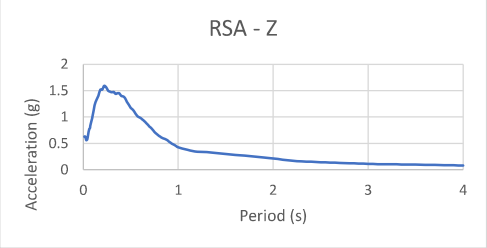


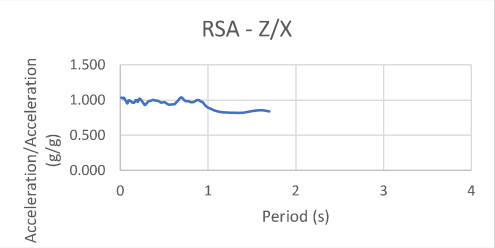


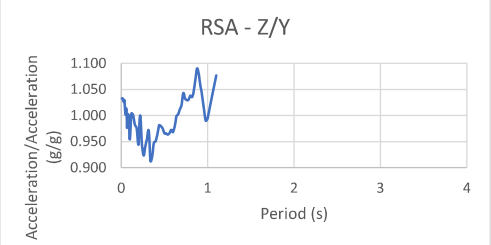


| | |
|---|---|
| Max UD (g) | 1.591482 |
| Per Max UD (s) | 0.22 |

| | |
|---|---|
| Max UD/EW (g) | 1.037 |
| Per Max UD/EW (s) | 0.70 |

| | |
|---|---|
| Max UD/NS (g) | 1.090 |
| Per Max UD/NS (s) | 0.88 |

| RSA - X | | RSA - Y | | MAX( X, Y) | |
|---|---|---|---|---|---|
| PGA = | 0.609 | PGA = | 0.609 | PGA = | 0.609 |
| Ss = | 1.558 | Ss = | 1.610 | Ss = | 1.610 |
| S1 = | 0.480 | S1 = | 0.432 | S1 = | 0.480 |

# APPENDIX C:

## BASIN SITES RECORDED RSA DATA
## JAPAN & CHILE

Station: NIG024

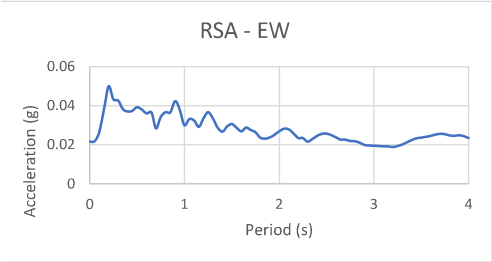


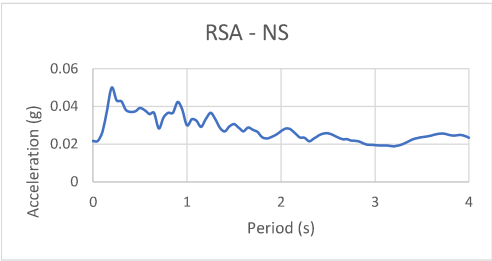


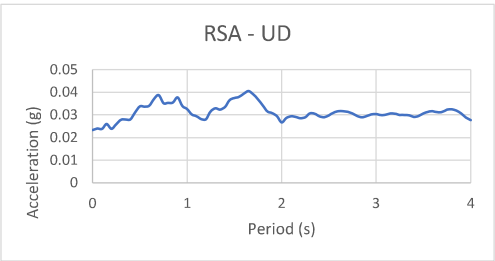


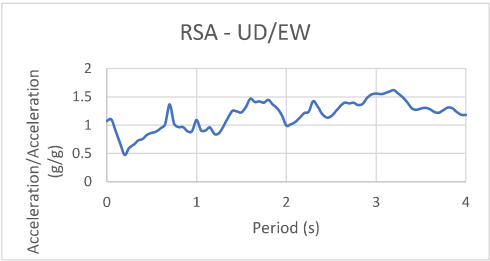


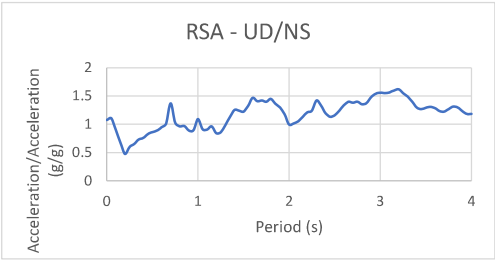


| | |
|---|---|
| Max UD (g) | 0.04055 |
| Per Max UD (s) | 1.65 |
| Max UD/EW (g) | 1.619 |
| Per Max UD/EW (s) | 3.20 |
| Max UD/NS (g) | 1.619 |
| Per Max UD/NS (s) | 3.20 |

| RSA - EW | | RSA - NS | | MAX( EW, NS) | |
|---|---|---|---|---|---|
| PGA = | 0.022 | PGA = | 0.022 | PGA = | 0.022 |
| Ss = | 0.050 | Ss = | 0.050 | Ss = | 0.050 |
| S1 = | 0.030 | S1 = | 0.030 | S1 = | 0.030 |

Station: NIG026

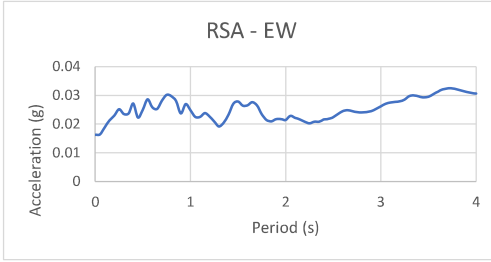


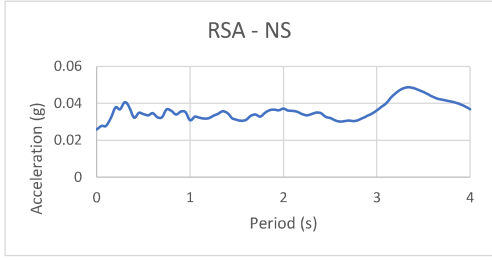


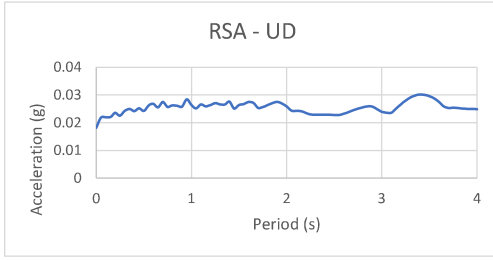


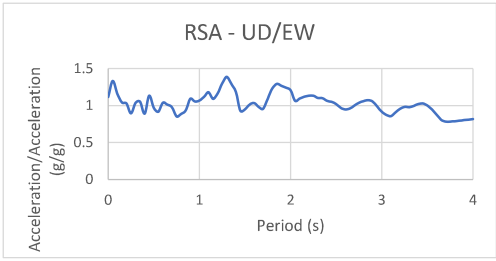


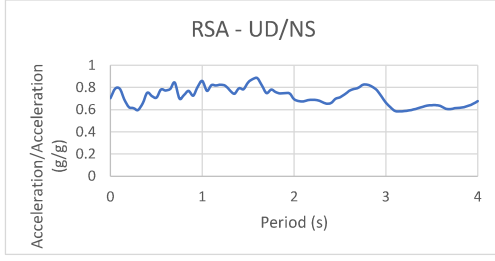


| | |
|---|---|
| Max UD (g) | 0.03016 |
| Per Max UD (s) | 3.40 |
| Max UD/EW (g) | 1.390 |
| Per Max UD/EW (s) | 1.30 |
| Max UD/NS (g) | 0.884 |
| Per Max UD/NS (s) | 1.60 |

| RSA - EW | | RSA - NS | | MAX( EW, NS) | |
|---|---|---|---|---|---|
| PGA = | 0.016 | PGA = | 0.026 | PGA = | 0.026 |
| Ss = | 0.023 | Ss = | 0.038 | Ss = | 0.038 |
| S1 = | 0.025 | S1 = | 0.031 | S1 = | 0.031 |

Station: NIG016

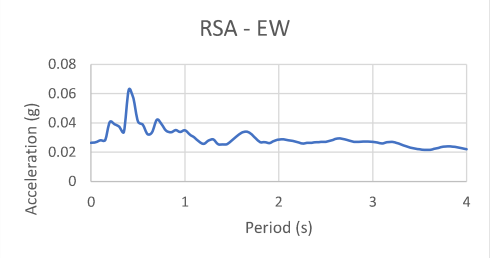


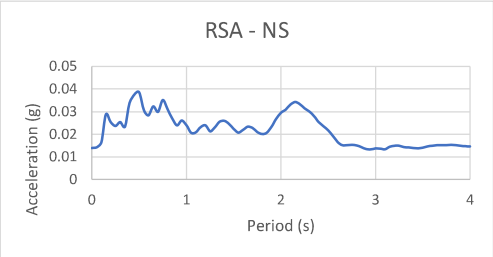


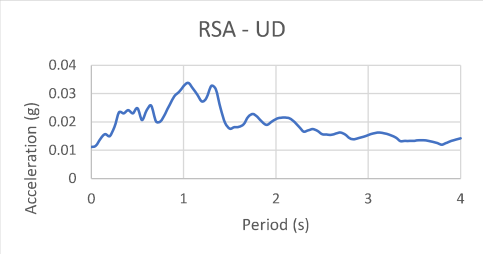


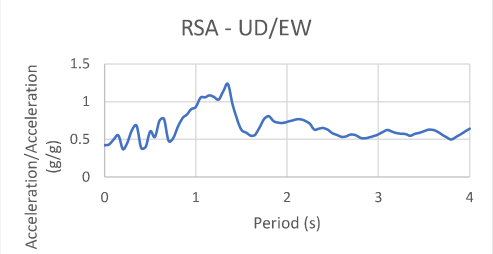


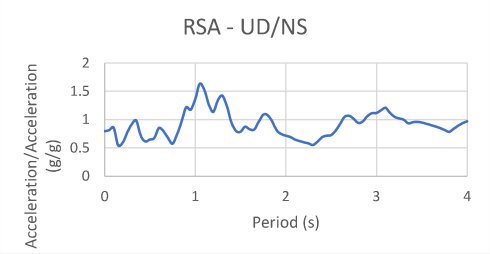


| | |
|---|---|
| Max UD (g) | 0.03382 |
| Per Max UD (s) | 1.05 |
| Max UD/EW (g) | 1.236 |
| Per Max UD/EW (s) | 1.35 |
| Max UD/NS (g) | 1.631 |
| Per Max UD/NS (s) | 1.05 |

| RSA - EW | | RSA - NS | | MAX( EW, NS) | |
|---|---|---|---|---|---|
| PGA = | 0.026 | PGA = | 0.014 | PGA = | 0.026 |
| Ss = | 0.041 | Ss = | 0.025 | Ss = | 0.041 |
| S1 = | 0.035 | S1 = | 0.024 | S1 = | 0.035 |

Station: NIG013

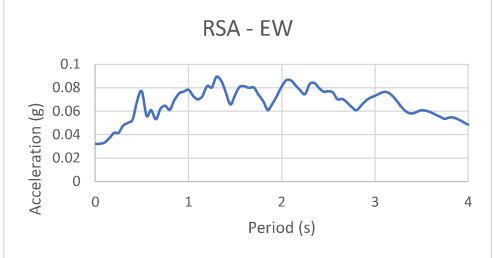


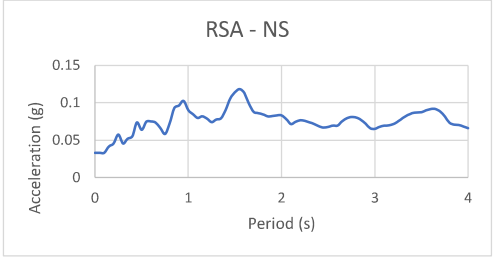


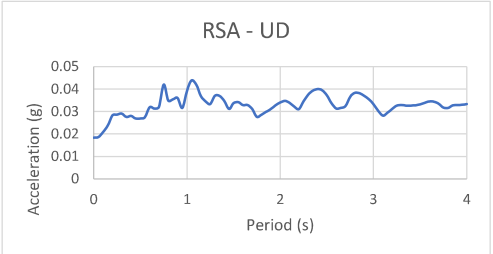


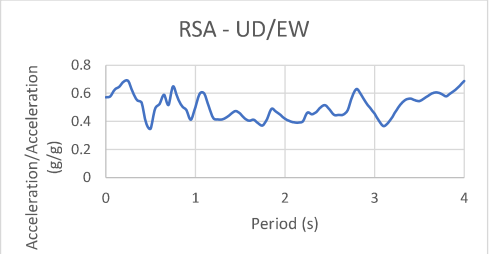


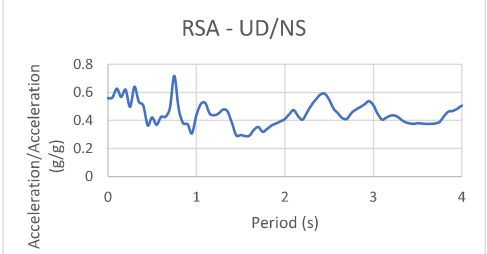


| | |
|---|---|
| Max UD (g) | 0.04381 |
| Per Max UD (s) | 1.05 |
| Max UD/EW (g) | 0.689 |
| Per Max UD/EW (s) | 4.00 |
| Max UD/NS (g) | 0.718 |
| Per Max UD/NS (s) | 0.75 |

| RSA - EW | | RSA - NS | | MAX( EW, NS) | |
|---|---|---|---|---|---|
| PGA = | 0.032 | PGA = | 0.033 | PGA = | 0.033 |
| Ss = | 0.041 | Ss = | 0.045 | Ss = | 0.045 |
| S1 = | 0.078 | S1 = | 0.090 | S1 = | 0.090 |

Station: NIG010

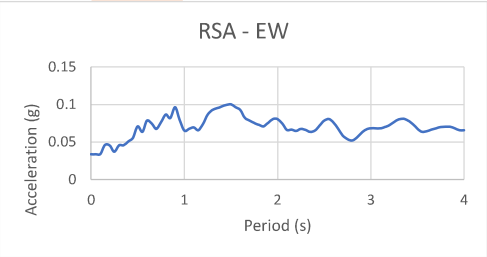


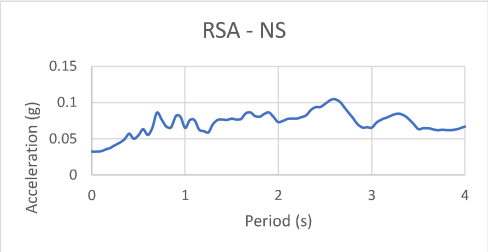


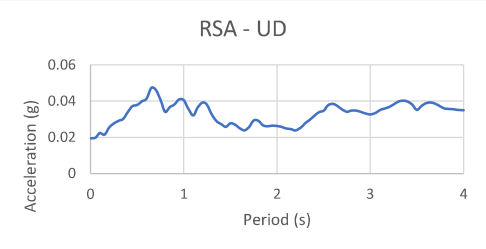


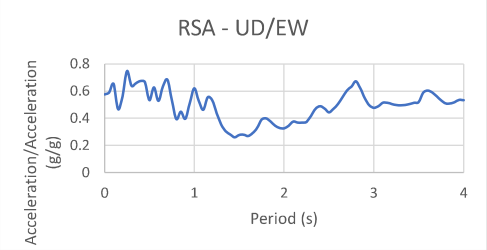


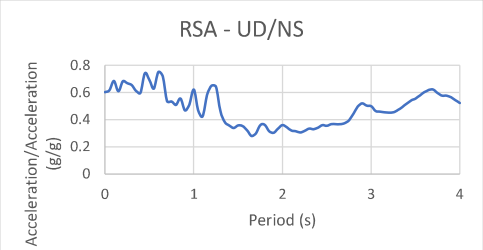


| | |
|---|---|
| Max UD (g) | 0.04732 |
| Per Max UD (s) | 0.65 |
| Max UD/EW (g) | 0.748 |
| Per Max UD/EW (s) | 0.25 |
| Max UD/NS (g) | 0.751 |
| Per Max UD/NS (s) | 0.60 |

| RSA - EW | | RSA - NS | | MAX( EW, NS) | |
|---|---|---|---|---|---|
| PGA = | 0.034 | PGA = | 0.032 | PGA = | 0.034 |
| Ss = | 0.045 | Ss = | 0.037 | Ss = | 0.045 |
| S1 = | 0.065 | S1 = | 0.065 | S1 = | 0.065 |

Station: NIG025

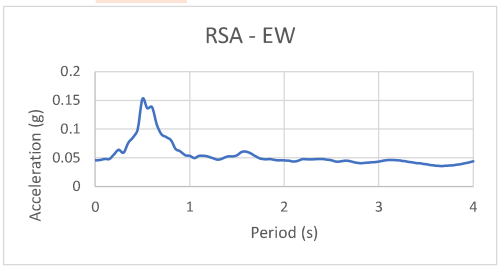


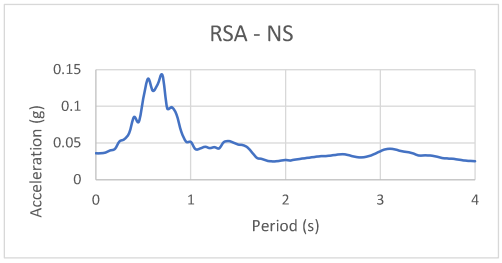


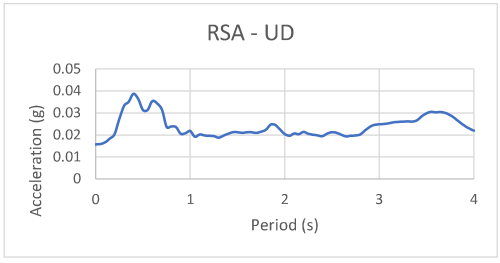


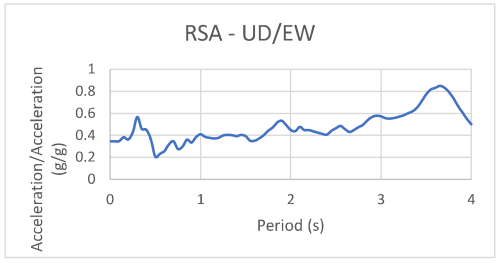


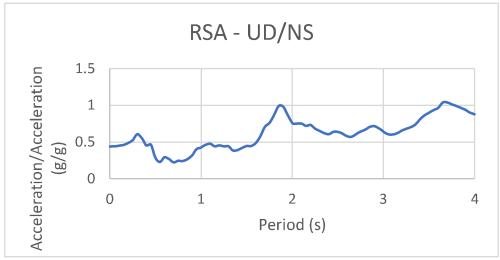


| | |
|---|---|
| Max UD (g) | 0.03871 |
| Per Max UD (s) | 0.40 |
| Max UD/EW (g) | 0.850 |
| Per Max UD/EW (s) | 3.65 |
| Max UD/NS (g) | 1.040 |
| Per Max UD/NS (s) | 3.70 |

| RSA - EW | | RSA - NS | | MAX( EW, NS) | |
|---|---|---|---|---|---|
| PGA = | 0.046 | PGA = | 0.036 | PGA = | 0.046 |
| Ss = | 0.056 | Ss = | 0.042 | Ss = | 0.056 |
| S1 = | 0.053 | S1 = | 0.051 | S1 = | 0.053 |

Station: CHB026

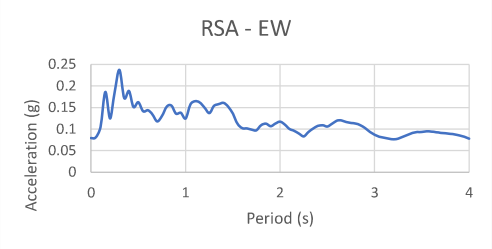


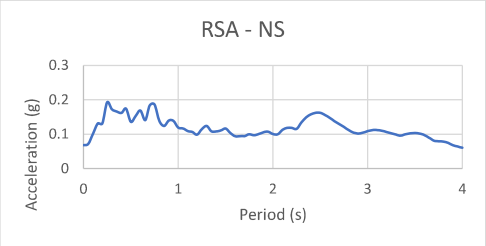


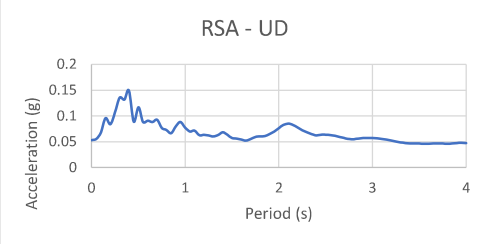


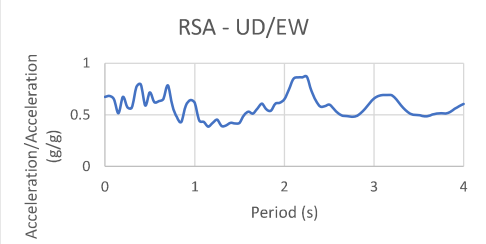


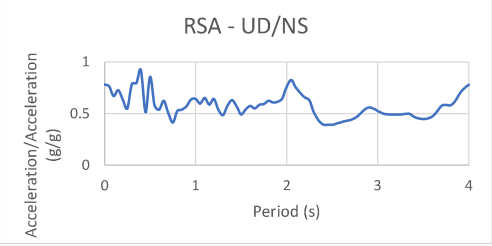


| | |
|---|---|
| Max UD (g) | 0.14914 |
| Per Max UD (s) | 0.40 |
| Max UD/EW (g) | 0.869 |
| Per Max UD/EW (s) | 2.25 |
| Max UD/NS (g) | 0.923 |
| Per Max UD/NS (s) | 0.40 |

| RSA - EW | | RSA - NS | | MAX( EW, NS) | |
|---|---|---|---|---|---|
| PGA = | 0.079 | PGA = | 0.068 | PGA = | 0.079 |
| Ss = | 0.124 | Ss = | 0.131 | Ss = | 0.131 |
| S1 = | 0.125 | S1 = | 0.120 | S1 = | 0.125 |

Station: CHB013

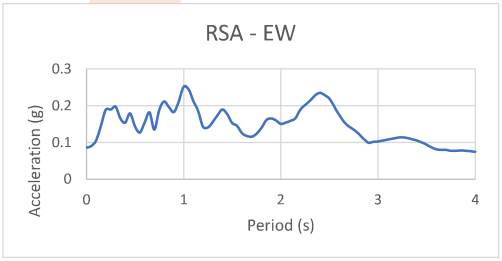


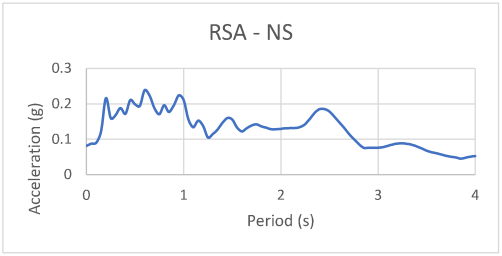


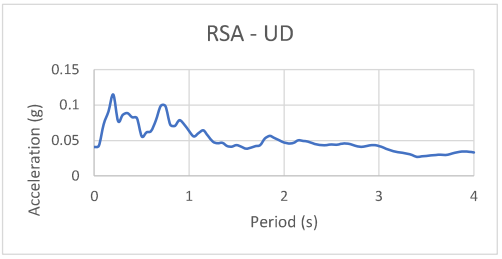


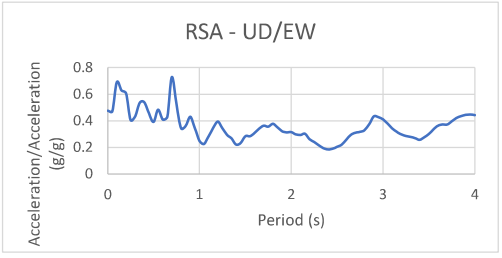


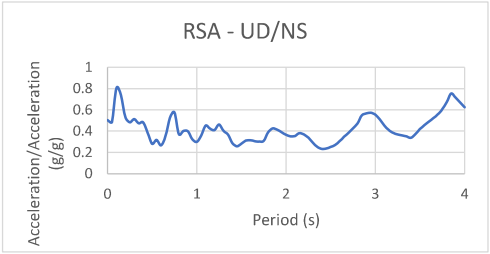


| | |
|---|---|
| Max UD (g) | 0.1149 |
| Per Max UD (s) | 0.20 |
| Max UD/EW (g) | 0.728 |
| Per Max UD/EW (s) | 0.70 |
| Max UD/NS (g) | 0.806 |
| Per Max UD/NS (s) | 0.10 |

| RSA - EW | | RSA - NS | | MAX( EW, NS) | |
|---|---|---|---|---|---|
| PGA = | 0.086 | PGA = | 0.081 | PGA = | 0.086 |
| Ss = | 0.189 | Ss = | 0.216 | Ss = | 0.216 |
| S1 = | 0.252 | S1 = | 0.210 | S1 = | 0.252 |

Station: CHB017

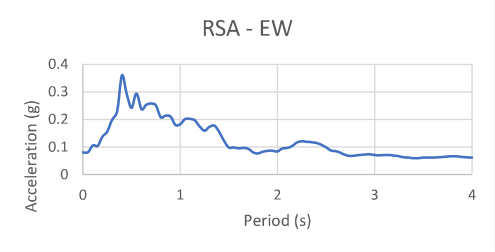


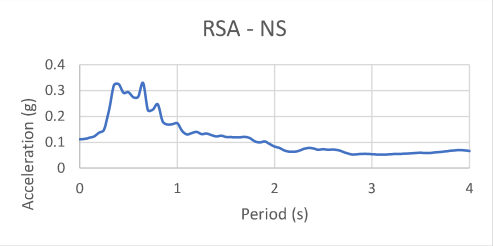


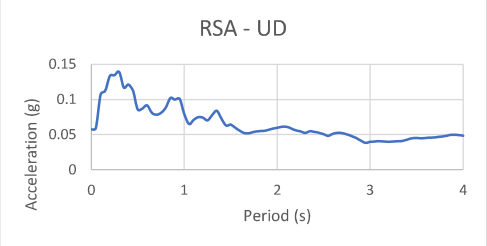


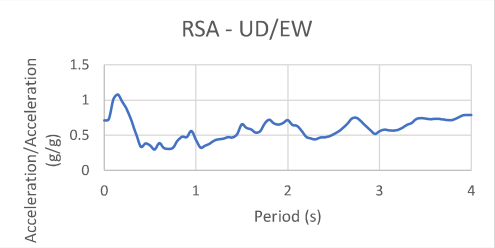


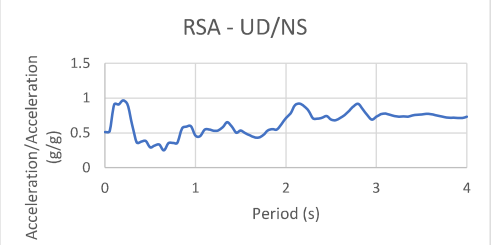


| | |
|---|---|
| Max UD (g) | 0.1391 |
| Per Max UD (s) | 0.30 |
| Max UD/EW (g) | 1.078 |
| Per Max UD/EW (s) | 0.15 |
| Max UD/NS (g) | 0.970 |
| Per Max UD/NS (s) | 0.20 |

| RSA - EW | | RSA - NS | | MAX( EW, NS) | |
|---|---|---|---|---|---|
| PGA = | 0.081 | PGA = | 0.112 | PGA = | 0.112 |
| Ss = | 0.138 | Ss = | 0.138 | Ss = | 0.138 |
| S1 = | 0.182 | S1 = | 0.174 | S1 = | 0.182 |

Station: CHBH10

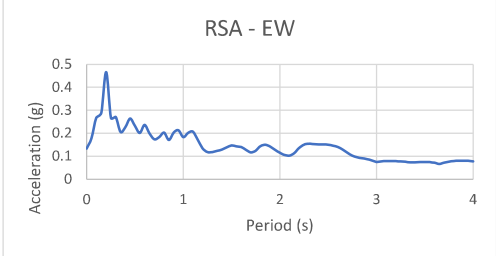


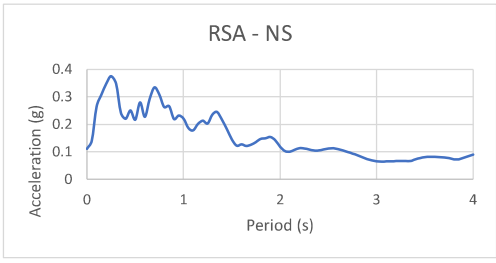


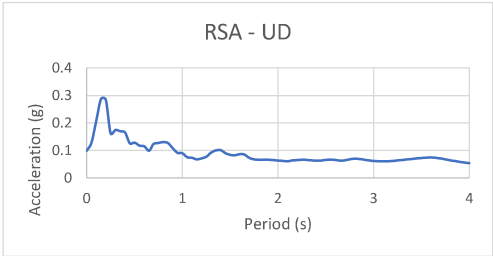


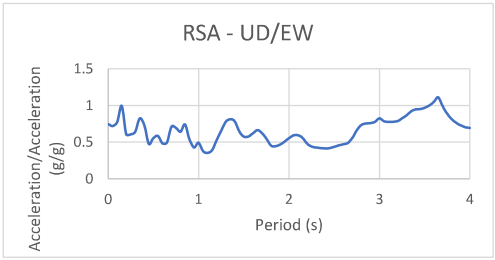


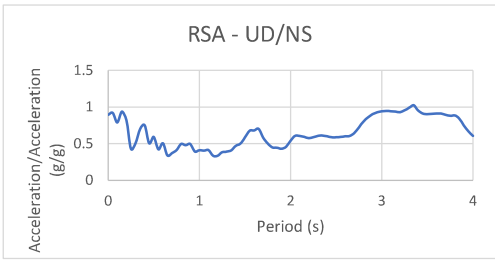


| | |
|---|---|
| Max UD (g) | 0.28829 |
| Per Max UD (s) | 0.15 |
| Max UD/EW (g) | 0.997 |
| Per Max UD/EW (s) | 0.15 |
| Max UD/NS (g) | 0.938 |
| Per Max UD/NS (s) | 0.15 |

| RSA - EW | | RSA - NS | | MAX( EW, NS) | |
|---|---|---|---|---|---|
| PGA = | 0.133 | PGA = | 0.111 | PGA = | 0.133 |
| Ss = | 0.467 | Ss = | 0.347 | Ss = | 0.467 |
| S1 = | 0.183 | S1 = | 0.220 | S1 = | 0.220 |

Station: CHB015

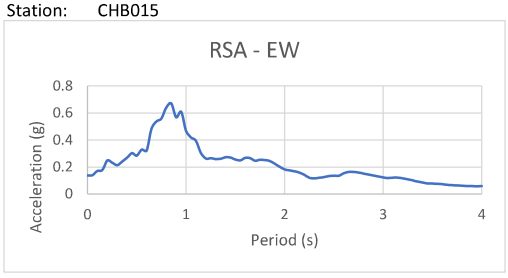


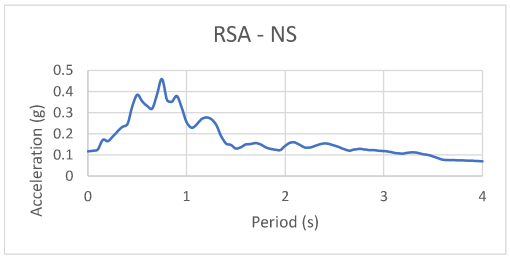


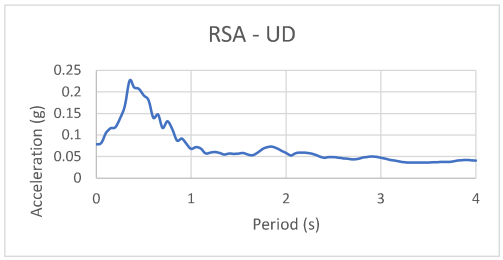


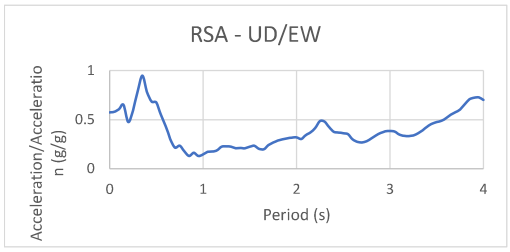


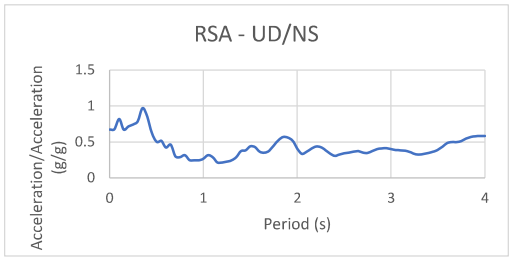


| | |
|---|---|
| Max UD (g) | 0.22631 |
| Per Max UD (s) | 0.35 |
| Max UD/EW (g) | 0.947 |
| Per Max UD/EW (s) | 0.35 |
| Max UD/NS (g) | 0.971 |
| Per Max UD/NS (s) | 0.35 |

| RSA - EW | | RSA - NS | | MAX( EW, NS) | |
|---|---|---|---|---|---|
| PGA = | 0.137 | PGA = | 0.117 | PGA = | 0.137 |
| Ss = | 0.247 | Ss = | 0.165 | Ss = | 0.247 |
| S1 = | 0.468 | S1 = | 0.256 | S1 = | 0.468 |

Station: TKY007

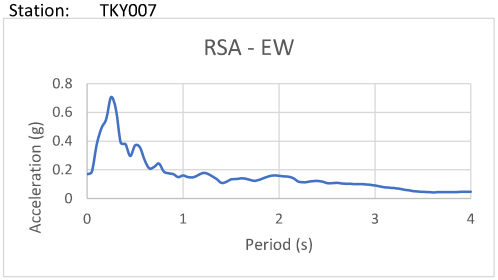


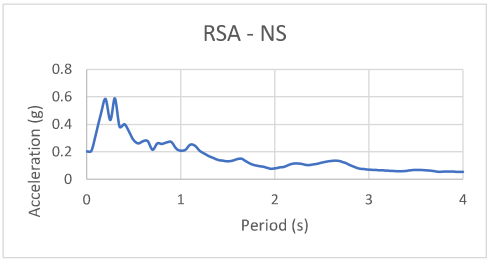


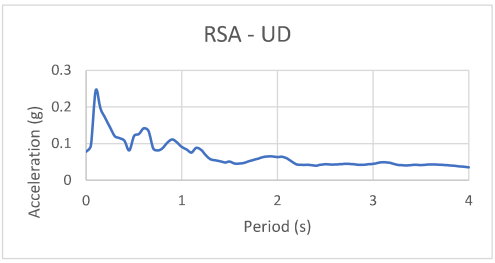


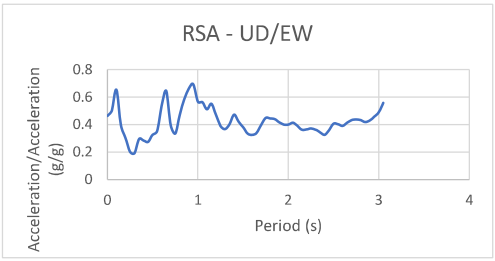


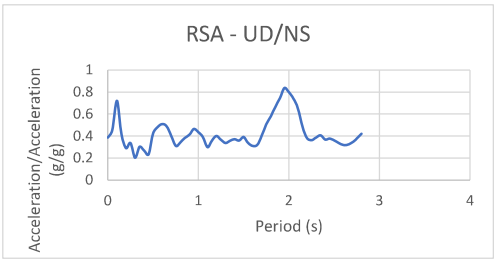


| | |
|---|---|
| Max UD (g) | 0.24445 |
| Per Max UD (s) | 0.10 |
| Max UD/EW (g) | 0.694 |
| Per Max UD/EW (s) | 0.95 |
| Max UD/NS (g) | 0.836 |
| Per Max UD/NS (s) | 1.95 |

| RSA - EW | | RSA - NS | | MAX( EW, NS) | |
|---|---|---|---|---|---|
| PGA = | 0.169 | PGA = | 0.202 | PGA = | #### |
| Ss = | 0.556 | Ss = | 0.584 | Ss = | #### |
| S1 = | 0.161 | S1 = | 0.209 | S1 = | #### |

Station: CHB012

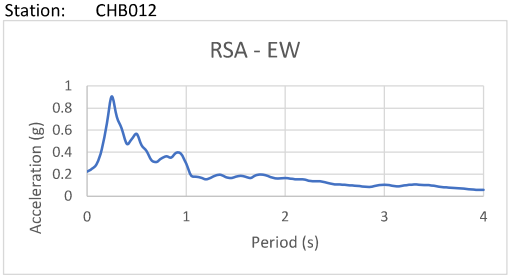


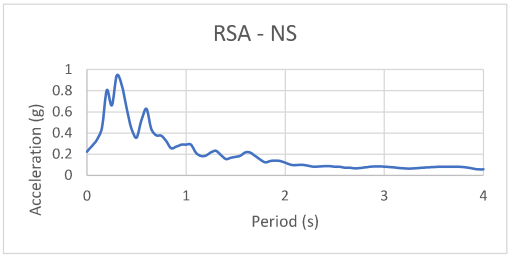


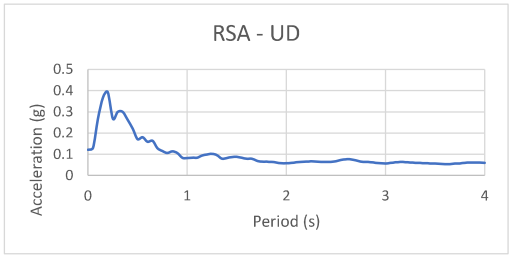


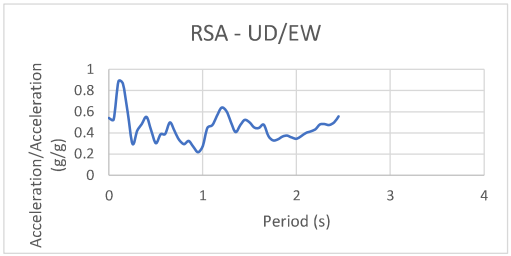


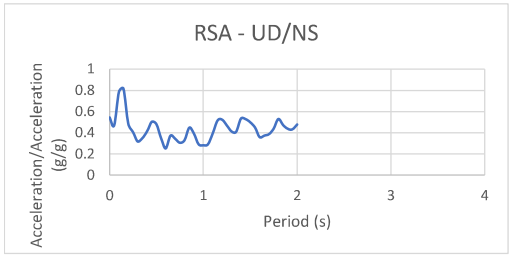


| | |
|---|---|
| Max UD (g) | 0.39229 |
| Per Max UD (s) | 0.20 |

| | |
|---|---|
| Max UD/EW (g) | 0.887 |
| Per Max UD/EW (s) | 0.10 |

| | |
|---|---|
| Max UD/NS (g) | 0.815 |
| Per Max UD/NS (s) | 0.15 |

| RSA - EW | | RSA - NS | | MAX( EW, NS) | |
|---|---|---|---|---|---|
| PGA = | 0.223 | PGA = | 0.223 | PGA = | 0.223 |
| Ss = | 0.662 | Ss = | 0.804 | Ss = | 0.804 |
| S1 = | 0.295 | S1 = | 0.291 | S1 = | 0.295 |

# APPENDIX D:

# BASIN SITE M9 CSZ RSA DATA

Site: Seattle 1

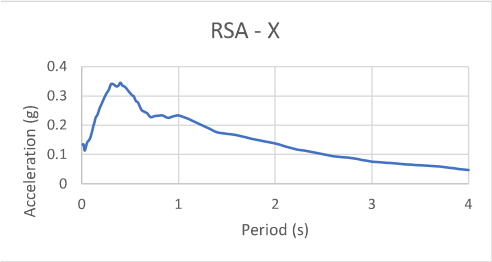


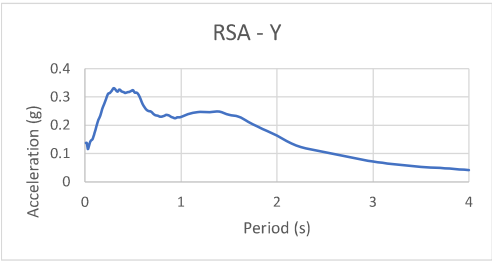


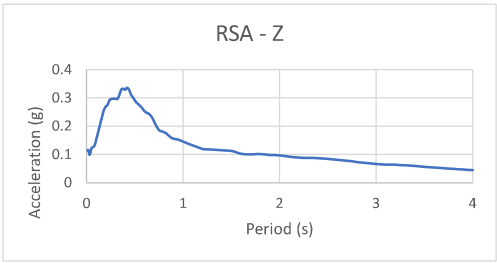


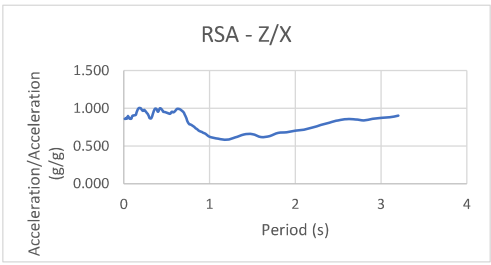


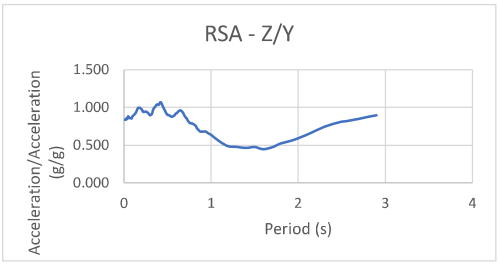


| | |
|---|---|
| Max UD (g) | 0.33612 |
| Per Max UD (s) | 0.42 |
| Max UD/EW (g) | 1.004 |
| Per Max UD/EW (s) | 0.18 |
| Max UD/NS (g) | 1.069 |
| Per Max UD/NS (s) | 0.42 |

| RSA - X | | RSA - Y | | MAX( X, Y) | |
|---|---|---|---|---|---|
| PGA = | 0.134 | PGA = | 0.138 | PGA = | 0.138 |
| Ss = | 0.270 | Ss = | 0.275 | Ss = | 0.275 |
| S1 = | 0.234 | S1 = | 0.229 | S1 = | 0.234 |

Site: Seattle 2

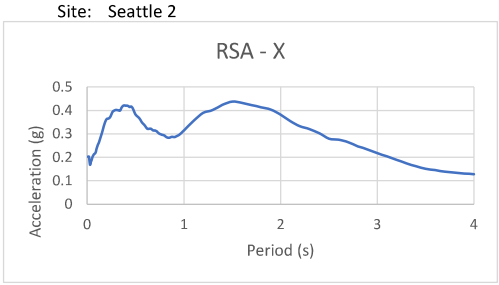


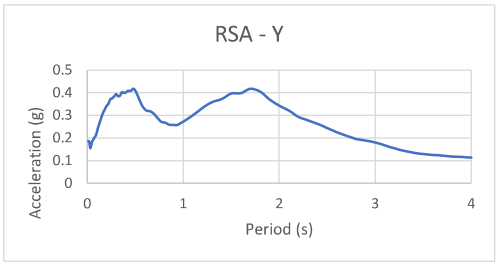


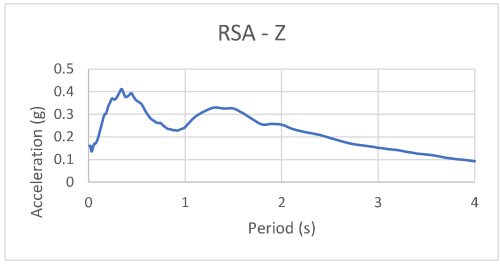


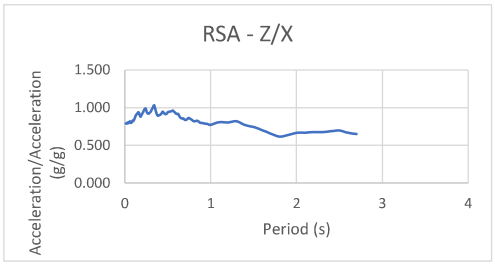


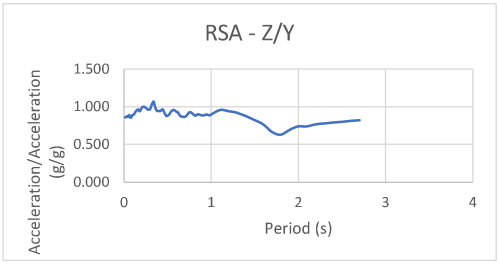


| | |
|---|---|
| Max UD (g) | 0.411615 |
| Per Max UD (s) | 0.34 |
| Max UD/EW (g) | 1.031 |
| Per Max UD/EW (s) | 0.34 |
| Max UD/NS (g) | 1.067 |
| Per Max UD/NS (s) | 0.34 |

| RSA - X | | RSA - Y | | MAX( X, Y) | |
|---|---|---|---|---|---|
| PGA = | 0.202 | PGA = | 0.185 | PGA = | 0.202 |
| Ss = | 0.363 | Ss = | 0.340 | Ss = | 0.363 |
| S1 = | 0.315 | S1 = | 0.272 | S1 = | 0.315 |

Station: Seattle 3

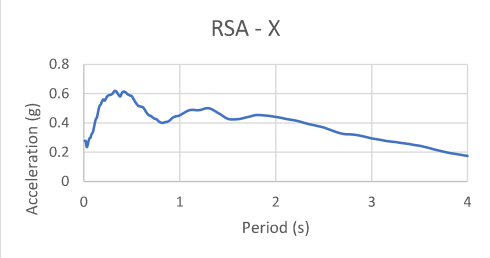


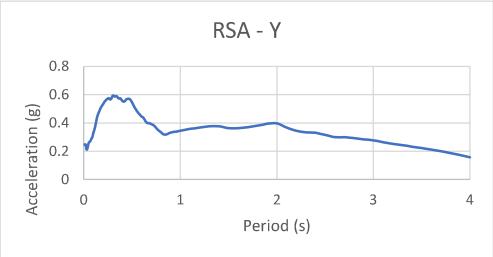


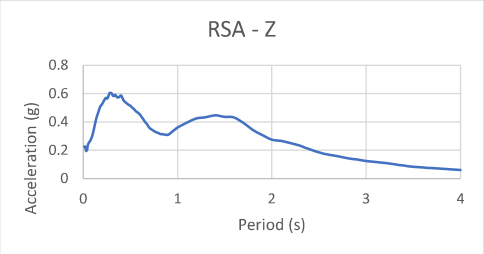


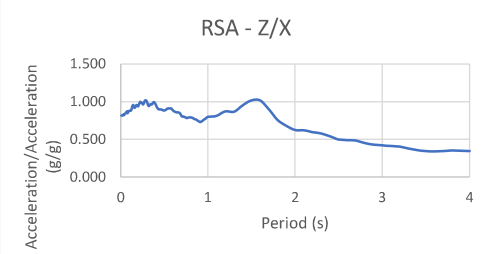


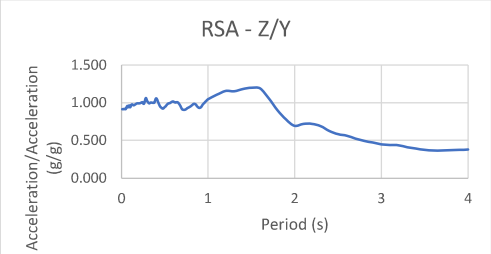


| | |
|---|---|
| Max UD (g) | 0.60377 |
| Per Max UD (s) | 0.30 |
| Max UD/EW (g) | 1.017 |
| Per Max UD/EW (s) | 0.28 |
| Max UD/NS (g) | 1.200 |
| Per Max UD/NS (s) | 1.50 |

| RSA - X | | RSA - Y | | MAX( X, Y) | |
|---|---|---|---|---|---|
| PGA = | 0.276 | PGA = | 0.247 | PGA = | 0.276 |
| Ss = | 0.560 | Ss = | 0.530 | Ss = | 0.560 |
| S1 = | 0.451 | S1 = | 0.344 | S1 = | 0.451 |

Station: Portland 1

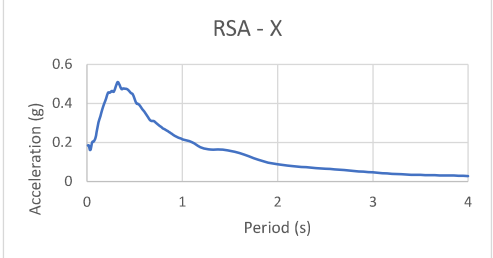


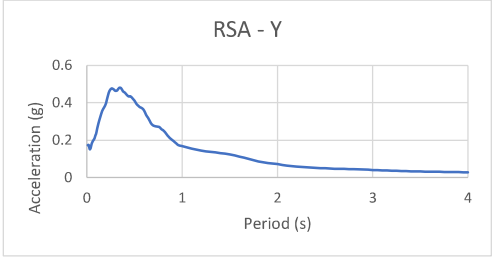


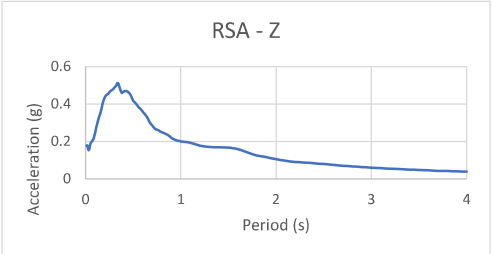


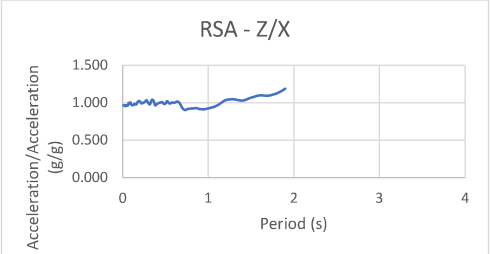


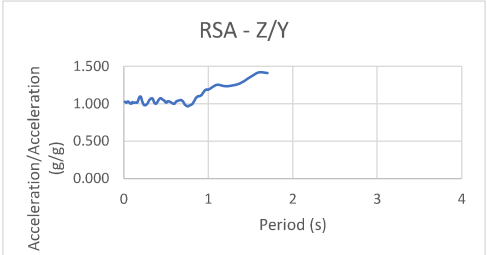


| | |
|---|---|
| Max UD (g) | 0.512885 |
| Per Max UD (s) | 0.34 |
| Max UD/EW (g) | 1.187 |
| Per Max UD/EW (s) | 1.90 |
| Max UD/NS (g) | 1.418 |
| Per Max UD/NS (s) | 1.60 |

| RSA - X | | RSA - Y | | MAX( X, Y) | |
|---|---|---|---|---|---|
| PGA = | 0.185 | PGA = | 0.174 | PGA = | 0.185 |
| Ss = | 0.426 | Ss = | 0.398 | Ss = | 0.426 |
| S1 = | 0.217 | S1 = | 0.169 | S1 = | 0.217 |

Station: Portland 2

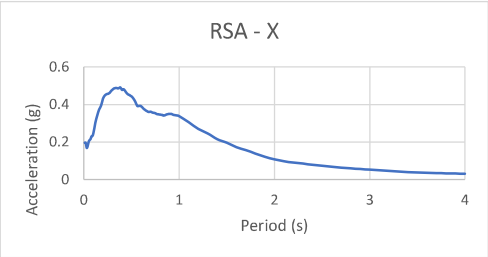


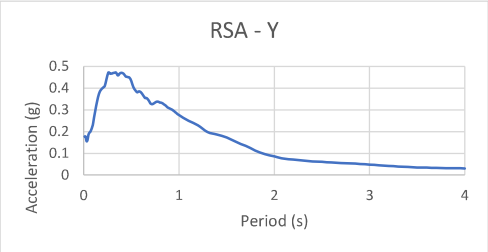


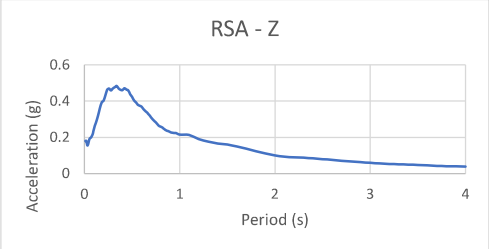


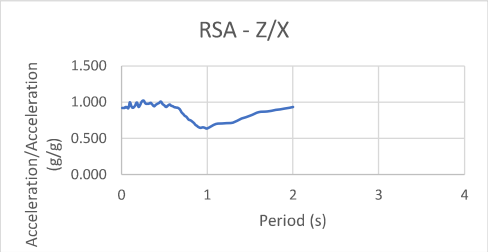


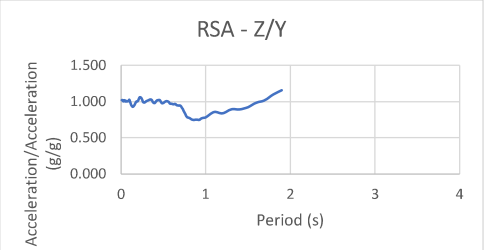


| | |
|---|---|
| Max UD (g) | 0.483944 |
| Per Max UD (s) | 0.34 |
| Max UD/EW (g) | 1.023 |
| Per Max UD/EW (s) | 0.26 |
| Max UD/NS (g) | 1.157 |
| Per Max UD/NS (s) | 1.90 |

| RSA - X | | RSA - Y | | MAX( X, Y) | |
|---|---|---|---|---|---|
| PGA = | 0.196 | PGA = | 0.177 | PGA = | 0.196 |
| Ss = | 0.431 | Ss = | 0.401 | Ss = | 0.431 |
| S1 = | 0.338 | S1 = | 0.275 | S1 = | 0.338 |

Station: Portland 3

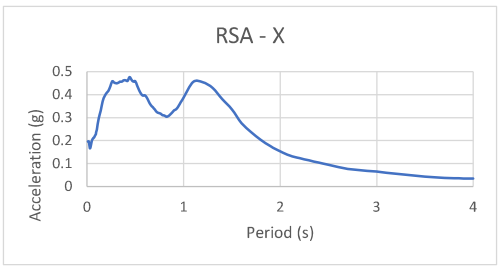


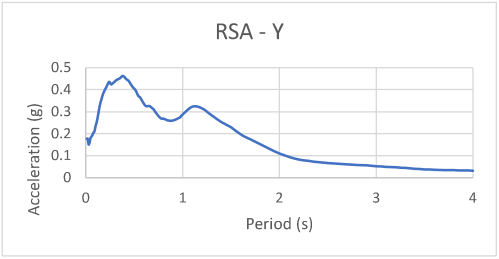


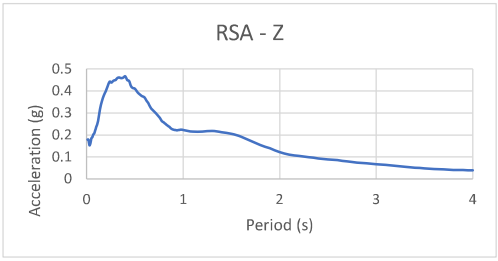


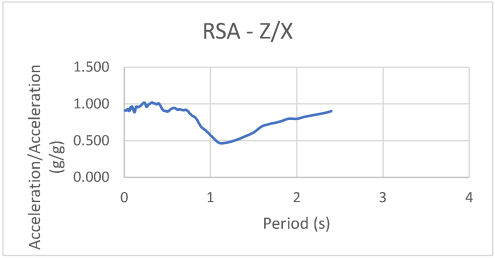


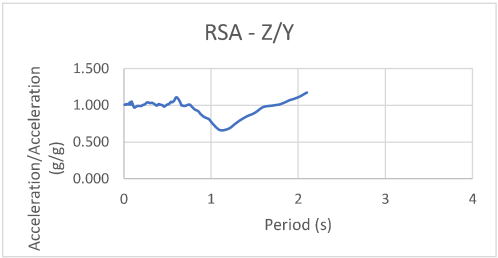


| | |
|---|---|
| Max UD (g) | 0.466228 |
| Per Max UD (s) | 0.40 |
| Max UD/EW (g) | 1.021 |
| Per Max UD/EW (s) | 0.32 |
| Max UD/NS (g) | 1.174 |
| Per Max UD/NS (s) | 2.10 |

| RSA - X | | RSA - Y | | MAX( X, Y) | |
|---|---|---|---|---|---|
| PGA = | 0.196 | PGA = | 0.177 | PGA = | 0.196 |
| Ss = | 0.406 | Ss = | 0.402 | Ss = | 0.406 |
| S1 = | 0.386 | S1 = | 0.287 | S1 = | 0.386 |